NASA/TM-2009-215699

Trade Study of Multiple Thruster Options for the Mars Airplane Concept

Christopher A. Kuhl, Steven W. Gayle, Craig A. Hunter, Patrick S. Kenney, Salvatore Scola, David A. Paddock, Henry S. Wright, and Joseph F. Gasbarre
Langley Research Center, Hampton, Virginia

March 2009

NASA STI Program . . . in Profile

Since its founding, NASA has been dedicated to the advancement of aeronautics and space science. The NASA scientific and technical information (STI) program plays a key part in helping NASA maintain this important role.

The NASA STI program operates under the auspices of the Agency Chief Information Officer. It collects, organizes, provides for archiving, and disseminates NASA's STI. The NASA STI program provides access to the NASA Aeronautics and Space Database and its public interface, the NASA Technical Report Server, thus providing one of the largest collections of aeronautical and space science STI in the world. Results are published in both non-NASA channels and by NASA in the NASA STI Report Series, which includes the following report types:

- TECHNICAL PUBLICATION. Reports of completed research or a major significant phase of research that present the results of NASA programs and include extensive data or theoretical analysis. Includes compilations of significant scientific and technical data and information deemed to be of continuing reference value. NASA counterpart of peer-reviewed formal professional papers, but having less stringent limitations on manuscript length and extent of graphic presentations.

- TECHNICAL MEMORANDUM. Scientific and technical findings that are preliminary or of specialized interest, e.g., quick release reports, working papers, and bibliographies that contain minimal annotation. Does not contain extensive analysis.

- CONTRACTOR REPORT. Scientific and technical findings by NASA-sponsored contractors and grantees.

- CONFERENCE PUBLICATION. Collected papers from scientific and technical conferences, symposia, seminars, or other meetings sponsored or co-sponsored by NASA.

- SPECIAL PUBLICATION. Scientific, technical, or historical information from NASA programs, projects, and missions, often concerned with subjects having substantial public interest.

- TECHNICAL TRANSLATION. English-language translations of foreign scientific and technical material pertinent to NASA's mission.

Specialized services also include creating custom thesauri, building customized databases, and organizing and publishing research results.

For more information about the NASA STI program, see the following:

- Access the NASA STI program home page at *http://www.sti.nasa.gov*

- E-mail your question via the Internet to help@sti.nasa.gov

- Fax your question to the NASA STI Help Desk at 443-757-5803

- Phone the NASA STI Help Desk at 443-757-5802

- Write to:
  NASA STI Help Desk
  NASA Center for AeroSpace Information
  7115 Standard Drive
  Hanover, MD 21076-1320

NASA/TM-2009-215699

Trade Study of Multiple Thruster Options for the Mars Airplane Concept

Christopher A. Kuhl, Steven W. Gayle, Craig A. Hunter, Patrick S. Kenney, Salvatore Scola, David A. Paddock, Henry S. Wright, and Joseph F. Gasbarre
Langley Research Center, Hampton, Virginia

National Aeronautics and
Space Administration

Langley Research Center
Hampton, Virginia 23681-2199

March 2009

Available from:

NASA Center for AeroSpace Information
7115 Standard Drive
Hanover, MD 21076-1320
443-757-5802

Table of Contents

List of Figures

List of Tables

1.0 Introduction

The ARES baseline airplane, proposed in 2003 to the Office of Space Science for the Mars Scout Program[1], required a thruster that could produce roughly 40 N of thrust and have a 50% margin to accommodate climbs and accelerations. The Aerojet 14-lbf (62N) AJ10-220 thruster was selected for the propulsion system, which is the only thruster available in this range of thrust. With concerns about the availability of tooling for manufacturing this thruster, as well as the non-recurring costs that would be imposed on the program, other options needed to be considered.

A trade study was performed at NASA Langley Research Center under the Planetary Airplane Risk Reduction (PARR) project (2004-2005) to examine the option of using multiple, smaller thrusters in place of a single large thruster on the Mars airplane concept with the goal to reduce overall cost, schedule, and technical risk.

The 5-lbf (22N) thruster is a common reaction control thruster on many satellites. Thousands of these types of thrusters have been built and flown on numerous programs, including MILSTAR and Intelsat VI. This study has examined the use of three 22N thrusters for the Mars airplane propulsion system and compared the results to those of the baseline single thruster system.

This report covers:

- Overview of the single thruster and multiple thruster propulsion system options.
- Thruster to airframe mounting concepts.
- Thermal analysis of the thrusters and heat soak-back into the airframe.
- Plume calculations for the various thruster arrangements.
- System mass estimates and overall performance of the thruster options.
- Direct comparison of the 62N thruster option and the multiple 22N thruster options.
- Thruster system down-select methodology and results.

2.0 Review of ARES Baseline Propulsion System

2.1 Single 62N Thruster System Overview

The ARES baseline propulsion system was designed to use a bi-propellant, pulsed control with MMH fuel and MON-3 oxidizer. Propellant is stored in two identical titanium tanks each with a screen-and-channel propellant management device (PMD) for fuel and oxidizer extraction. The fuel flow is controlled through a regulated helium blow-down system where helium is stored at high pressure in a composite over-wrapped pressure vessel. Propulsion system components integrated into the airframe are shown in Figure 1.

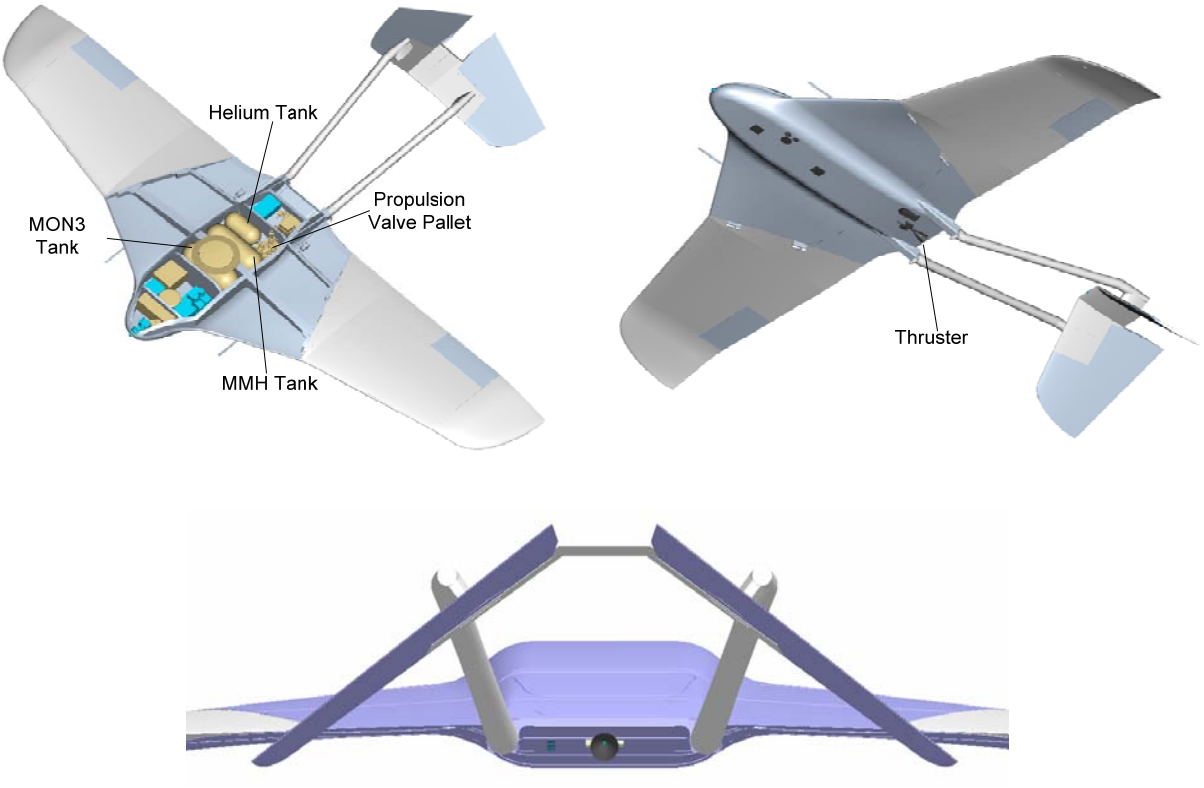

Figure 1. Single 62N Thruster Configuration.

2.2 Single 62N Propulsion System Schematic

The ARES airplane baseline propulsion system is a regulated bi-propellant system with pulsed thruster control. Major components of this system consist of fuel and oxidizer tanks, helium pressure tank, and a thruster. Fuel and oxidizer tanks are isolated before flight using normally-closed pyrotechnic valves and isolated during operation using redundant parallel check valves. The schematic layout of the ARES propulsion subsystem is shown in Figure 2.

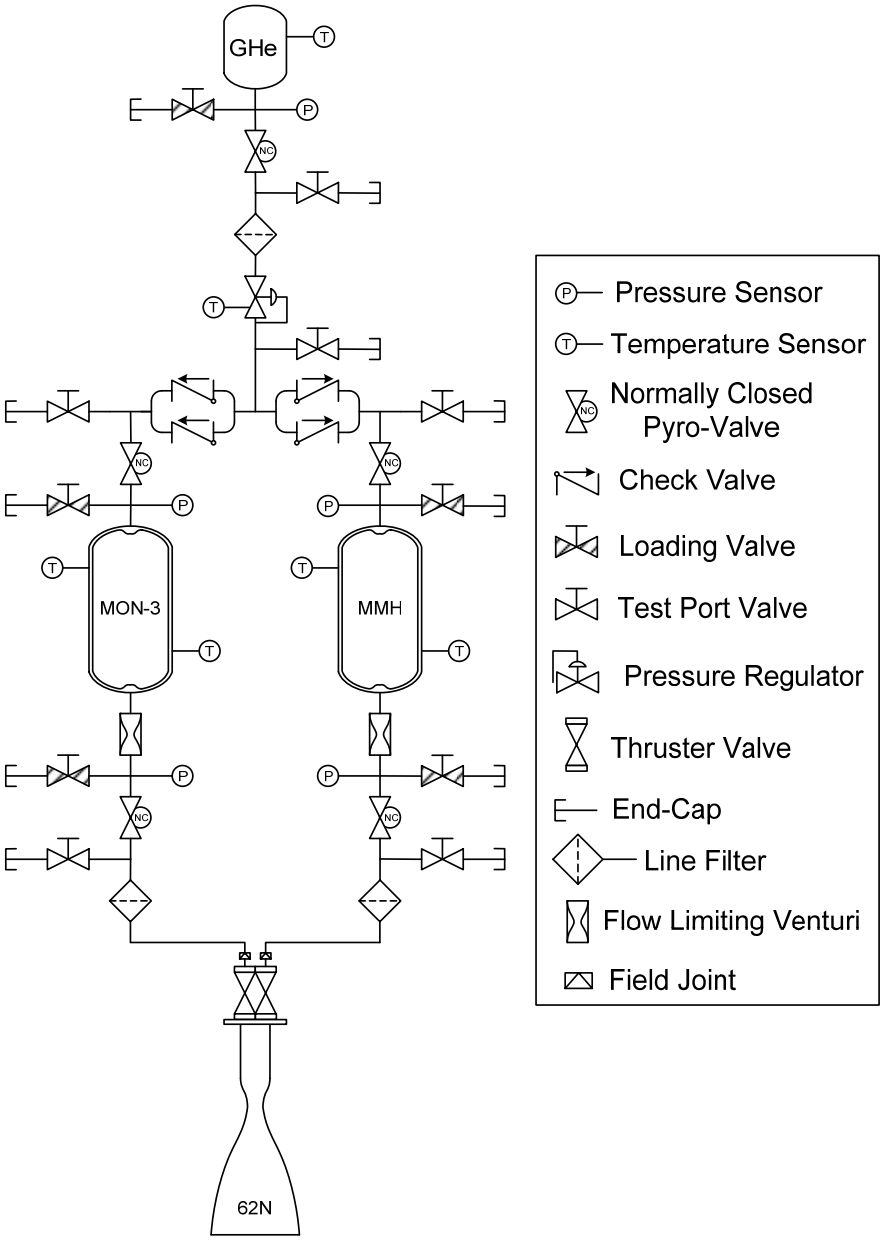

Figure 2. Single 62N Thruster Propulsion System Schematic.

2.3 Single 62N Baseline Thruster - Aerojet 14lbf (62N) AJ10-220

The 14lbf Aerojet AJ10-220 bi-propellant thruster, shown in Figure 3, is derived from Lockheed's "Bus-1", a previously classified US Air Force spacecraft. "Bus-1" is a modular bus developed by Lockheed that is qualified for STS and ELV's. The bus provides propulsion, GN&C, Communications, & Data Management. The Bus-1 unit consisted of 6 reaction control thruster modules (RCTM) each of which contained two 14 lbf thrusters, making a total of 12 thrusters per unit. These thrusters were qualified over a 10-22 lbf (44.5 – 97.9 N) thrust range and have a demonstrated chamber life of greater than 40 hours of operation. At the 14 lbf level, the specific impulse is approximately 285s. The thruster incorporates fuel film cooling and series redundant valves to provide a redundant leak protection. A total of 54 production RCTMs were delivered for the "Bus-1" program from 1987 to 1992. Table 1 lists the performance parameters of the AJ10-220 thruster.

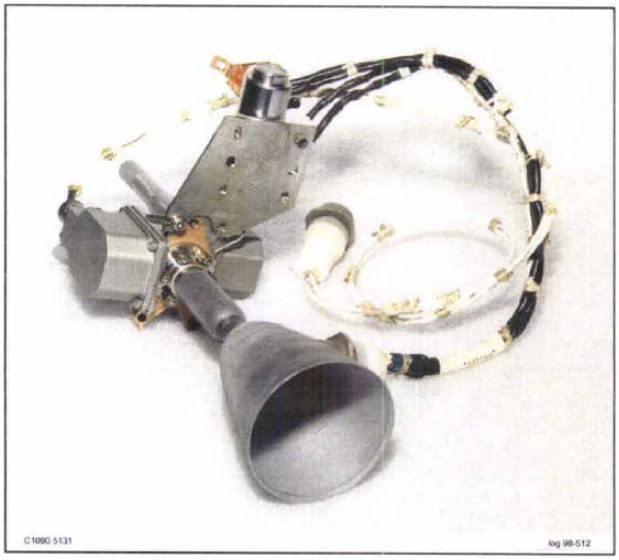

Figure 3. Aerojet AJ10-220 62N Thruster.[2]

A follow-on thruster design was conducted by Aerojet to improve the life of the thruster by using an Iridium/Rhenium chamber as opposed to the production Columbium chamber. The Ir/Re 14 lbf engine has demonstrated through hot-fire tests to deliver a specific impulse of 305 s and a predicted life over 40 hours. The Ir/Re 14 lbf is similar to the production model with the exception of an Ir/Re chamber, a heater circuit, and the thrust plate and frame are modified to accommodate different spacecraft interfaces.

Some, but not all, of the tooling exists in storage at Aerojet for the Columbium production engine. The current thruster design uses shunts and a frame to direct heat away from the valve during hot-fire, and valve overheating will occur unless the chamber heat is shunted to some other structure. Current thruster design uses a frame with vibration isolators to manage launch vibration loads and any change in thruster mounting will require a new dynamic analysis. Depending on the magnitude of changes from the qualified thruster, non-recurring costs start at approximately $1M for a Mars Airplane program.

Table 1. Aerojet AJ10-220 62N Thruster Parameters[2]

Fuel	Monomethyl Hydrazine (MMH)
Oxidizer	Nitrogen Tetroxide (MON3)
Inlet Pressure	140 – 375 psia
Propellant Inlet Temp	40°F – 110°F
Thrust @ 220 psia	14 ± 0.7 lbf (62 ± 3 N)
Thrust @ 140 – 375 psia	9.5 – 22.0 lbf (42 – 98N)
SS Isp @ 220 psi	285 nominal, 265 min
MR @ 220 psia	1.65 ± 0.05
Expansion Ratio	75:1
Weight	4.3 lb (1950 grams)
Length	7.5 inches (19 cm)
Diameter	2.3 inches (5.8 cm)
Valve Voltage	28 ± 4 VDC

2.4 Airframe Thruster Mounting Concepts

To mount the thrusters to the airplane, additional support structure was designed for this study that was not part of the original ARES Step-2 baseline design. The airframe structure concept for mounting of thruster assemblies into existing Mars Airplane airframe design is shown in Figure 4. The thruster ribs and bulkheads are composite sandwich structure similar to existing Mars Airplane airframe design. Figure 5 shows a typical rib or bulkhead cross-section. The upper and lower flanges of the thruster ribs and bulkheads are bonded directly to the center-body skins. The aft thruster bulkhead is mechanically joined to the center-body main ribs. The thruster ribs are mechanically joined to the aft thruster bulkhead and the center-body aft spar. The thruster forward bulkhead is mechanically joined to the thruster ribs. Loads sustained by the thruster assembly are passed directly into the center-body airframe.

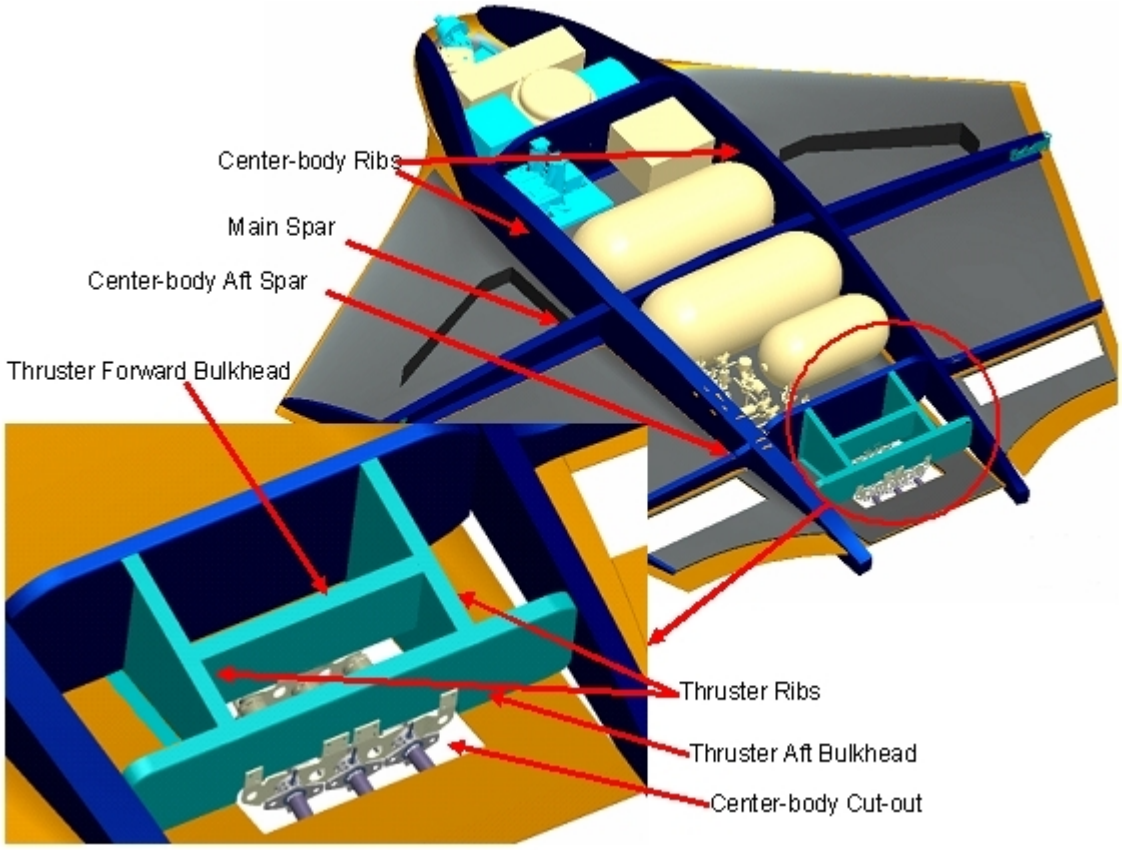

Figure 4. Airframe Support Structure for Thruster Mounting
(New structure shown in light-green)

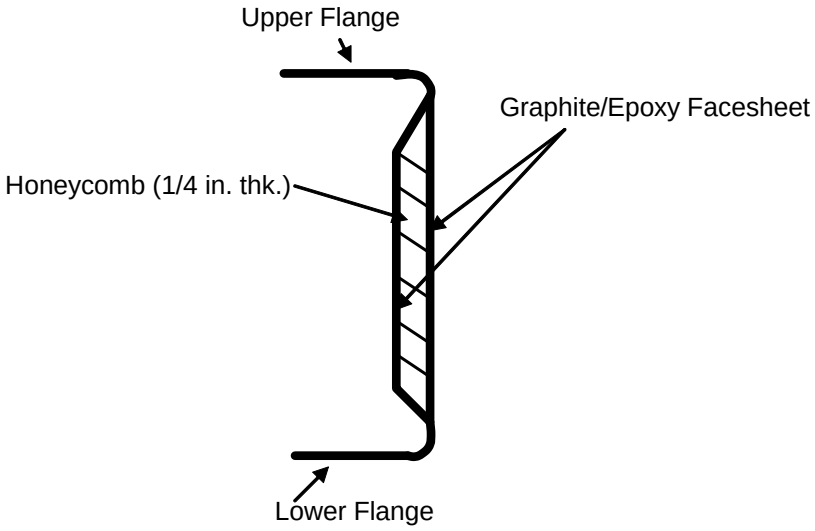

Figure 5. Airplane Support Composite Structure

The composite structure was analyzed with Pro-Engineer Mechanica Finite Element Analysis (FEA). Preliminary lay-up schedules for laminates and honeycomb sizing have been determined to enable mass estimates for composite support structure. The analysis approach was to conservatively size the composite structure to mount either of the three thruster configurations considered in this study. Launch loads, cases 1a and 1b from Appendix B, were determined to be the critical load cases the composite structure would sustain, therefore they were applied to the FEA model. After multiple design iterations, a final preliminary design was developed based on the required design factor of safety of 2.0 for composite materials, show in Appendix B. Preliminary mass estimates are shown in Table 2.

Table 2. Airplane Thruster Support Structure Mass Breakdown

Component	Material	Weight (lbf)	Mass (kg)
Aft Thruster Bulkhead	Composite Sandwich	0.289	0.131
Forward Thruster Bulkhead	Composite Sandwich	0.158	0.072
Thruster Ribs	Composite Sandwich	0.180	0.082
Total		**0.627**	**0.284**

2.5 Single 62N Thruster Mounting and Support System

The orientation of the 62N thruster in relation to the airplane is shown in Figure 6. The thruster tilts 5.88° from the horizontal reference so that the thrust vector is directed through the airplane center of gravity, shown in Figure 7.

The AJ10-220 thruster mounting bracket is titanium alloy bolted directly to the thruster injector flange, shown in Figure 8. Mounting scheme is typical for this thruster. The thruster bracket is mounted to the airframe similar to the 22N thruster assemblies. The mounting bracket is bolted directly to composite bulkhead. A structural analysis was performed on the 62N thruster mounting bracket with Pro-Engineer Mechanica FEA. Load case 1a and 1b were applied to the FEA model.

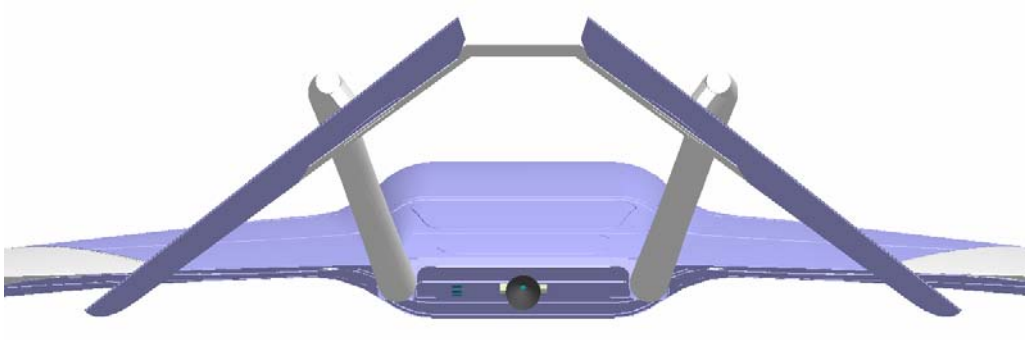

Figure 6. Single 62N Thruster Configuration on Airplane

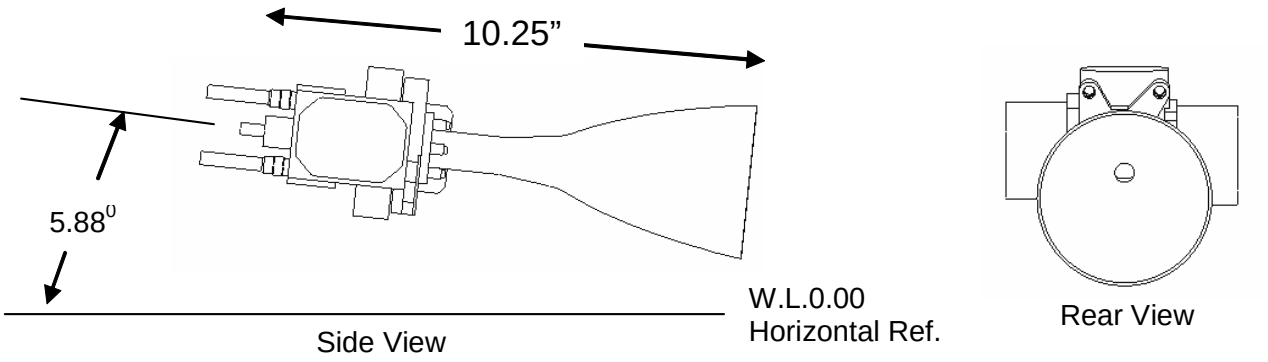

Figure 7. Aerojet AJ10-220 62N Thruster Orientation
(Thruster is tilted 5.88° to direct thrust vector through the center of gravity)

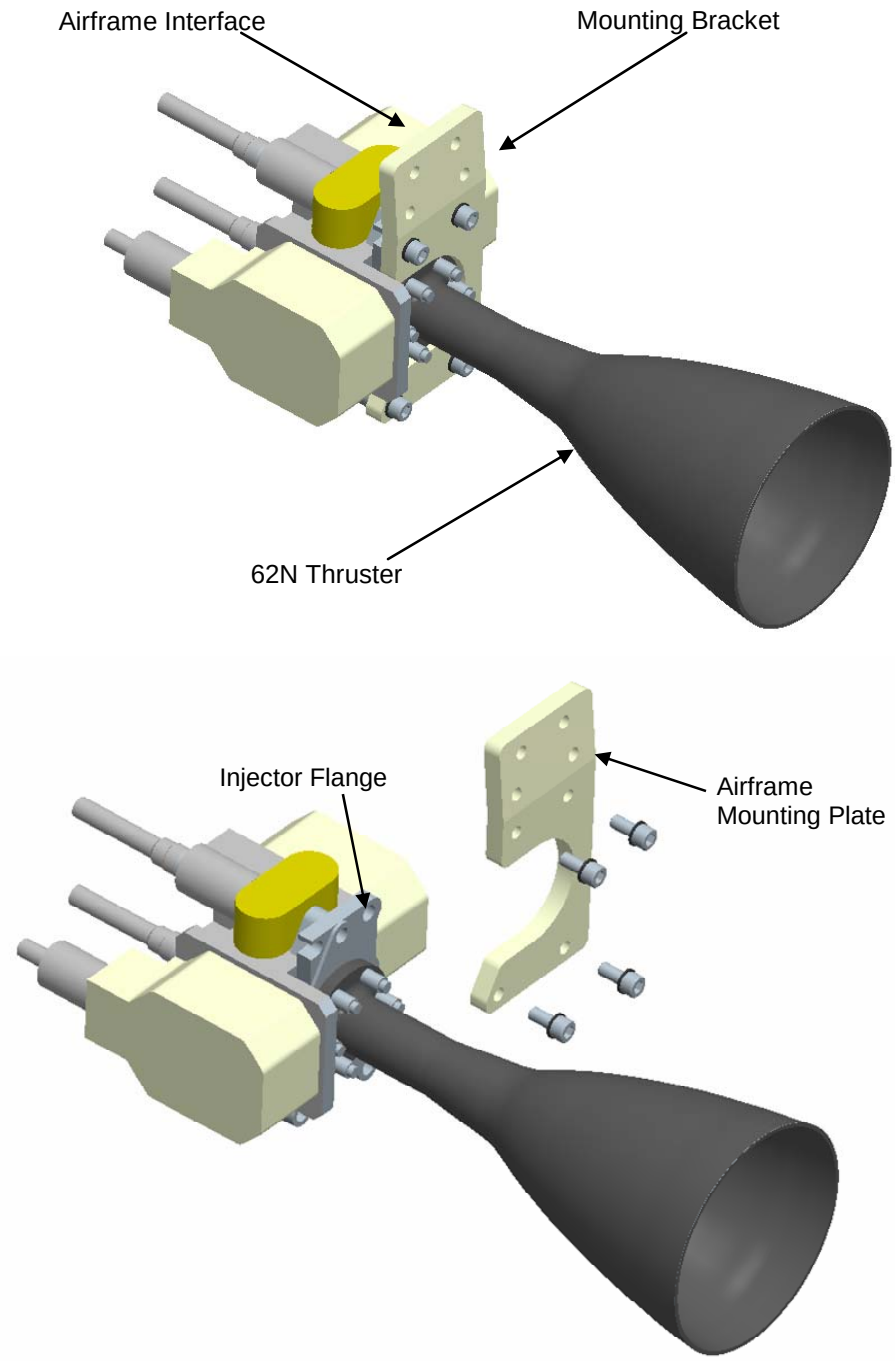

Figure 8. Aerojet 62N Thruster Mounting Concept

Similar to the composite structure, launch load cases (1a and 1b in Appendix B) were determined to be the critical load cases applied to the 62N thruster due to the large "g" loads seen during launch. The mass of a single 62N thruster is equal to 1.95 kg. Based on Figure 77, Appendix B, the MAC value for the thruster is 50. Therefore the "g" force applied to the thruster for load case 1a in the axial direction would be 52.8 and for load case 1b would be 50 in any direction. Based on F = ma the force on each thruster for the axial direction of load case 1a would be 227 lbf and for load case 1b 215 lbf. The preliminary mounting bracket design was sized according to design factors of safety. Preliminary mass estimates for mounting hardware are shown in Table 3.

Table 3. Mass Breakdown of Mounting Concept for AJ10-220 62N Thruster

Component	Material	Density (lbf/in^3)	Weight (lbf)	Mass (kg)
Thruster Bracket	Titanium Alloy	0.16	0.159	0.072
Mounting Hardware	CRES	0.29	0.100	0.045
Total			0.259	0.117

2.6 *Single 62N Thruster Thermal Analysis*

As part of the acceptance testing of the 14 lbf production engine, thrusters were hot-fired three times for 100 seconds. The time requirement for these thrusters was 214 seconds at 14 lbf thrust level. Table 4 shows results of hot fire testing at a duty cycle similar to that of the Step-2 ARES mission. Maximum temperature of the valve face never exceeds 110°F. Figure 9 shows the temperature data for a 100 sec hot-fire steady-state test of the Ir/Re engine[3]. The flange temperature (TF2) reaches a maximum temperature of 160°F at 95 seconds and climbs to 255°F after a few seconds of coast due to thermal soakback.

Table 4. Hot Fire Testing Results for AJ10-220 62N Thruster[3]

Fuel Inlet Pressure [psia]	Ox Inlet Pressure [psia]	Burn Time [sec]	Cycle:[sec]	Coast [sec]	Max Chamber Temp [°F]	Max Flange Temp [°F]	Max Valve Temp [°F]
225	225	60	5 on /5 off	20	1300-1700	190-215	105
145	170	60	5 on /5 off	20	1250-1650	140-190	100
340	380	60	5 on /5 off	20	1450-1650	210-235	110
375	375	60	5 on /5 off	20	1425-1625	200-230	110

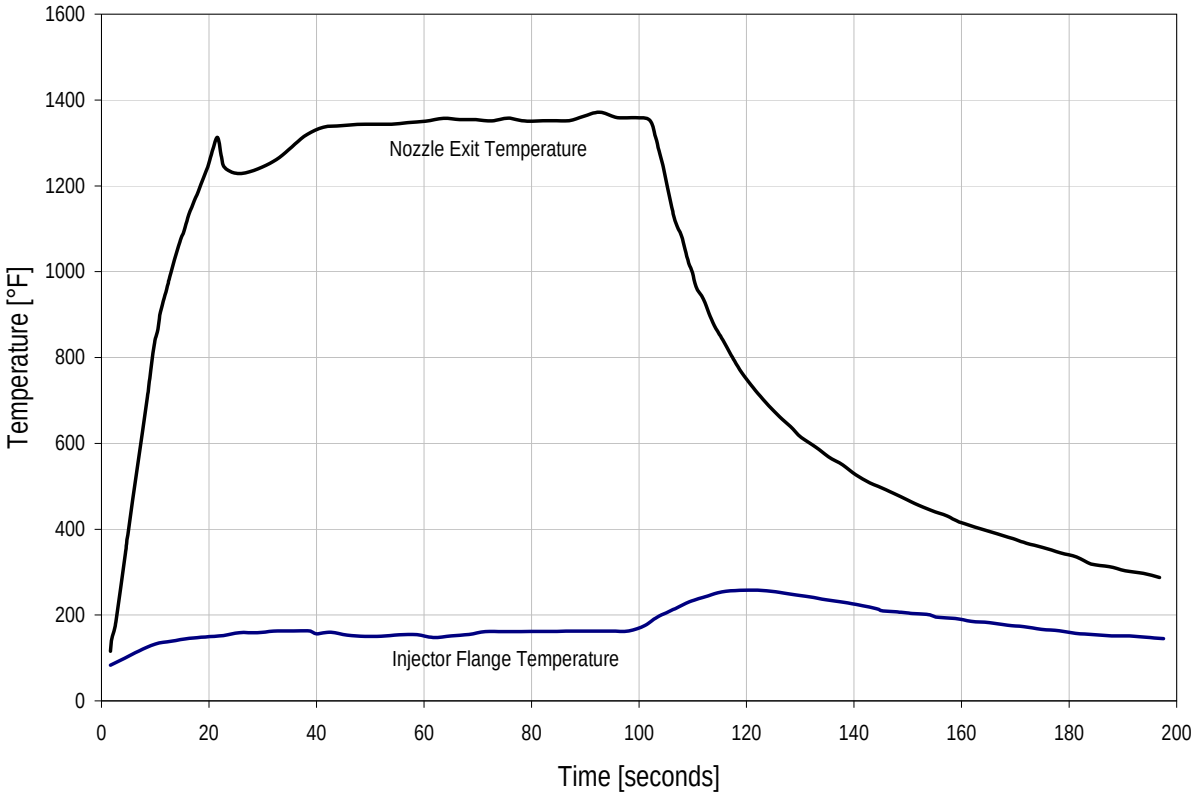

Figure 9. Time Varying Temperature Data for AJ10-220 (Ir-Re) Thruster[3]

2.7 Single 62N Thruster Plume Analysis

In order to evaluate the potential impact of the rocket plume on the aircraft's tail structure, an isolated plume CFD simulation was conducted[4]. Color contours of Mach number are shown in Figure 10, along with a line contour indicating the thermal edge of the plume at To=220K. The nozzle stagnation temperature is 3395K and the free-stream stagnation temperature is 199K. This analysis shows that there is sufficient clearance between the 220K edge of the plume and the tail surfaces and support booms to preclude any thermal impingement effects. In addition, the limited influence of the plume on the surrounding free-stream indicates that flow around the tail surfaces will not be changed dramatically by the presence of the plume.

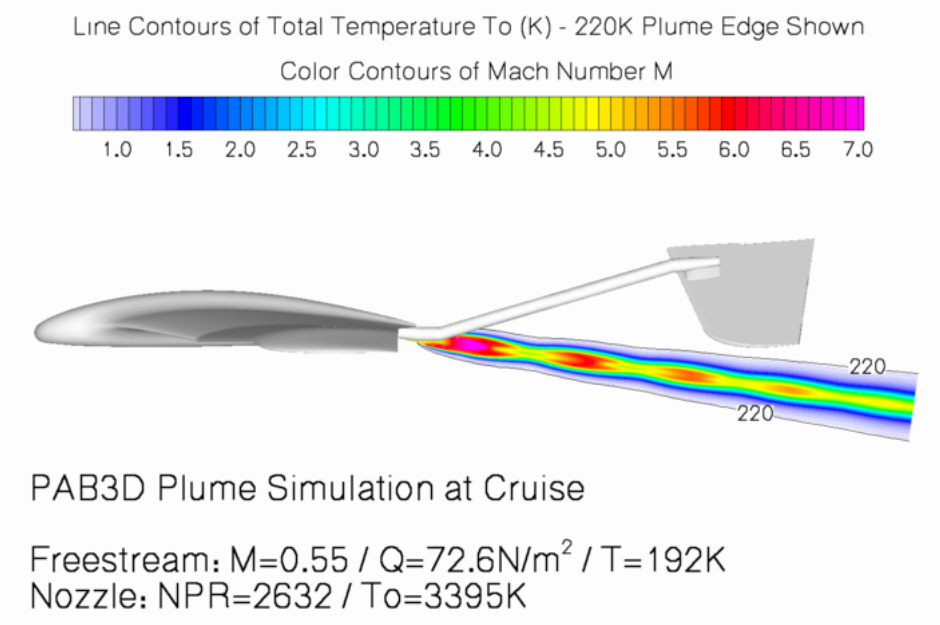

Figure 10. Single 62N Thruster Rocket Plume CFD Analysis[4]

2.8 *Single 62N Thruster Mission Performance*

The flight simulation of the Mars airplane was evaluated using a 6 degree-of-freedom model from the Langley Standard Real-Time Simulation application framework[5]. Control logic was incorporated to hold the aircraft's speed while flying a mission profile. Since the airplane uses a pressure-blowdown propulsion system, the thruster is not throttled; instead duty cycle adjustments provide the needed thrust modulation. The thruster control law was also modified to accommodate the pulsing mode of the thruster. The law uses two key elements, a thrust period and a duty cycle. The two elements define how long the thruster is on (period * duty cycle) and off. Once a thrust period has ended the duty cycle is modified to reflect the error between the commanded Mach number and the average Mach number for the period. Two atmospheric conditions were simulated, one with no turbulence, and the other condition with severe atmospheric turbulence. Thruster duty cycles for the flight condition with no turbulence are shown in Figure 11. The histogram shows a predominant duty cycle between 45% and 60 % for the majority of the flight. During severe turbulence, the data shown in Figure 12 provide no predominant duty cycle which suggests that the flight controls are trying to keep up with the fast changing flight conditions.

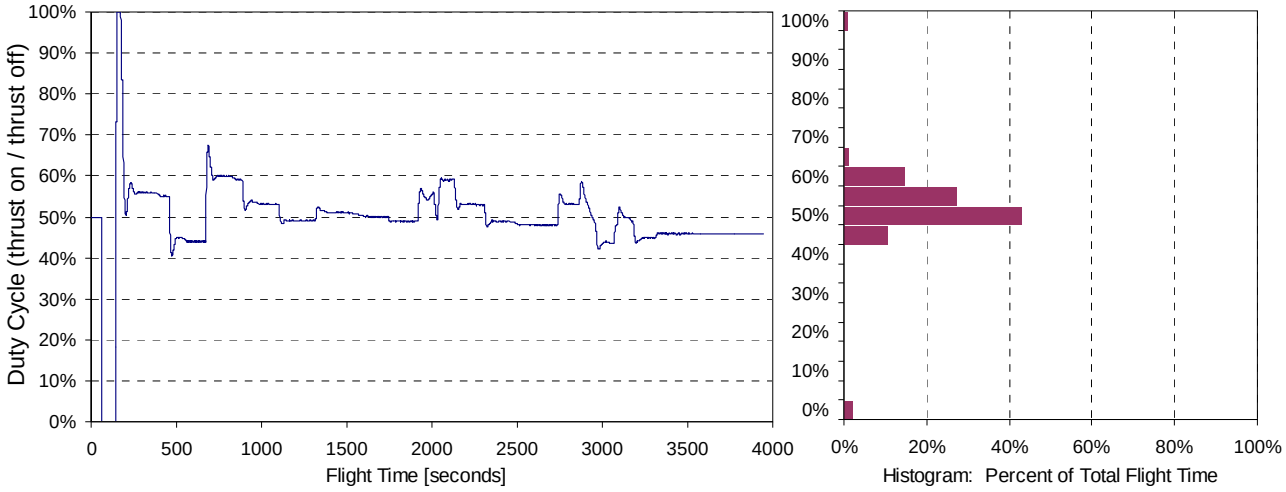

Figure 11. Single Thruster Duty Cycles - No Turbulence

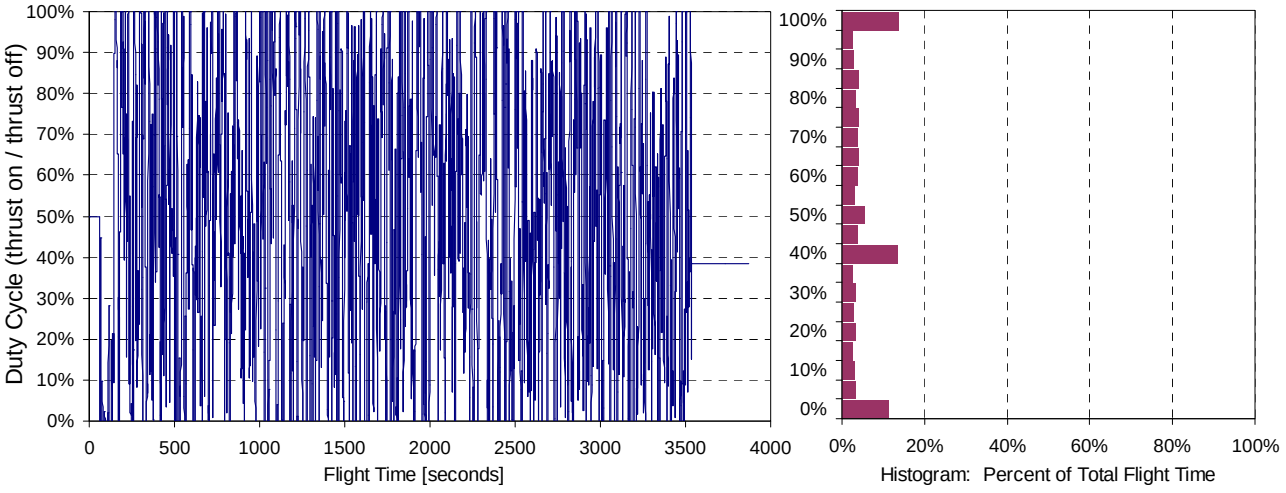

Figure 12. Single Thruster Duty Cycles - Severe Turbulence

2.9 Single 62N Thruster System Summary

The results of the simulation show that for the airplane with a single 62N thruster flying in no-turbulence conditions, the flight range with 40 kg of propellant is about 527 km. In severe turbulence conditions for the same fuel load, the flight range is reduced to about 520 km (Table 5). The total mass of the single thruster propulsion system is broken down into components shown in Table 6. Based on commercially available components, estimates from vendors, and analysis, the current best estimate for the 62N thruster system is 13.18 kg. Incorporating the contingencies assigned to each component, the total mass increases to a growth mass of 15.95 kg.

Table 5. Single Thruster System Performance Summary

Parameter	Value
Total AFS Mass	145 kg
Propulsion Mass	15.95 kg
Propellant Load	40 kg
Fuel	15 kg - MMH
Oxidizer	25 kg - MON3
Thrust	62 N
Isp	~285 s
No Turbulence	
Flight Duration	65.75 min
Range	527 km
Avg Fuel Usage	13.2 km/kg
Severe Turbulence	
Flight Duration	64.47 min
Range	520 km
Avg Fuel Usage	13.0 km/kg

Table 6. Single 62N Thruster System Mass Breakdown

Common Components	QTY	CBE Each [kg]	Total [kg]	Cont [%]	CBE + Cont [kg]	Vendor	Part Number
Pressure Transducer	5	0.15	0.75	20%	0.90	GP50	7200
Normally Closed Pyro Valve	5	0.15	0.75	15%	0.86	CONAX	1832-205
GHe Filter	1	0.25	0.25	25%	0.31	Vacco	F1D10636-01
High Pressure Service Valve	11	0.113	1.243	10%	1.37	Vacco	V1E10430-01
Helium Regulator	1	0.363	0.363	10%	0.40	Vacco	66250
Check Valve	4	0.02	0.08	25%	0.10	Vacco	V1D10856-02
Liquid Filter	2	0.18	0.36	25%	0.45	Vacco	F1D10638-01
GHe Tank	1	1.2	1.2	25%	1.50	Lincoln	220131-1
Oxidizer Tank	1	2.87	2.87	25%	3.59		
Fuel Tank	1	2.87	2.87	25%	3.59		
Tank Support Brackets	4	0.1	0.4	25%	0.50		
Subtotal			*10.74*		*13.07*		
Single Thruster Option							
Thruster	1	1.09	1.09	10%	1.20	Aerojet	AJ10-220
Thruster Valves	1	0.86	0.86	10%	0.95	Moog	52-189B
Flow Venturi	2	0.04	0.08	5%	0.08		
Misc Tubing, Brackets	1	0.25	0.25	25%	0.31		
PIA & PCA Plates	2	0.08	0.16	25%	0.20		
Engine Support Structure	1	0.117	0.117	25%	0.15		
Total Propulsion Mass			*13.18*		***15.95***		

3.0 Triple 22N Thruster Propulsion System Options

3.1 Bi-Propellant Thruster Options

An alternative to the single 14 lbf (62N) system is the concept of using three 22N bi-propellant thrusters. The options that exist are shown in Table 7. Based on the recommendation by Lockheed Martin following a contracted trade study[6], the AMPAC-In-Space Propulsion (ARC) 22N thruster was chosen as the baseline thruster for the three-thruster trade study. This thruster was qualified under the Intelsat VI satellite program and over 1000 units have flown to date. (It should be noted that the Aerojet R-6C is an almost identical engine with similar production numbers and similar heritage and can be considered as a backup for future development).

Table 7. Mars Airplane Commercial Thruster Options[6]

Vendor	Aerojet	Aerojet	Aerojet	Aerojet	AMPAC-ISP (ARC)	AMPAC-ISP (ARC)	Astrium - EADS
Model	AJ10-220	AJ10-220+	R-6C	R-6D	5 lbf	5 lbf	S22-02
Chamber Material	C103	Ir/Re	C103	C103	C103	Pt/Rh	Pt/Rh
Status	Existing Design	Modified Design	COTS Item	Existing Design	COTS Item	Existing Design	Existing Design
Thrust	14 lbf	14 lbf	5 lbf	5 lbf	5 lbf	5 lbf	5 lbf
Thrust	62 N	62 N	22 N	22 N	22 N	22 N	22 N
Isp [sec]	282	282	293	294	291	300	285
Area Ratio	75	75	150	150	150	150	150
Mixture Ratio (nom)	1.65	1.65	1.65	1.65	1.65	1.6	1.65
Feed Press [psia]	140 - 375	140-375	220	220	220	220	290
Chamber Press [psia]	125	125	116	125	125	125	125
Valve Model	Mg 52-189	EKV ACS	Mg 51-330	Mg 51-136	Mg 51-178	Mg 51-178	Mg 51-178
Thruster Mass [kg]	1.95	1.125	0.54	0.4	0.45	0.47	0.49
Valve Mass [kg]	0.86	0.62	0.14	0.27	0.19	0.19	0.19
Total Mass [kg]	1.09	1.063	0.68	0.67	0.64	0.66	0.68
ROM Cost [M$]	>$1M	>$1M	> $100k	unkn	<$100k	<$200k	unkn
Qual Status	Full	In-Develop	Full	In-Develop	Full	In-Qual	In-Develop
Number Flown	>100	0	>600	0	>1000	0	0
Heritage	Lockheed BUS-1 (DoD)	Evolve from AJ10-220 C103 chamber	MILSTAR GOES ISRO Insat 2B	Evolve from R-6C Thruster	Telecom Intelsat VI	Evolve from C103 5lbf Thruster	Astrium 10N Thruster

3.2 Triple 22N Propulsion System Schematic

The triple thruster propulsion system is identical to the ARES baseline 62N system shown in Figure 2 with the exception of the three thrusters, three sets of flow venturis, and a tubing manifold to route the fuel and oxidizer to the thruster valves of each thruster. A schematic of this system is shown in Figure 13.

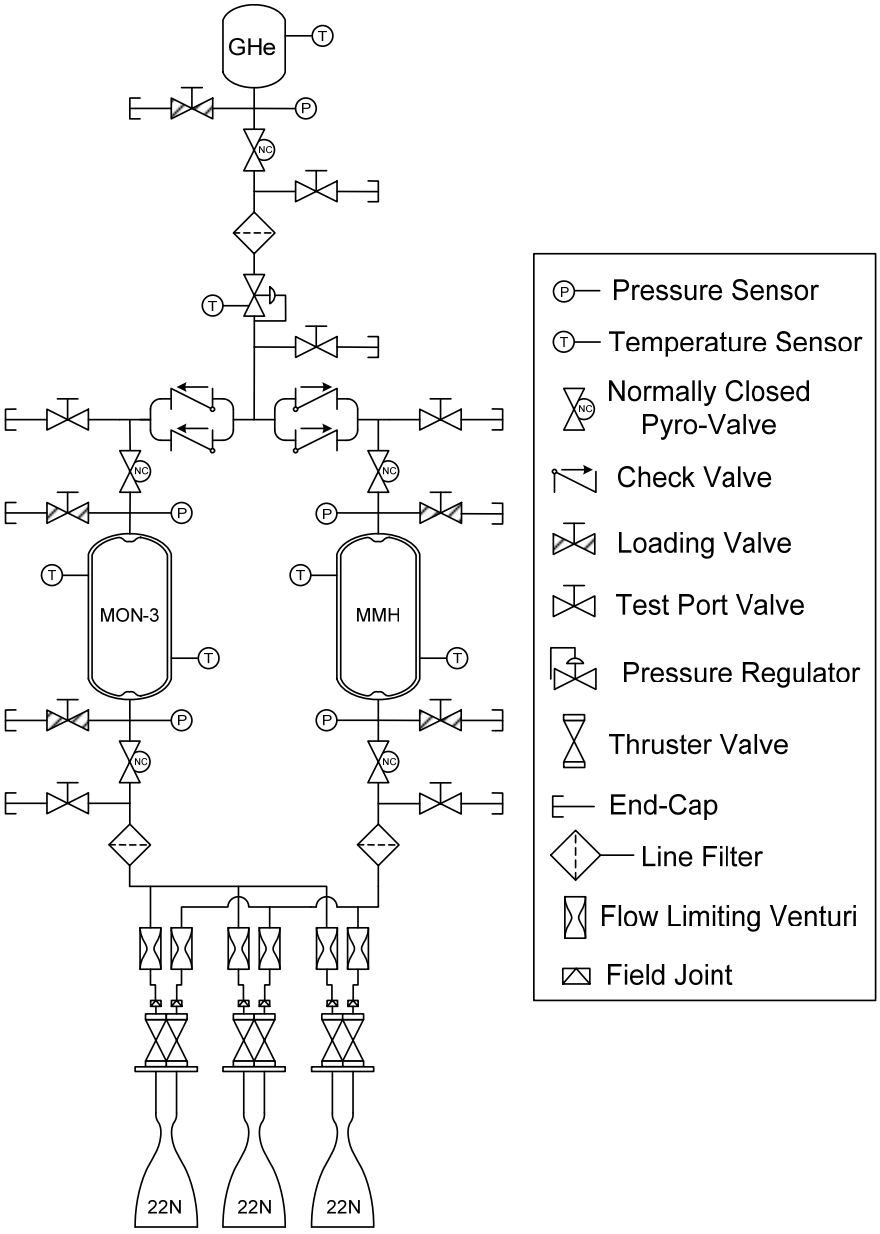

Figure 13. Triple 22N Propulsion System Schematic

3.3 Triple 22N Thruster Selection

AMPAC-In-Space Propulsion (formerly Bell Aerospace and Atlantic Research Corporation) developed a family of 5 lbf bipropellant engines using different valve configurations ranging from dual seat solenoid valves to single seat torque motor valves. These engines have demonstrated extremely long life of 100,000 seconds on multiple units with high vacuum specific impulse ranging from 286-295s[7]. These engines have demonstrated wide flexibility of mission duty cycle operation by firing in any duty cycle ranging from 1-100% and accumulating over 325,000 firing pulses on multiple units with a minimum of 400,000 pulses on one unit. The engine uses a unique single element injector made of a coated columbium alloy orifice plate with titanium alloy feed tubes and support structure. The thrust chamber is made of columbium alloy and coated with R512E silicide coating for protection from the products of combustion internally and externally to allow for high emissivity for radiation cooling. The injector is electron beam welded to the thrust chamber to eliminate the potential of hot gas leakage. The valve is bolted to the injector using metal seals. The RCS thrusters were designed, built, and qualified for the Intelsat VI series spacecraft. A summary of performance characteristics of the 22N thruster is shown in Table 8.

Table 8. ARC 22N Thruster Characteristics[7]

Fuel	MMH
Oxidizer	NTO
Thrust	22N
Specific Impulse	293 s
Area Ratio	150:1
Inlet Pressure Range	6.5 – 27.6 bar
Feed Temperature	70°F Nominal 105°F Max SS Operation 160°F Pulsed Mode SS
Chamber Press (nom)	125 psia
Max Impulse	2,668,800 N-s
Min Impulse Bit	0.045 N-s
Mass	0.8 kg
Engine Length	~270 mm
Nozzle Exit Diameter	54 mm
Total Thruster Mass	0.8 kg

In 1996, AMPAC-ISP started an IR&D program to develop an improved 5 lbf (22N) bi-propellant thruster for satellite station keeping. These thrusters have longer combustion chamber life by using a Pt/Rh alloy combustion chamber with high temperature capability and superior oxidation resistance instead of the Silicide-coated columbium thrust chambers that would not meet steady-state propellant throughput requirements. In 1997, AMPAC-ISP demonstrated the DST-4 Pt/Rh thruster and during the development tests a single Pt/Rh chamber accumulated 33 hrs of test time and over 900 kg of propellant throughput with no damage. The thruster has been tested with both torque motor and solenoid valves and has passed a qualification level vibration test with solenoid valves[8].

Figure 14. AMPAC-Isp 22N Thruster Photos

A diagram of the 22N baseline thruster used in this study is shown in Figure 15. The total length of the thruster, including shown inlet tubing, is approximately 10.75 inches. The valve is shown with the Moog series redundant solenoid valve model Mg 51-178.

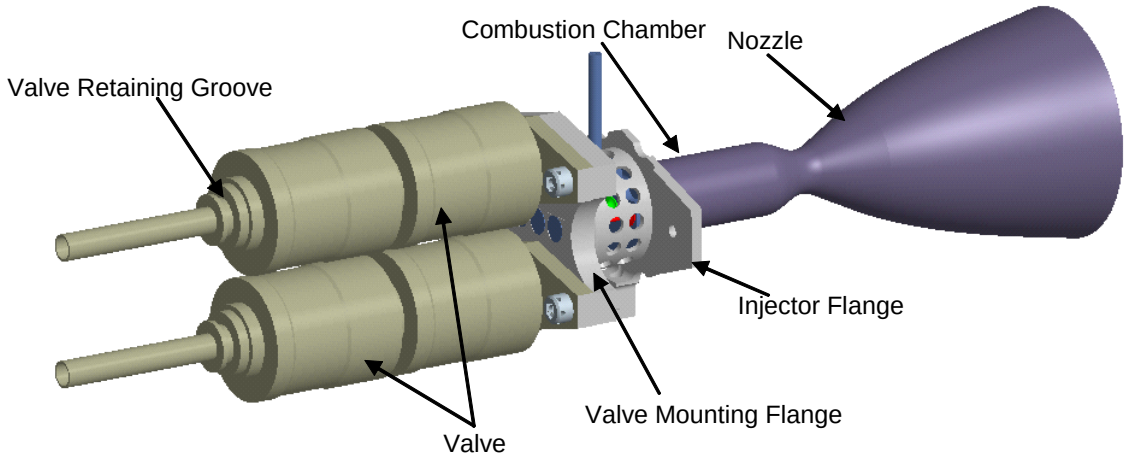

Figure 15. AMPAC-Isp 22N Thruster Details

3.4 Triple 22N Thruster Mounting and Support System

Two options for mounting the three thrusters on the airplane body were considered. The first is an "in-line" configuration where the outer two thrusters would be the primary driver and the center thruster used in instances where acceleration and climbing are needed. The second configuration consists of a triangular arrangement where the top two thrusters are primary and the bottom thruster is secondary.

Each thruster configuration requires that the thrust vector for each individual thruster, regardless of arrangement, passes through the specified flight vehicle's center of gravity (c.g.). The location of the vehicle's c.g. is centered between the flight vehicle's fuel tanks (Figure 1). The ARES center-body location for each thruster assembly was determined from the base-lined ARES airframe configuration[1].

Launch load cases 1a and 1b (Appendix B) were determined to be the critical load cases applied to the 22 N thruster due to the large "g" loads seen during launch. The mass of a single 22 N thruster is equal to 0.8 kg. Based on Figure 77, the MAC value for the thruster is 60. Therefore the "g" force applied to the thruster for load case 1a in the axial direction would be 62.8 and for load case 1b would be 60 in any direction. Based on F = ma the force on each 22 N thruster for the axial direction of load case 1a would be 111 lbf and for load case 1b 106 lbf.

3.4.1 Triple 22N In-Line Thruster Mounting Configuration

The triple thruster in-line configuration is an arrangement of three 22 N thrusters in a single row shown in Figure 16. Right hand and left hand thrusters were rotated about c.g. location 4.5° to allow for adequate clearance. The thrusters are tilted 5.88° from the horizontal reference to direct thrust vector through the airplane c.g., shown in Figure 17.

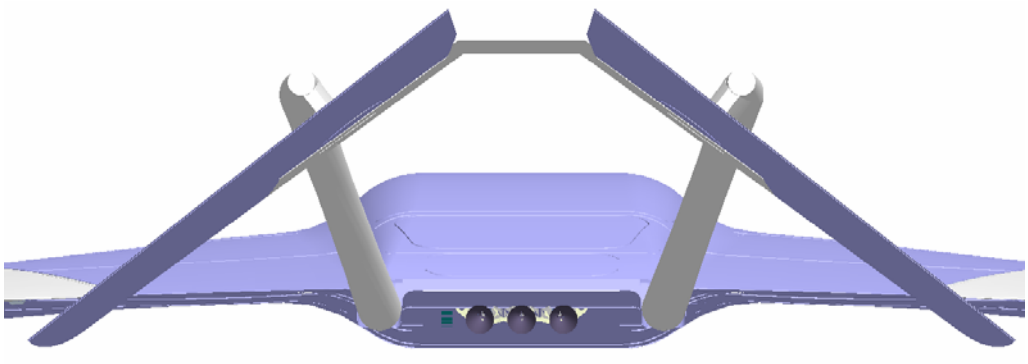

Figure 16. Triple 22 N Thruster In-Line Configuration on Airplane

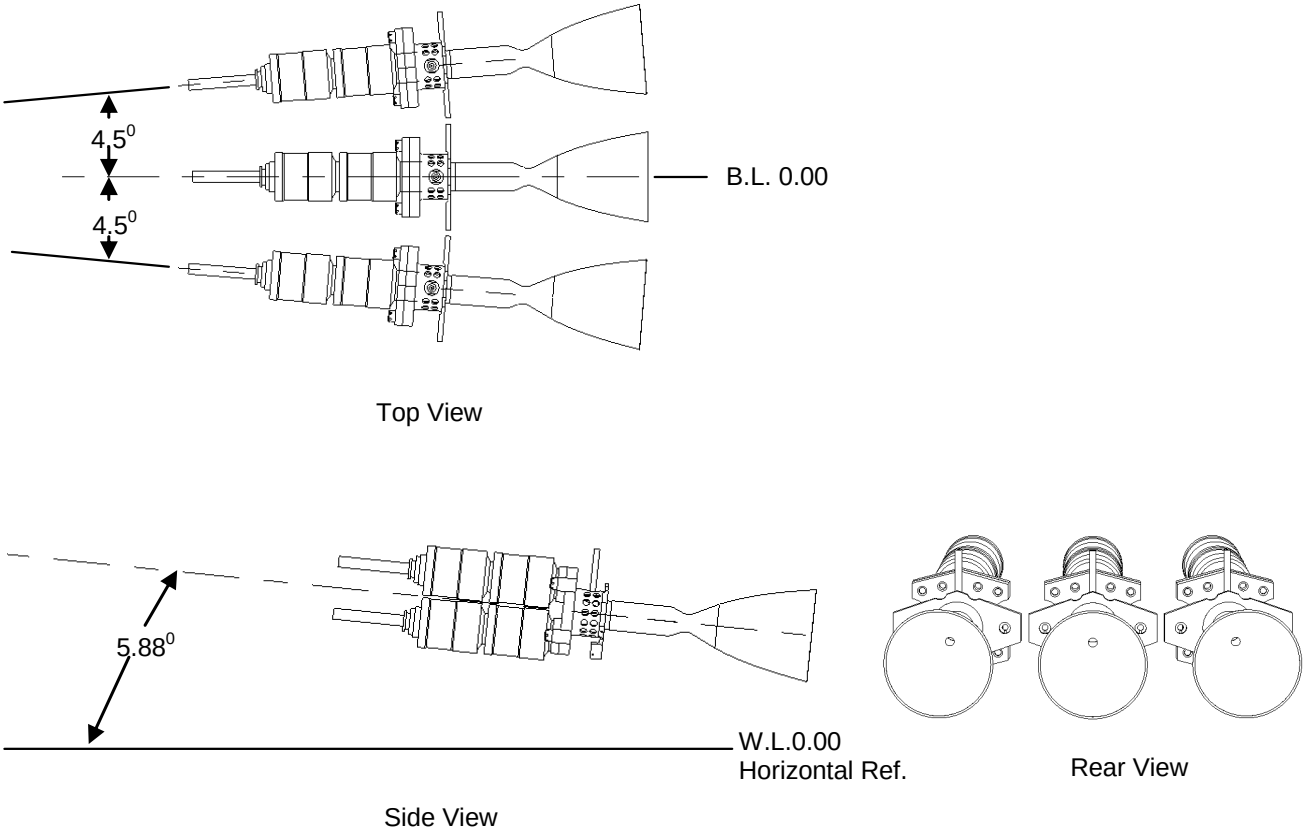

Figure 17. Triple 22N In-Line Thruster Orientation

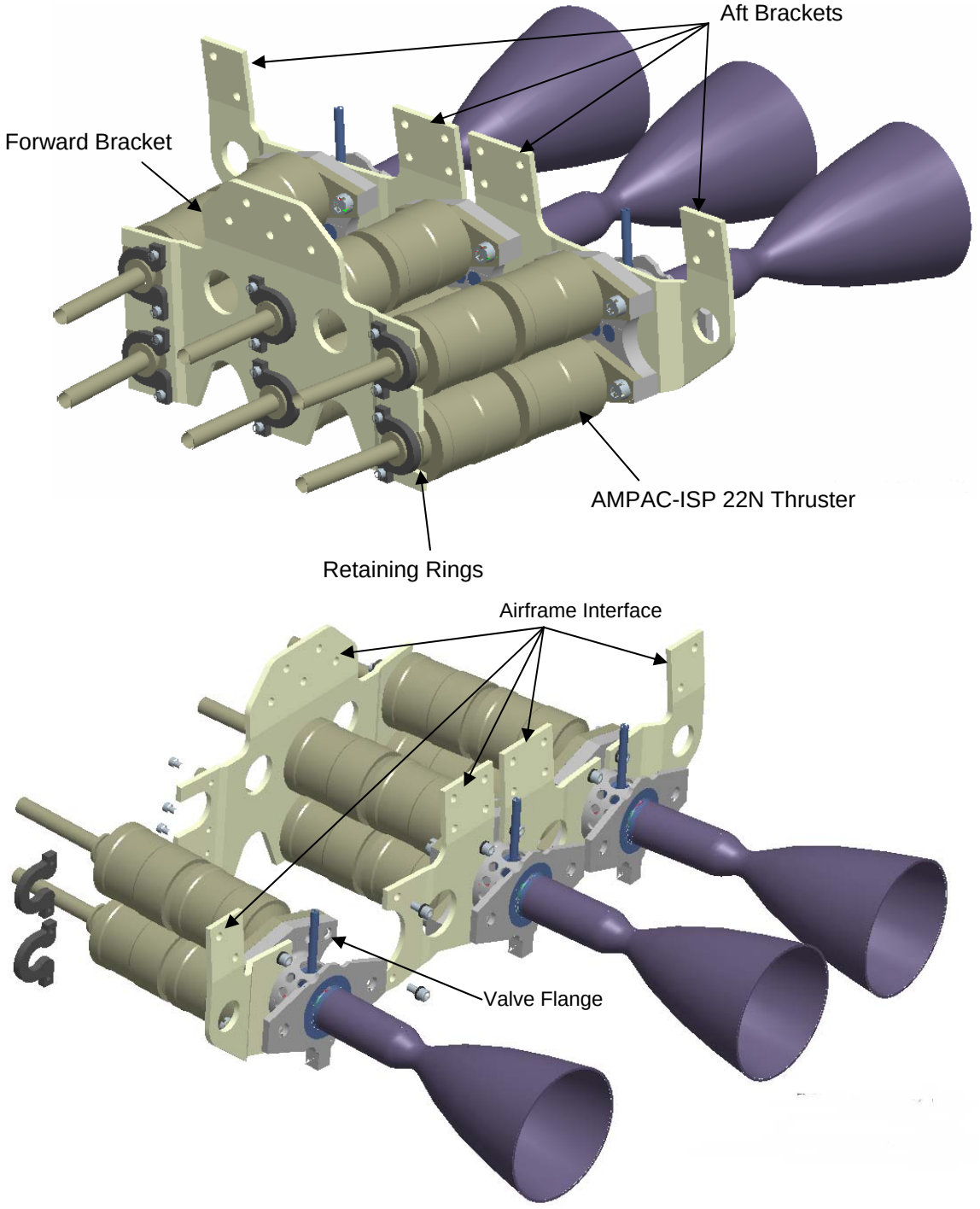

Figure 18. Triple 22N In-Line Thruster Mounting and Assembly

The aft and forward brackets are titanium alloy. Titanium alloy was selected because of its good strength-to-weight ratio, low density, and low coefficient of thermal expansion, good corrosion resistance, good toughness, and its performance at extreme temperatures (-320°F to 750°F). The brackets are fabricated to place thrusters in correct orientation. The aft brackets are bolted to the valve flange using existing mounting holes (see Figure 18). The thruster valve flange was chosen for bracket interface, because it reaches a maximum temperature of only 200°F at steady-state operation. The thrusters are also supported at the forward bracket and captured by titanium retaining rings. Once the retaining rings are

placed into existing groove in valves, they are fastened to the forward bracket. The forward and aft brackets are bolted to the composite airframe structure shown in Figure 19. The design approach was to enable the ability to readily assemble and disassemble the thrusters from the airframe and allow for repeatable location of thrusters.

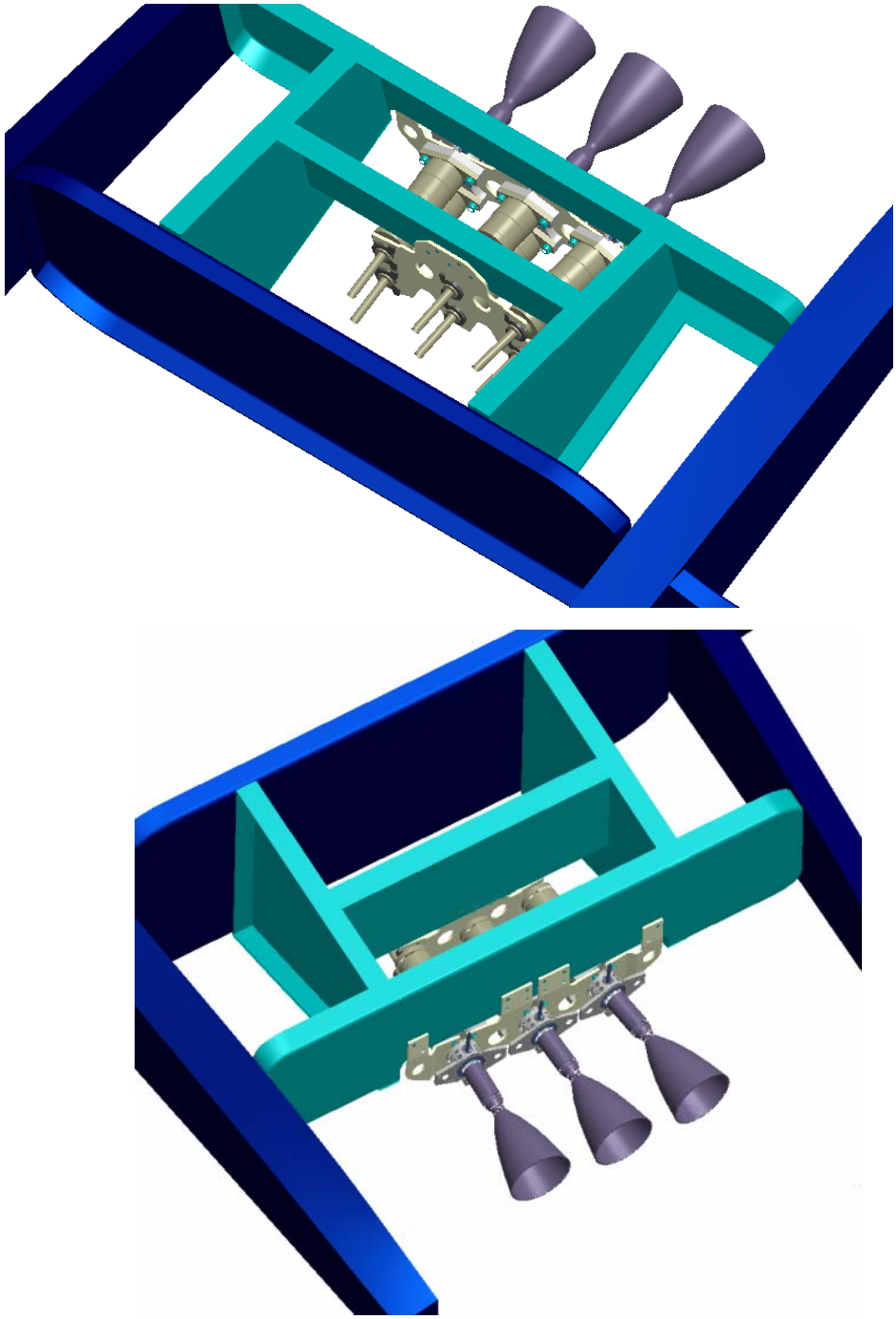

Figure 19. Triple 22N In-Line Thruster Assembly and Airframe Mounting Interface

The triple 22N thruster in-line configuration was analyzed with Pro-Engineer Mechanica Finite Element Analysis (FEA). Load case 1a and 1b from Appendix B, were determined to be the critical load cases the thruster assembly would sustain, therefore it was applied to FEA model. After multiple design iterations, a final preliminary design was developed based on required factors of safety of 1.5 for ultimate strength and 1.25 for yield strength, see Appendix B. Preliminary mass estimates are shown in Table 9.

Table 9. Triple 22N In-Line Mounting Component Mass Breakdown

Component	Material	Density (lbf/in^3)	Weight (lbf)	Mass (kg)
RH Center Thruster Aft Bracket	Titanium Alloy	0.16	0.060	0.027
LH Center Thruster Aft Bracket	Titanium Alloy	0.16	0.060	0.027
RH Outboard Thruster Aft Bracket	Titanium Alloy	0.16	0.048	0.022
LH Outboard Thruster Aft Bracket	Titanium Alloy	0.16	0.048	0.022
Valve Retaining Rings (6 Total)	Titanium Alloy	0.16	0.046	0.021
Valve Support Bracket	Titanium Alloy	0.16	0.170	0.077
Mounting Hardware	CRES	0.29	0.150	0.068
Total			**0.582**	**0.264**

3.4.2 Triple 22N Triangular Thruster Mounting Configuration

The second thruster configuration is an arrangement of three 22N thrusters in a triangular orientation (Figure 20). Right hand, left hand, and bottom thrusters were rotated about c.g. location until adequate clearance was achieved. Details of the rotation and orientation of the thrusters are shown in Figure 21.

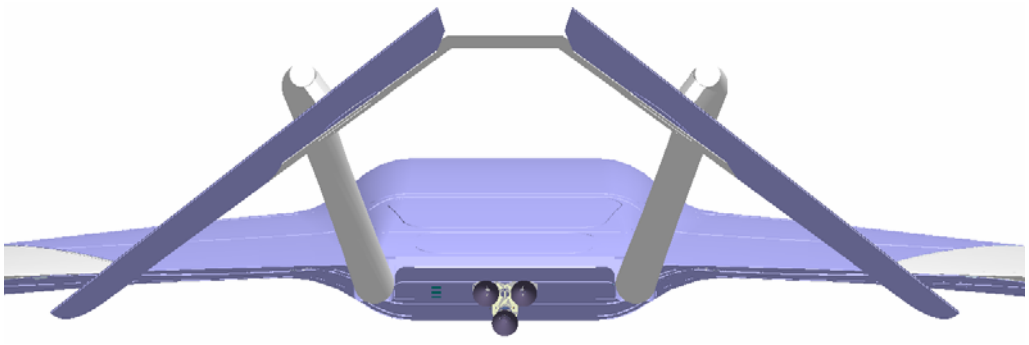

Figure 20. Triple 22N Thruster Triangular Configuration on Airplane

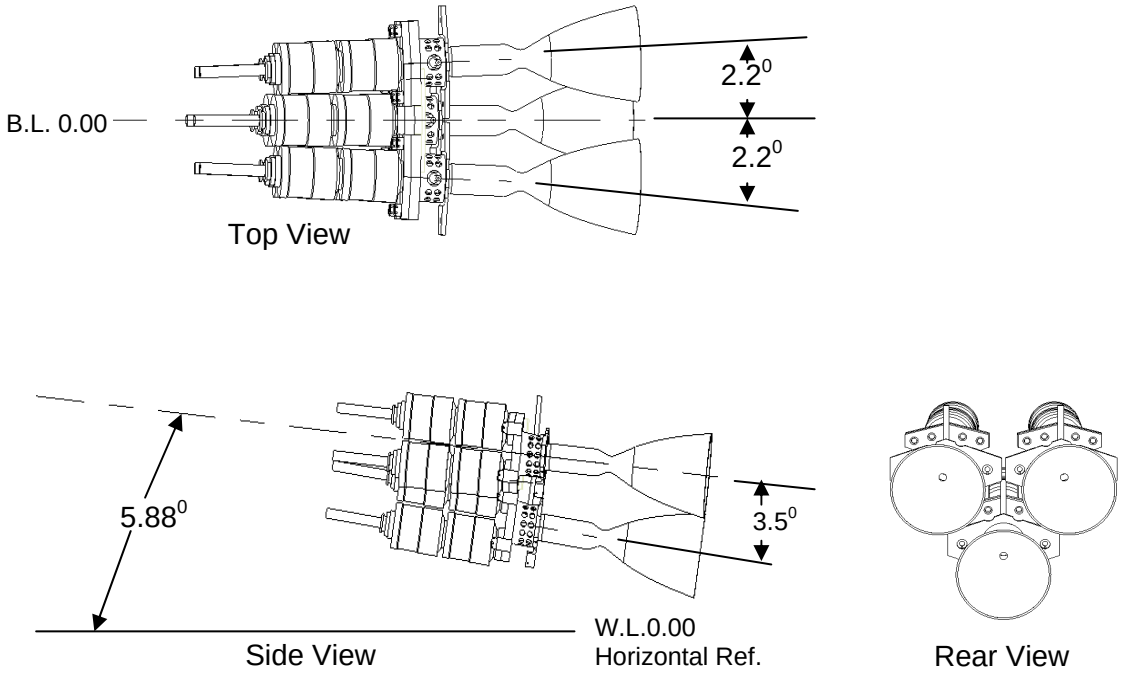

Figure 21. Triple 22N Triangular Thruster Orientation

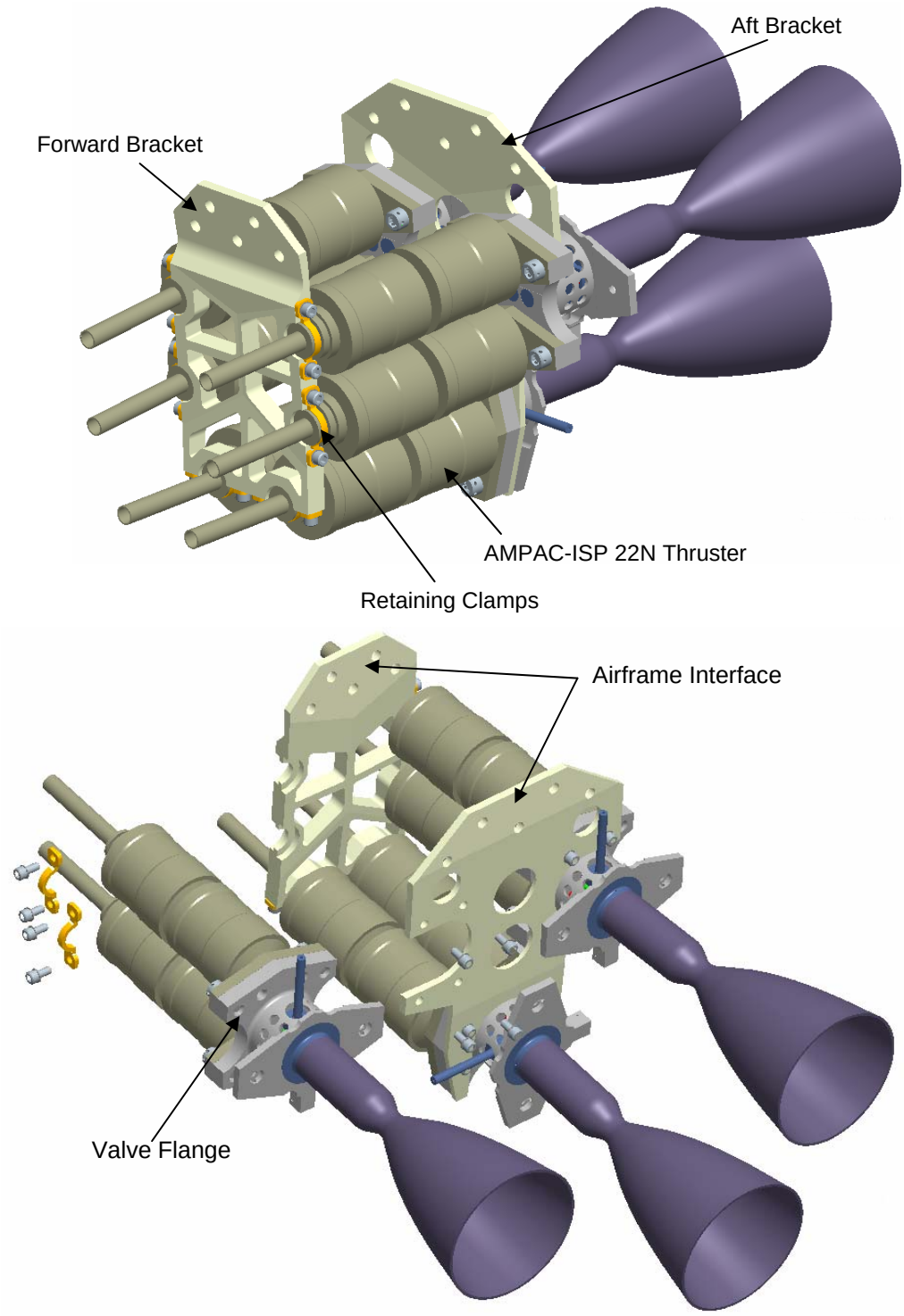

Figure 22. Triple 22N Triangular Thruster Mounting and Assembly

The aft and forward brackets are titanium alloy. The brackets are fabricated to place each thruster in correct orientation. The aft bracket is bolted to the valve flange using existing mounting holes (see Figure 22). The thruster valve flange was chosen for bracket interface, because it reaches a maximum temperature of only 160°F at steady-state operation (Figure 9). The thrusters are also supported at the forward bracket and captured by titanium retaining clamps. Once retaining clamps are placed into existing groove in valves, the retaining clamps are fastened to forward bracket. Note: the forward thruster bracket for the triangular configuration incorporates an alternative approach for mechanically fastening

the thruster valves, than the row configuration forward bracket. Either method could be developed for each thruster configuration. The forward and aft brackets are bolted to composite airframe structure, shown in Figure 23.

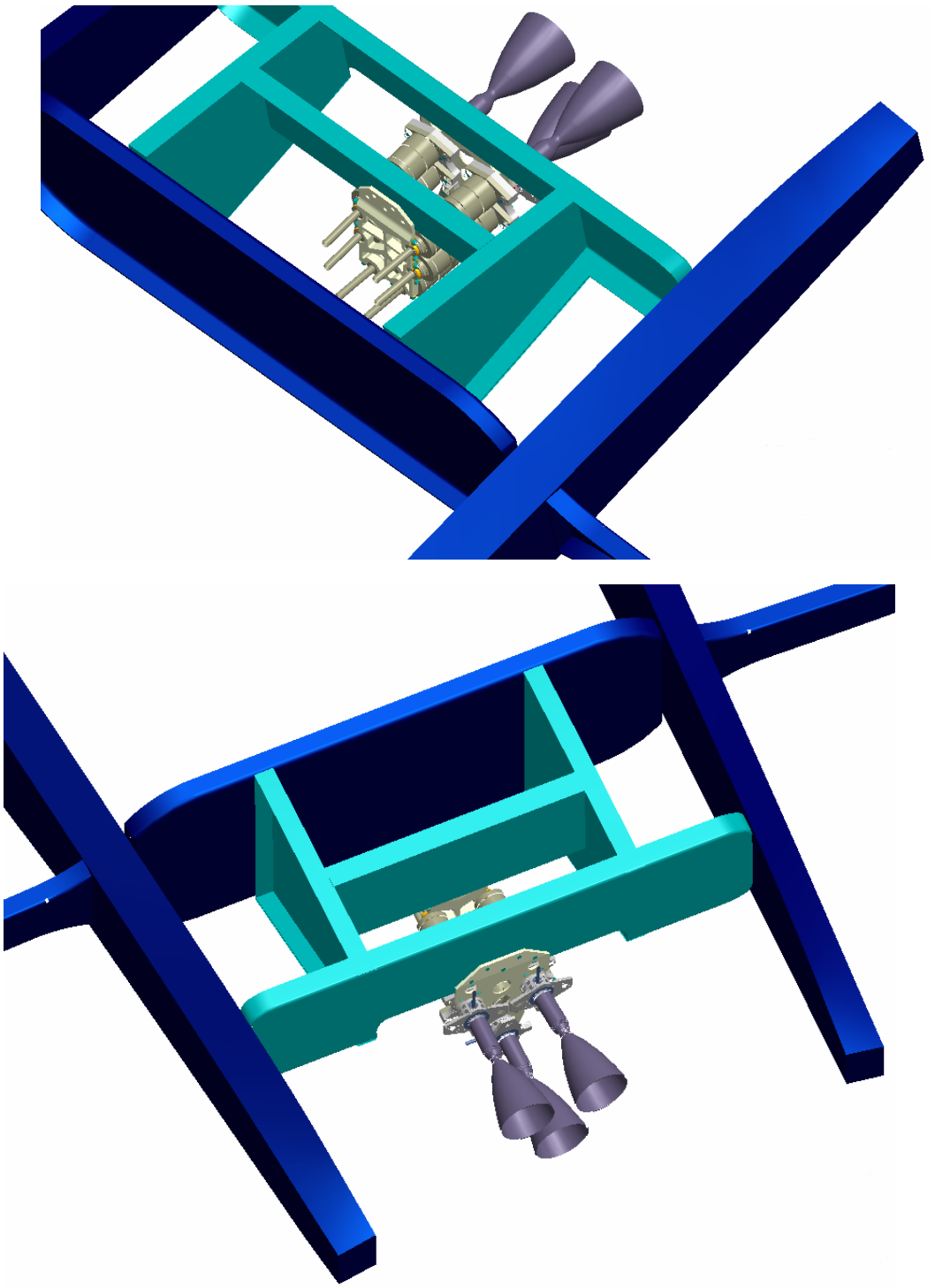

Figure 23. Triple 22N Triangular Thruster Assembly and Airframe Mounting Interface

A structural analysis was performed on the triple 22N triangular thruster assembly with Pro-Engineer Mechanica Finite Element Analysis (FEA). Load case 1a and 1b, Appendix B, were determined to be the critical load cases the thruster assembly would sustain, therefore it was applied to the FEA model. After multiple design iterations, a final preliminary design was developed based on required design factors of safety of 1.5 for ultimate strength and 1.25 for yield strength. Preliminary mass estimates are shown in Table 10.

Table 10. Triple 22N Triangular Mounting Component Mass Breakdown

Component	Material	Density (lbf/in^3)	Weight (lbf)	Mass (kg)
Aft Thruster Bracket	Titanium Alloy	0.16	0.154	0.070
Forward Support Bracket	Titanium Alloy	0.16	0.178	0.081
Valve Clamp (6 Total)	Titanium Alloy	0.16	0.010	0.005
Mounting Hardware	CRES	0.29	0.130	0.059
Total			**0.472**	**0.214**

3.5 Thermal Analysis of Triple 22N Thruster System

3.5.1 22N Thruster Thermal Characteristics

During operation, the thrusters reach temperatures significantly greater than the Mars ambient temperature of approximately -60°C. For continuous firing at room temperature, the combustion chambers of the thrusters reach approximately 1000°C in 45 seconds. This creates a temperature difference between the thrusters and outer fuselage of almost 1100°C, which will cause a large radiative heat transfer between the two components.

The fuselage of the aircraft is a composite structure designed by Aurora Flight Sciences Corporation[9] consisting of an aluminum honeycomb core surrounded by face sheets of carbon fabric. The adhesive holding the carbon face sheets to the aluminum honeycomb will begin to break down at approximately 250°C. The goals of the thermal analysis of these thrusters in simulated operation are:

- To determine if there is any thermal benefit of using one configuration over the other
- To determine if the fuselage will remain under 250°C, and
- Suggest ways to lower the fuselage temperature if it is found to reach temperatures greater than 250°C.

During development of this thruster, Aerojet performed a test firing of a single thruster in order to determine the temperatures at different locations on the thruster[10]. Seven thermocouples were mounted to the thruster as shown in Figure 24. A temperature vs. time profile for each thermocouple was provided for 120 seconds of continuous firing in a vacuum at room temperature. The thruster appeared to reach thermal equilibrium after approximately 45 seconds.

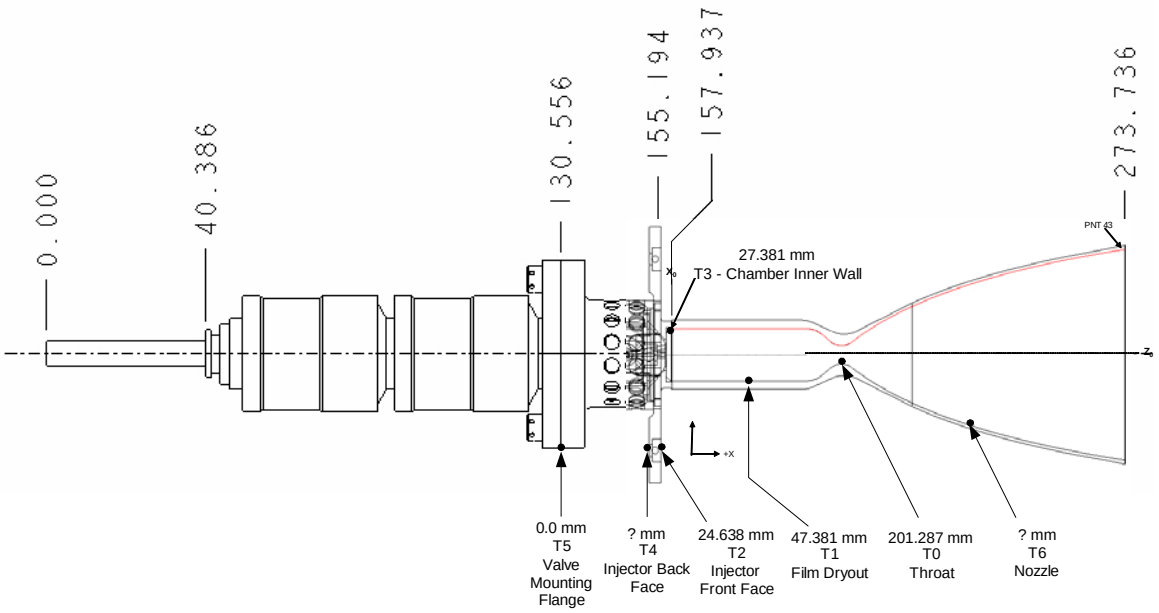

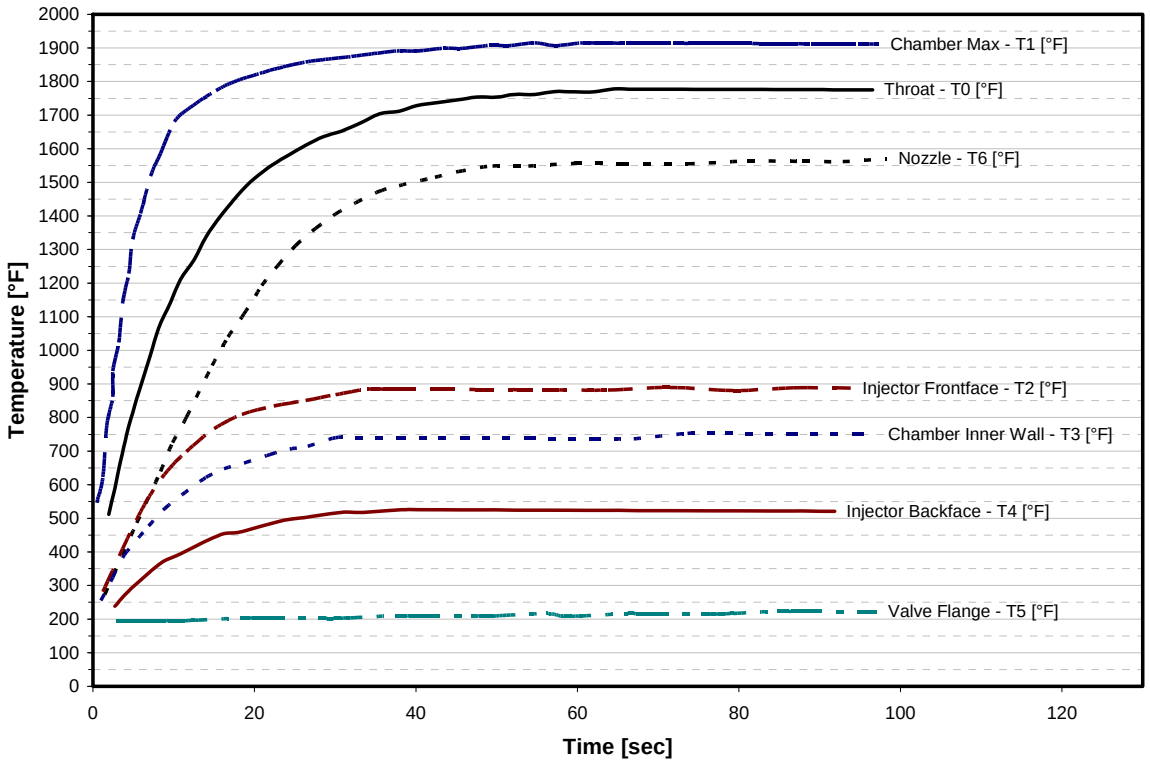

Figure 24. Thermocouple locations during test firing, and corresponding data[10].

During flight, two thrusters will be continuously firing. These two thruster will reach an equilibrium temperature profile similar to the one provided by the test firing, however it will be slightly cooler due to the much lower ambient temperature on Mars and forced convection from the thrusters to the atmosphere. The third thruster will be turned on and off as needed during flight.

3.5.2 Modeling and Assumptions

Each of the two configurations described in the previous sections consist of three AMPAC-Isp 22N thrusters mounted to the airframe through the additional support structure shown again in Figure 25. The thrusters are connected to each other and to the inner spar structure of the aircraft by two titanium mounting brackets. These brackets are bolted to two separate bulkheads inside the vehicle. There is a rectangular cut out in the lower fuselage that allows the thrusters to protrude out of the aircraft; this can partially be seen in the right side of Figure 25. The nozzles are directly under a small section of the lower fuselage, and the combustion chambers are partially under this section, and partially under the cut out. Consequently, this allows for radiation transfer to the inner components of the aircraft as well as the lower fuselage. The locations of internal electronics, instruments and fuel tanks have not yet been decided and are not yet included in the design model.

A PRO-Engineer CAD model containing the ARES fuselage, inner support structure, and each thruster configuration described in this report was used for the thermal analysis. Locations for the instruments and other internal components had not yet been defined. An MSC.Patran.Thermal model of the aircraft had been built for a previous ARES thermal study[1] for the Step-2 proposal activity and this model was used as a starting point for a new MSC.Patran.Thermal model for the thruster investigation.

The fuselage of the aircraft had not changed since the previous study; however a cutout needed to be placed in the lower fuselage to accommodate the thrusters. The cutout was positioned to match the location of the cutout in the CAD model. The rest of the components in the model had to be removed; the inner support structure had changed, and the locations of the instruments and other internal components need to be redefined.

The fuselage and old support structure had been modeled as three separate surface layers in order to simulate the full composite structure; an inner carbon face sheet, an aluminum honeycomb core, and an outer carbon face sheet. From the CAD geometry, a new MSC.Patran support structure was created in this same fashion, with one layer for each part of the composite. According to the Aurora assembly drawings[9], the outer and inner faces of the carbon sheets were connected through the caps of the c-channel. The c-channels were therefore not directly modeled, and a box was created for the carbon layers with a surface inside for the honeycomb.

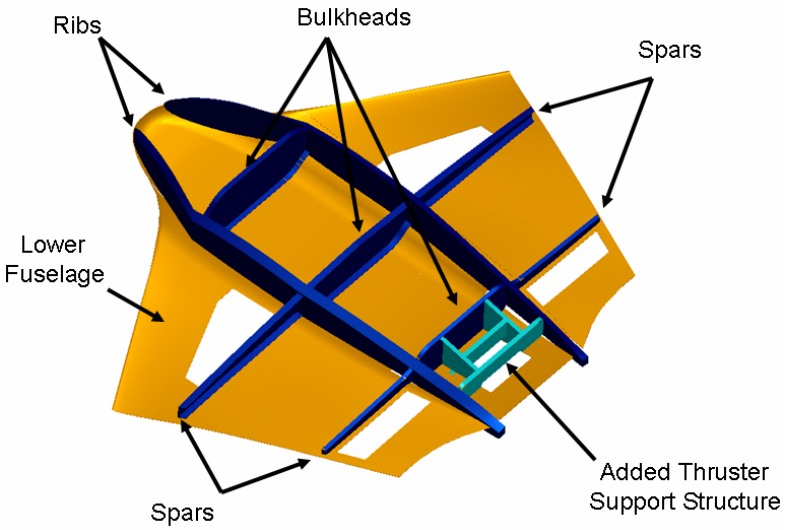

Figure 25. Airframe Structural Characteristics

An MSC.Patran version of each thruster configuration was created next, and imported into the model. Components of the thrusters were created as solids where possible, and the rest were approximated with surfaces. All fuel/oxidizer pipe lines and other internal components were removed. The thrusters were placed in the model at approximately the same vertical distance from the bottom of the fuselage as in the CAD geometry.

Surfaces were created to model two 0.5 mm aluminum heat shields for three analysis cases. They are designed to cover the portion of the fuselage directly above the thrusters. A larger heat shield was required for analyses including the thruster exhaust plumes. Figure 26 shows both heat shield configurations.

Thicknesses of shell components in the model were taken directly from the CAD model. Those that could not be obtained from the model were taken from Aurora assembly schematics of the composite structure[9]. Values from this source, such as carbon fabric thickness, are approximate; they were determined by multiplying the number of fabric sheets used in each face of the structure by 0.127 mm (thickness of each sheet). Table 18, Appendix C gives the thicknesses used in this investigation. Material properties for the carbon face sheets and honeycomb core were taken from the previous study. Component materials and material property sources are presented in Table 19, Appendix C.

3.5.3 Thermal Loads and Boundary Conditions

All three thrusters are given the same steady state temperature profile derived from Figure 24. This is a conservative assumption since one thruster will be pulsing on and off which should reduce the maximum temperature that it reaches. Convection and radiation inside the aircraft was ignored for this study (except in the rear-most inner compartment, which was included in the radiation view factor analysis). Convection would help to reduce and spread out the temperature on the hotter components, therefore neglecting it is a conservative assumption. Convection on the thrusters is also ignored. A turbulent forced convection model would need to be derived in order to model it accurately. Convection would help to reduce the steady state temperature reached by the thrusters, so neglecting it is a conservative assumption. However, the thrusters may heat the air passing over them enough to cause a convection heat load into the lower fuselage. This has also been ignored, and may need to be considered in a future study. Radiation from the thruster exhaust plumes is ignored for the primary trials. An analysis with estimated plume properties is done for the triangular thruster arrangement. When the CFD plume analysis is completed, and the geometry and temperature profile has been defined, an updated thermal analysis should be done including this information. The exhaust plumes will be hot, and will

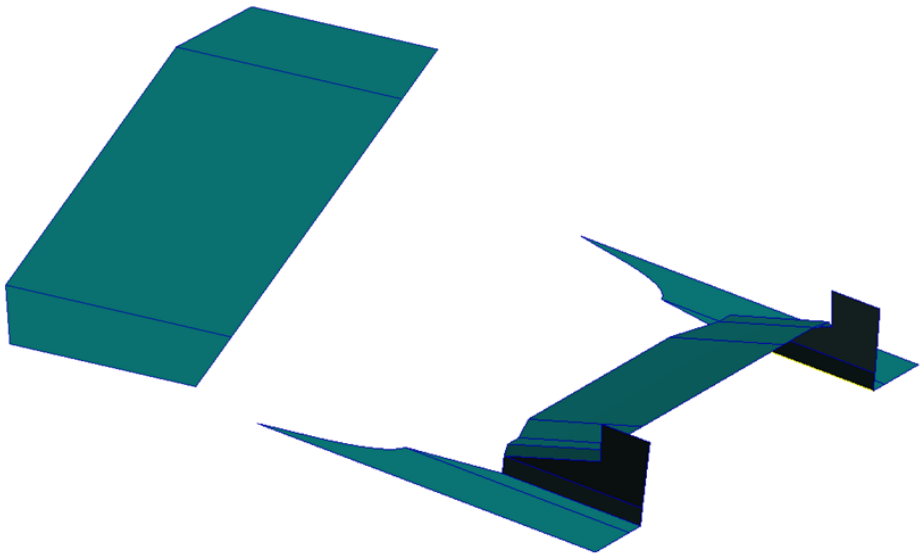

Figure 26. Heat Shield Options for Airplane Thermal Protection.
Small heat shield (upper left) and large heat shield (lower right).

contribute to the radiation transfer to the underside of the fuselage, and also to the tail. Table 20 and Table 21, Appendix C show the loads and boundary conditions applied to the model. Most of these conditions are always used in the analysis; however some trials will not contain a low emissivity paint or heat shield. Which ones are turned off for various runs are described in the next section.

3.5.4 Thermal Analysis Results

Three steady state analyses were done for each thruster configuration using the boundary conditions and loads given in Table 20 and Table 21, Appendix C respectively. The "View factor radiation calculations" in Table 21 are the only loads that are modified for each case, which are described below:

- **Baseline** – no paints or heat shield on the lower fuselage, bare carbon face sheets
- **Low Emissivity Paint** – A paint with an emissivity of 0.3 is applied to the fuselage directly above the thrusters and to the inner face sheet of the upper fuselage. A number of aluminum, and leafing aluminum paints can provide this emissivity, or lower. Chromeric Silver paint 586 can also provide this emissivity.
- **Heat Shield** – A 0.5 mm thick polished aluminum sheet is placed on the lower fuselage. The inner face sheet of the upper fuselage is coated with low emissivity paint.

Results for these trials are documented in Sections 3.5.4.1 and 3.5.4.2, and do not include radiation from the exhaust plumes. Section 3.5.4.3 provides results for the triangular configuration with the estimated exhaust plume properties given in Table 21. Analyses were completed for each of the three cases described above, however the painted area and heat shield area needed to be enlarged to protect more of the fuselage surface.

3.5.4.1 In-Line Thruster Configuration Results

Figure 27 shows the temperature profile across the thrusters. This profile is described in Table 20, Appendix C, and is used for each in-line configuration case.

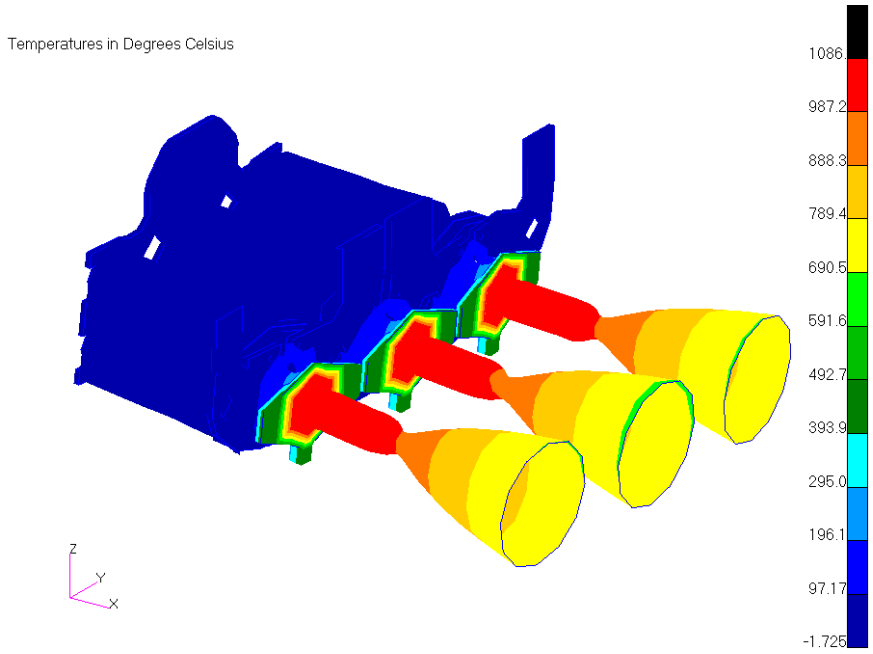

Figure 27. In-line thruster configuration temperature profile

3.5.4.1.1 Baseline Study Results

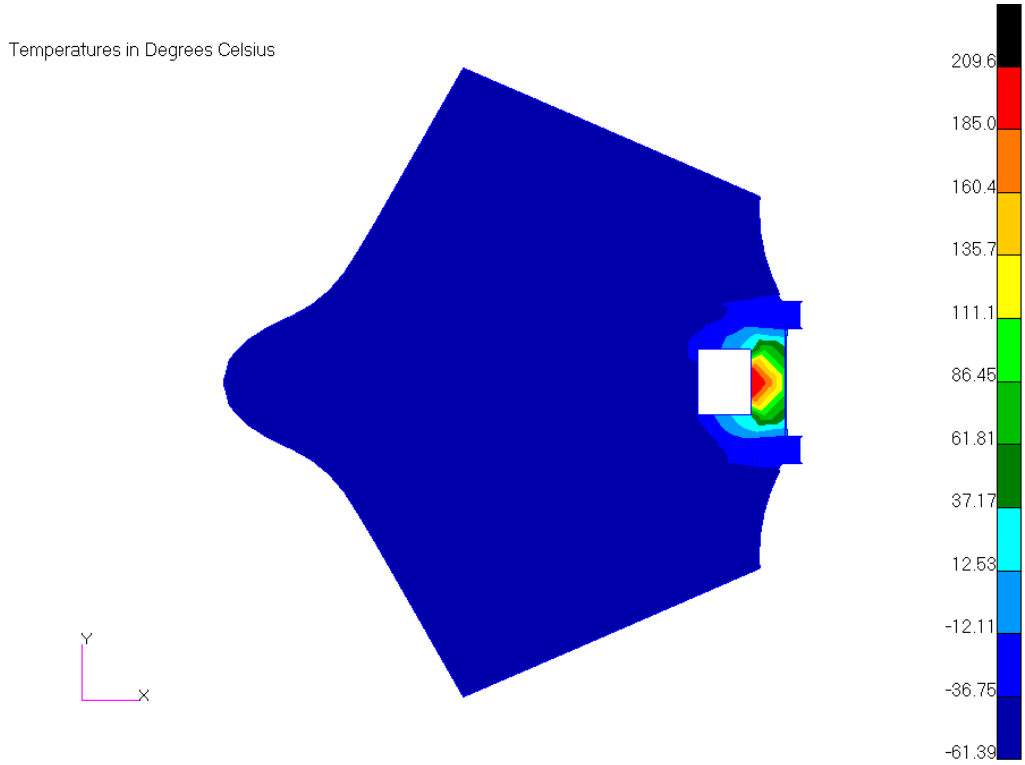

Figure 28. Temperature profile, lower fuselage, in-line configuration baseline study.
(Max Temperature = 209.6°C).

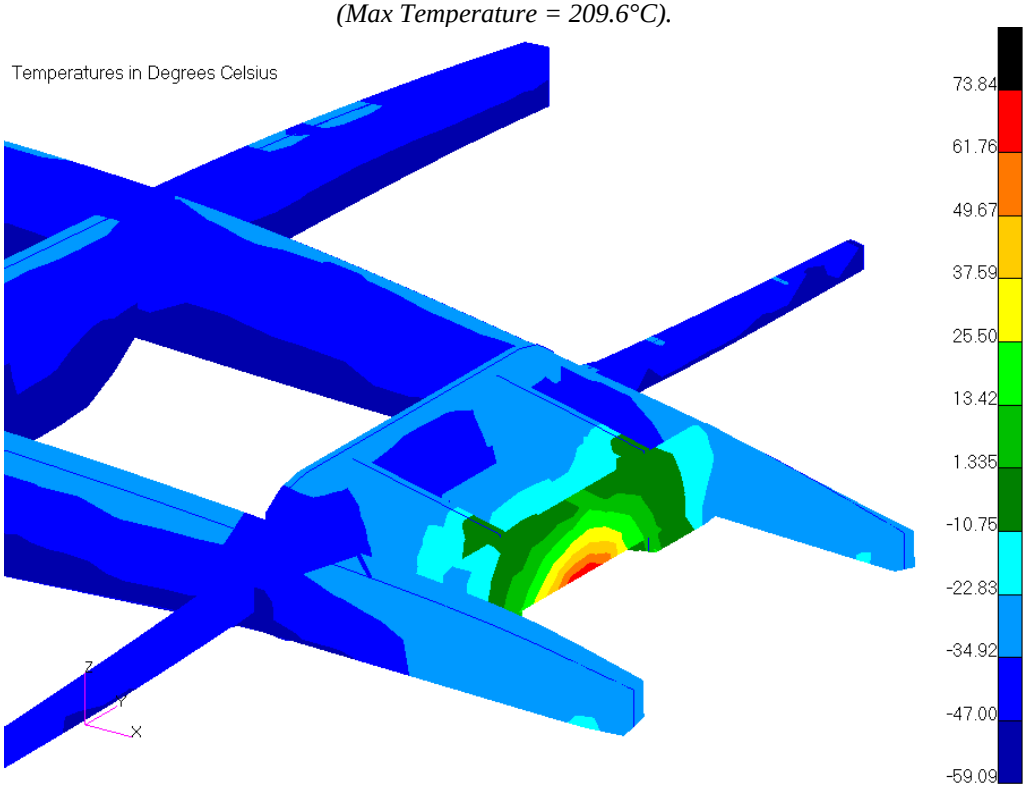

Figure 29. Temperature profile, support structure, in-line configuration baseline study.
(Max Temperature = 73.8°C).

3.5.4.1.2 Low Emissivity Paint Study Results

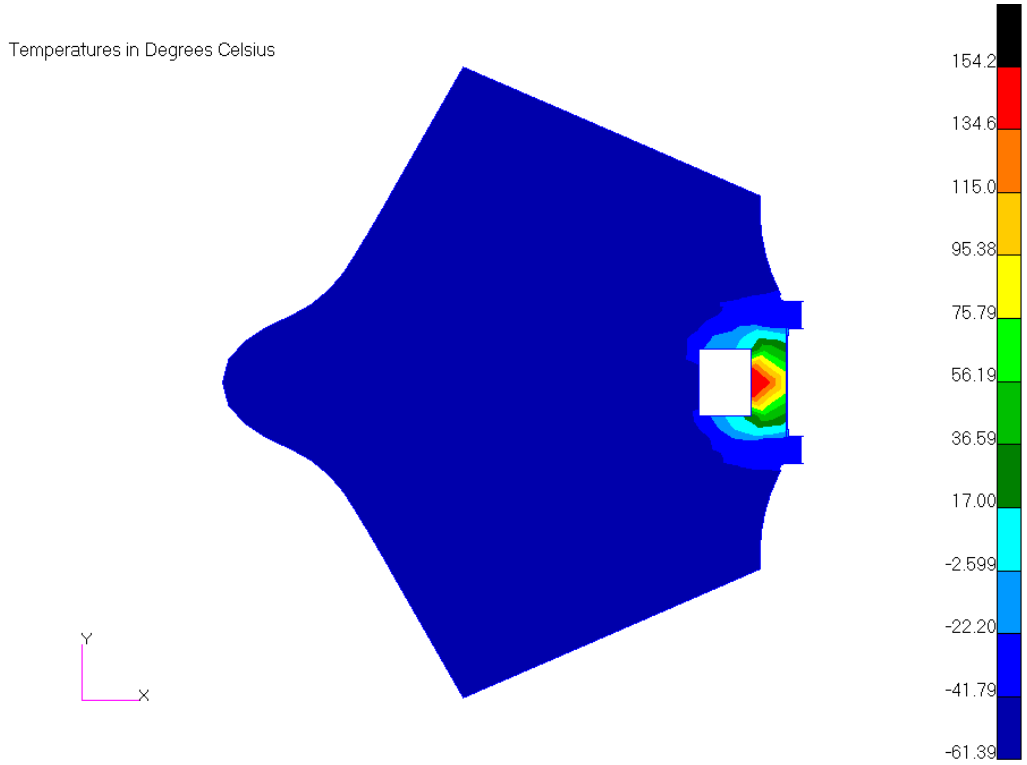

Figure 30. Temperature profile, lower fuselage, in-line configuration, low ε paint.
(Max Temperature = 154.2°C).

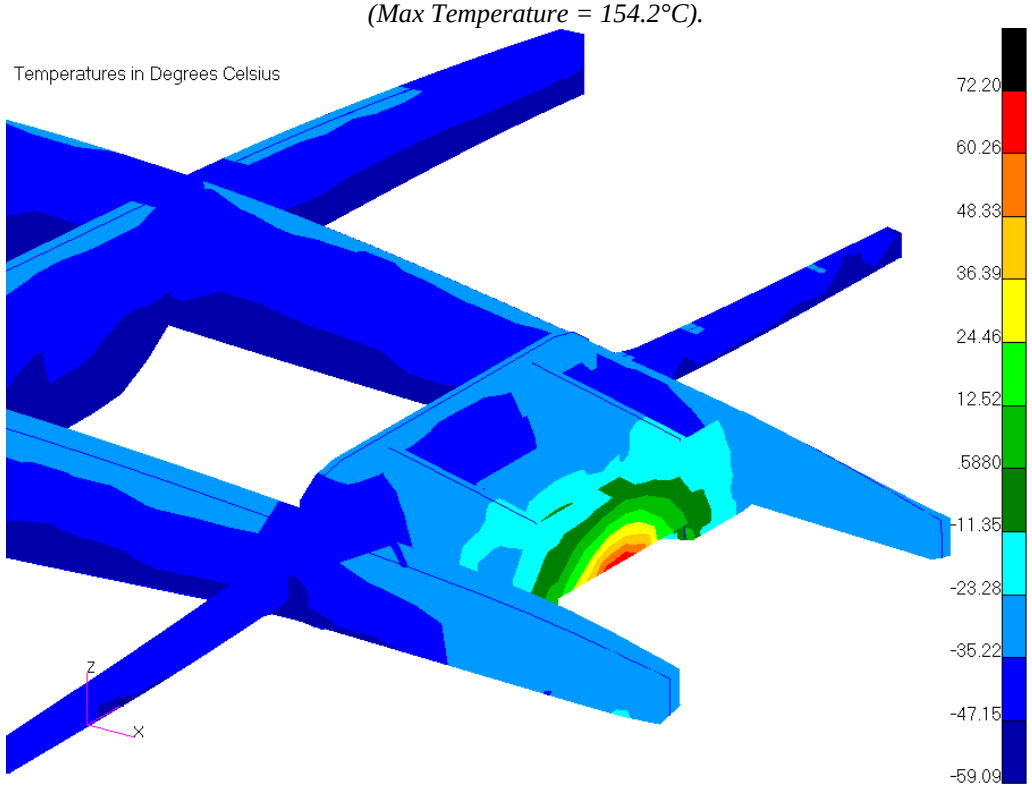

Figure 31. Temperature profile, lower fuselage, in-line configuration, low ε paint.
(Max Temperature = 72.2°C).

3.5.4.1.3 Heat Shield Study Results

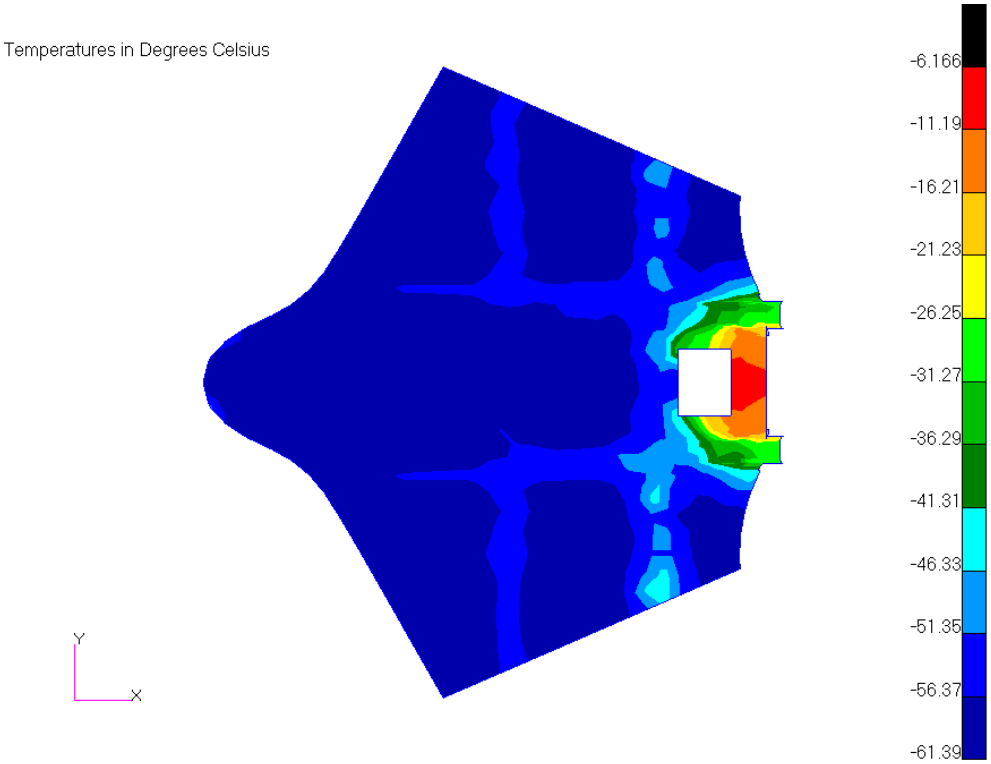

Figure 32. Temperature profile, lower fuselage, in-line configuration with heat shield. *(Max T = -6.17°C).*

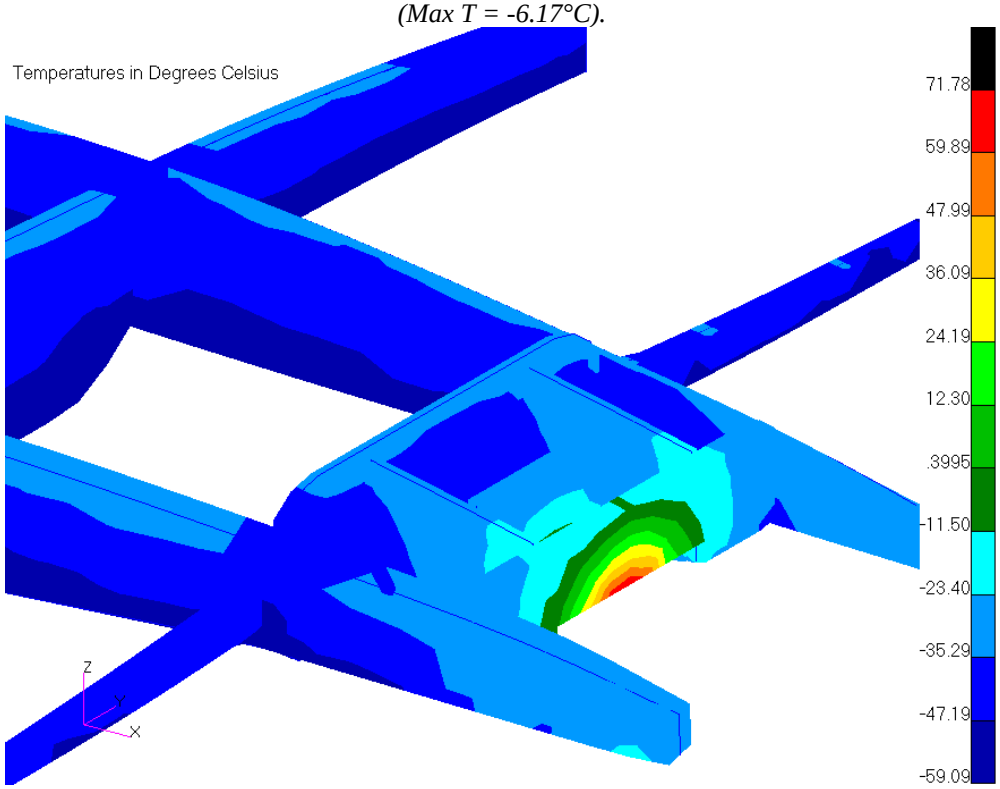

Figure 33. Temperature profile, lower fuselage, in-line configuration with heat shield. *(Max T = 71.8°C).*

3.5.4.2 Triangular Thruster Configuration Results

Figure 34 shows the temperature profile across the thrusters. This profile is described in Table 20, Appendix C, and is used for each triangular configuration case.

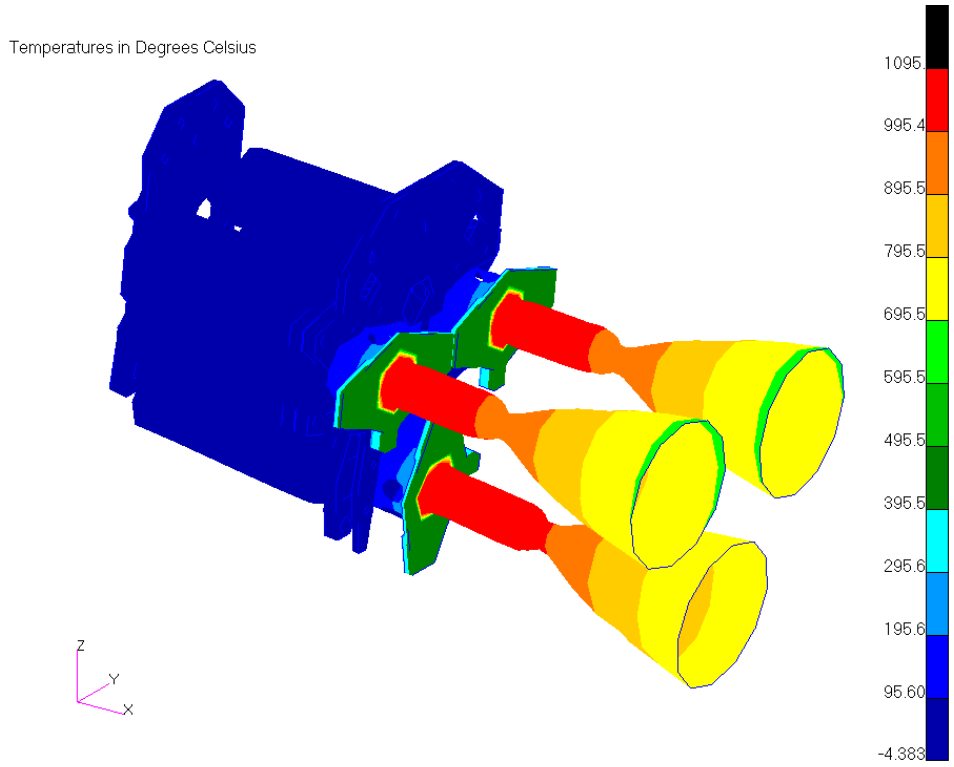

Figure 34. Triangular thruster configuration temperature profile

3.5.4.2.1 Baseline Study Results

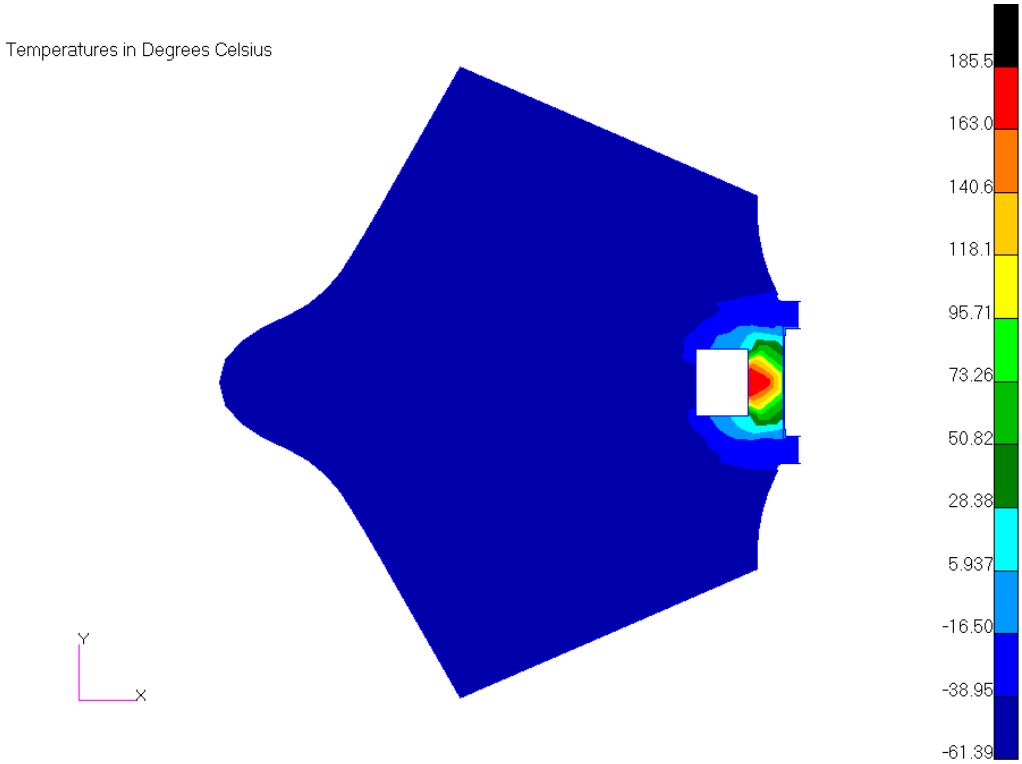

Figure 35. Temperature profile, lower fuselage, triangular configuration baseline study.
(Max Temperature = 185°C).

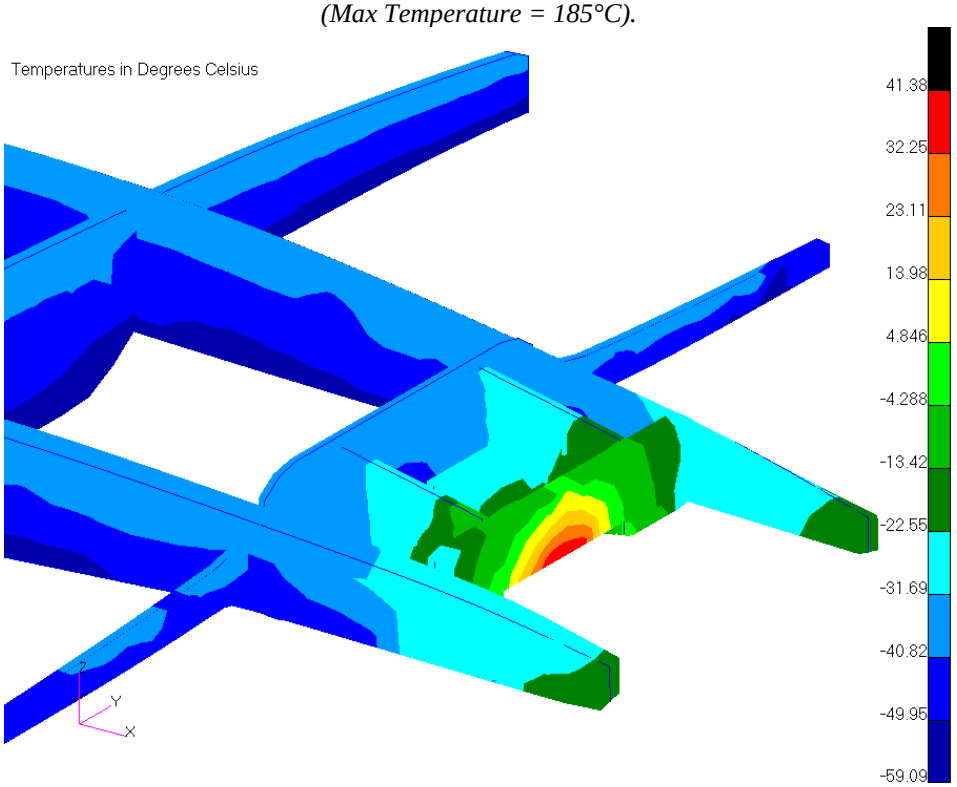

Figure 36. Temperature profile, support structure, triangular configuration baseline study.
(Max Temperature = 41.4°C).

3.5.4.2.2 Low Emissivity Paint Study Results

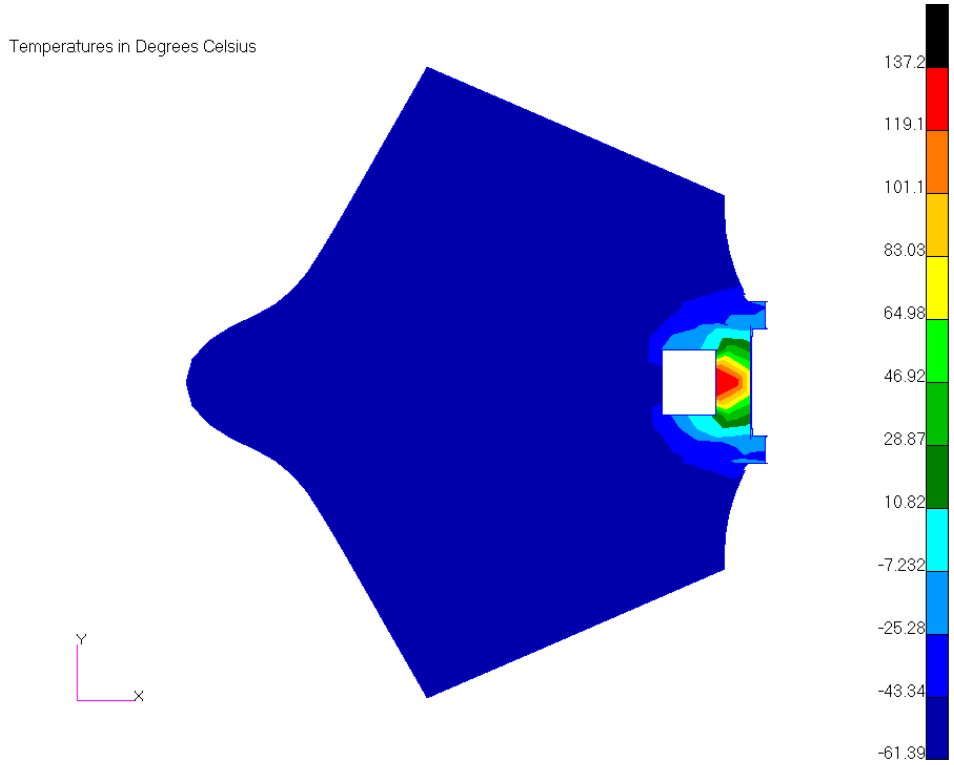

Figure 37. Temperature profile, lower fuselage, triangular configuration and low ε paint.
(Max Temperature = 137.2°C).

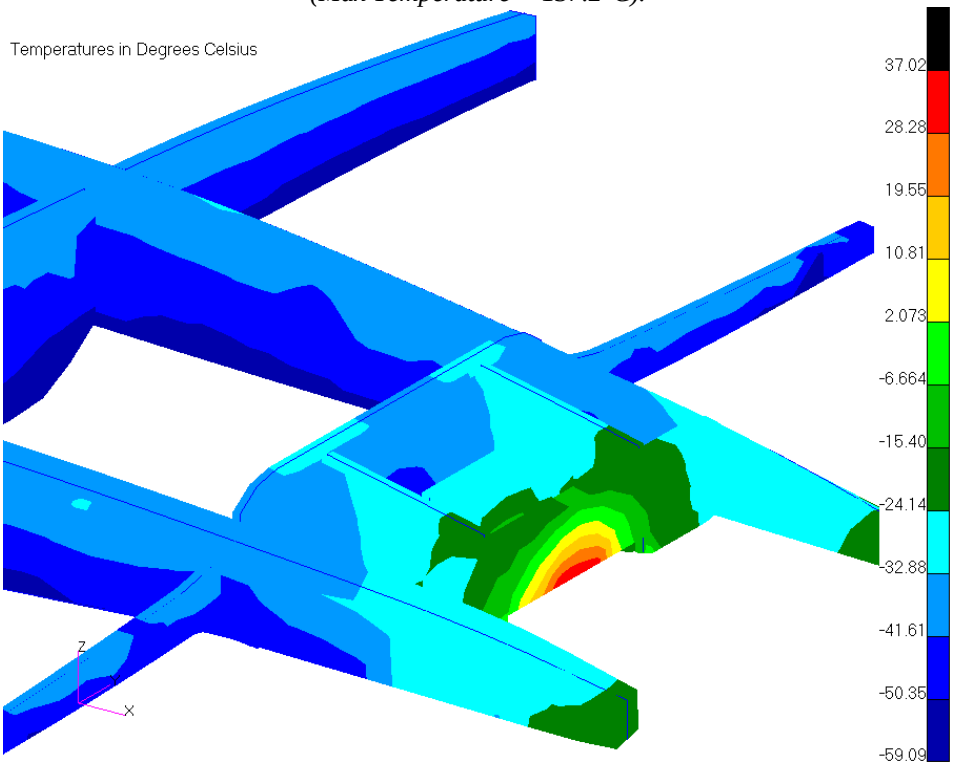

Figure 38. Temperature profile, support structure, triangular configuration and low ε paint.
(Max Temperature = 37.02°C).

3.5.4.2.3 Heat Shield Study Results

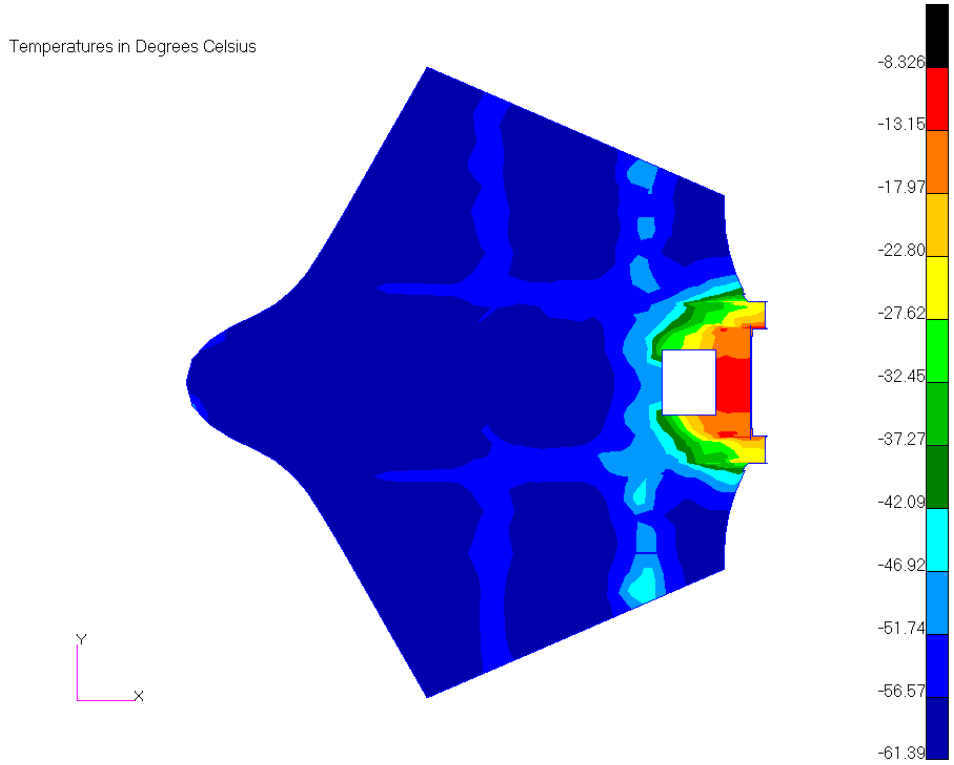

Figure 39. Temperature profile, lower fuselage, triangular configuration with heat shield.
(Max Temperature = -8.33°C).

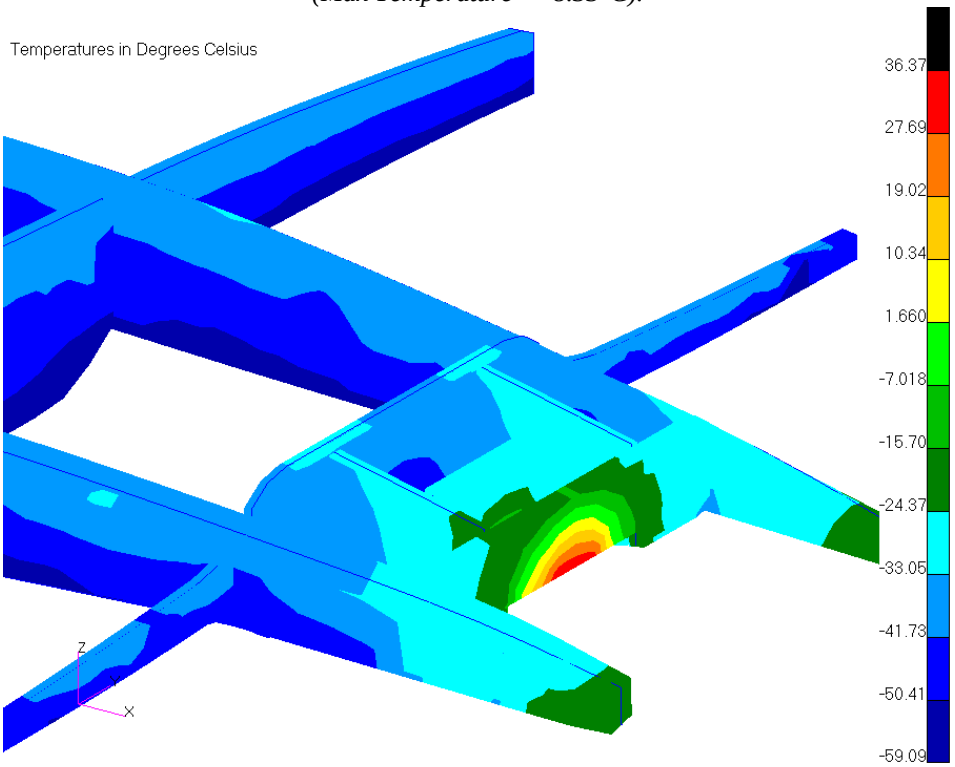

Figure 40. Temperature profile, lower fuselage, triangular configuration with heat shield.
(*Max Temperature = 36.4°C).*

3.5.4.3 Triangular Thruster Configuration Results with Estimated Plume

The full plume structure used in the analysis was approximately one quarter of the full plume length. The reason for this was to save computational time running the view factor analysis. The plume closest to the fuselage structure will contribute the most heating, and so the closest quarter is sufficient to get a general idea of the steady state temperatures resultant on the aircraft.

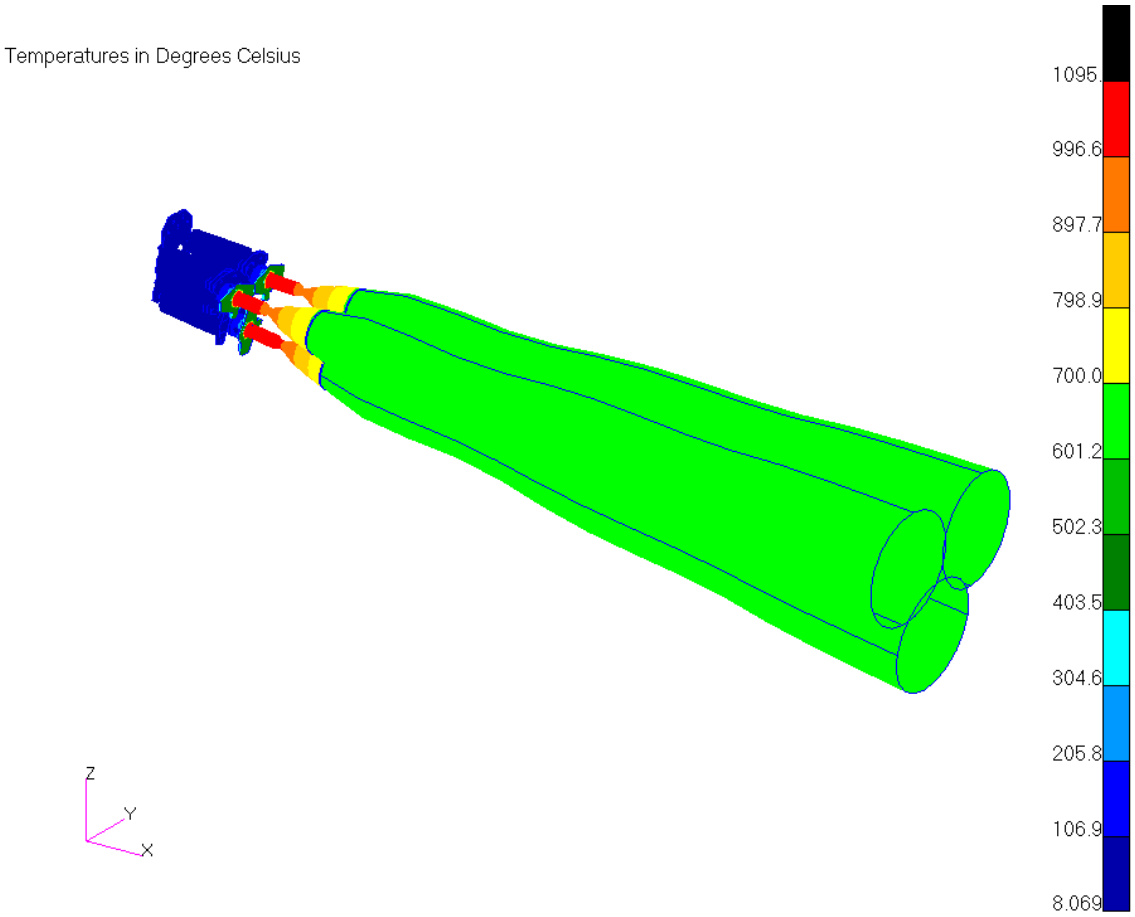

Figure 41. Triangular thruster plume configuration.
(Plumes shown at 700 °C.)

3.5.4.3.1 Baseline Study Results, 700 °C and 400 °C

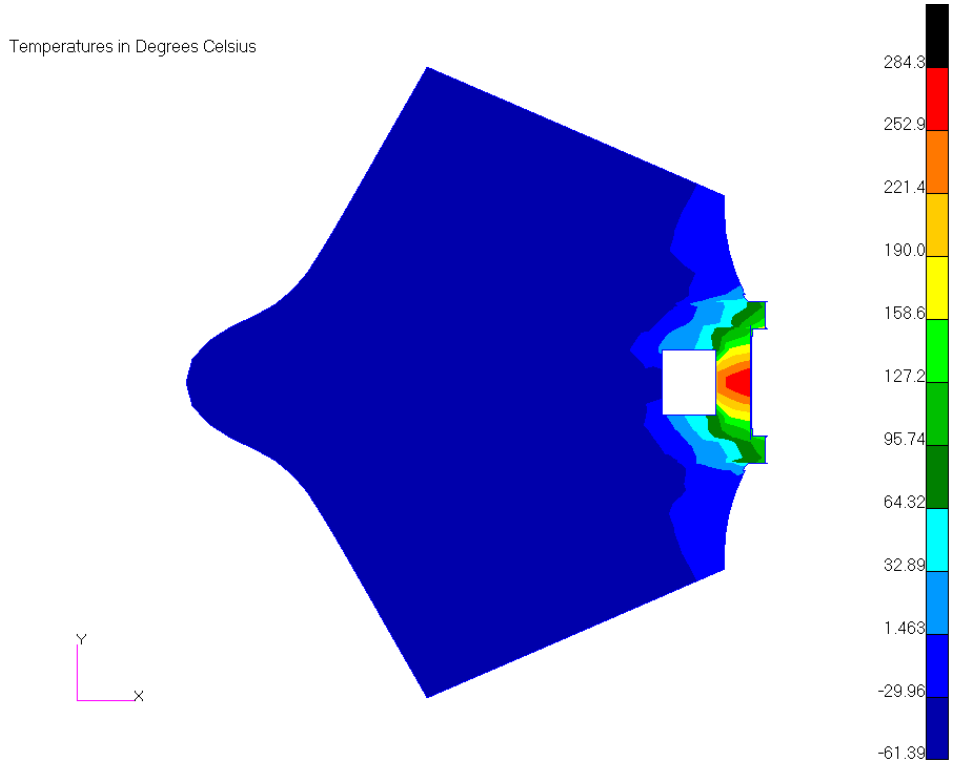

Figure 42. Temperature profile, lower fuselage, triangular configuration, 700°C plume.
(Max Temperature = 284°C).

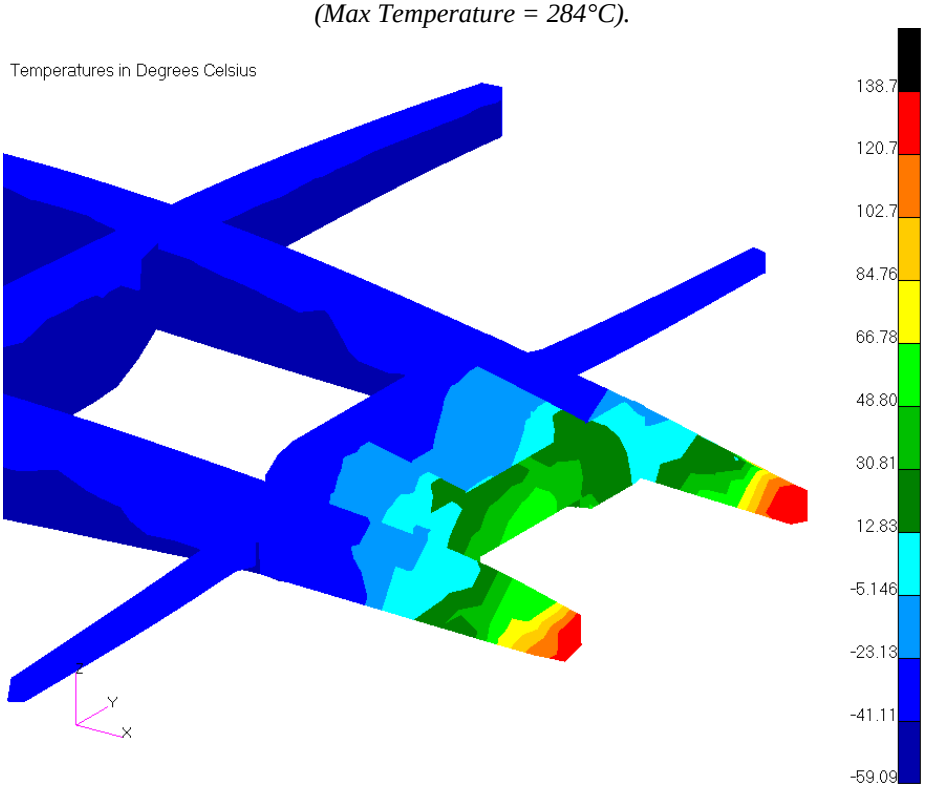

Figure 43. Temperature profile, support structure, triangular configuration, 700°C plume.
(Max Temperature = 139°C).

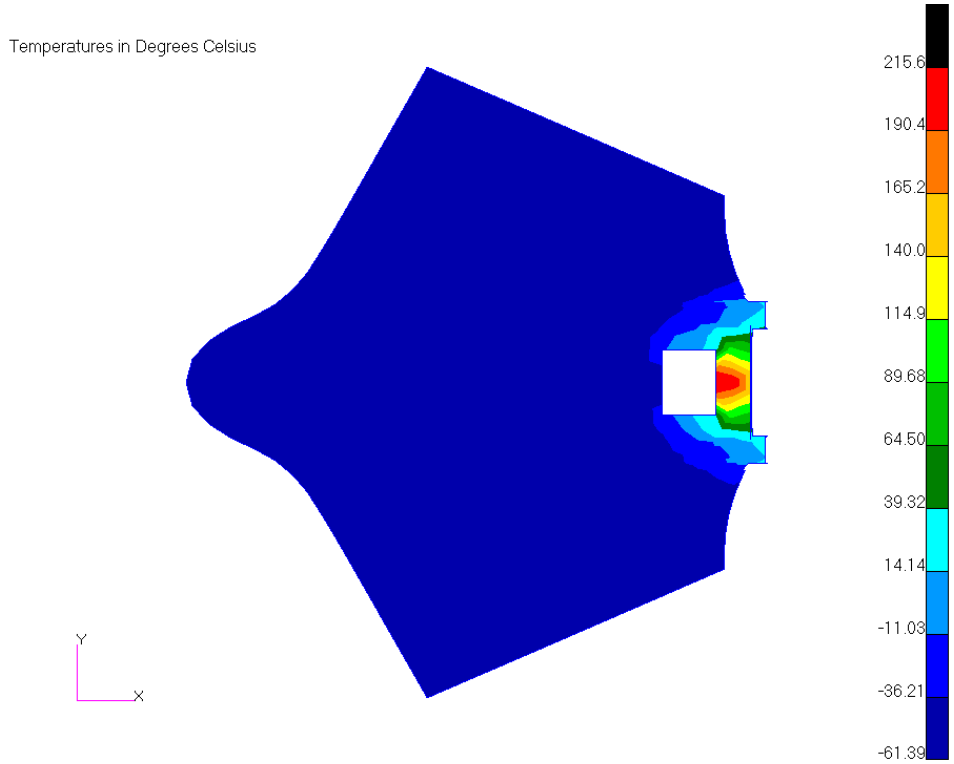

Figure 44. Temperature profile, lower fuselage, triangular configuration, 400°C plume.
(Max Temperature = 215°C).

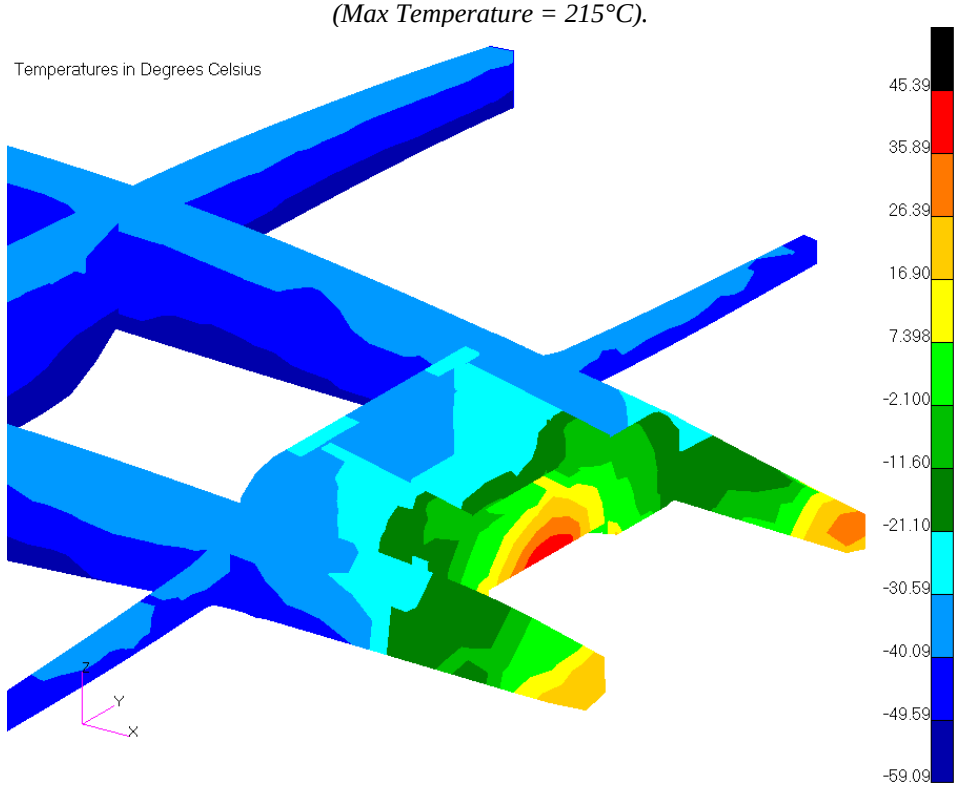

Figure 45. Temperature profile, support structure, triangular configuration, 400°C plume.
(Max Temperature= 45°C).

3.5.4.3.2 Low Emissivity Paint Study Results, 700 °C and 400 °C

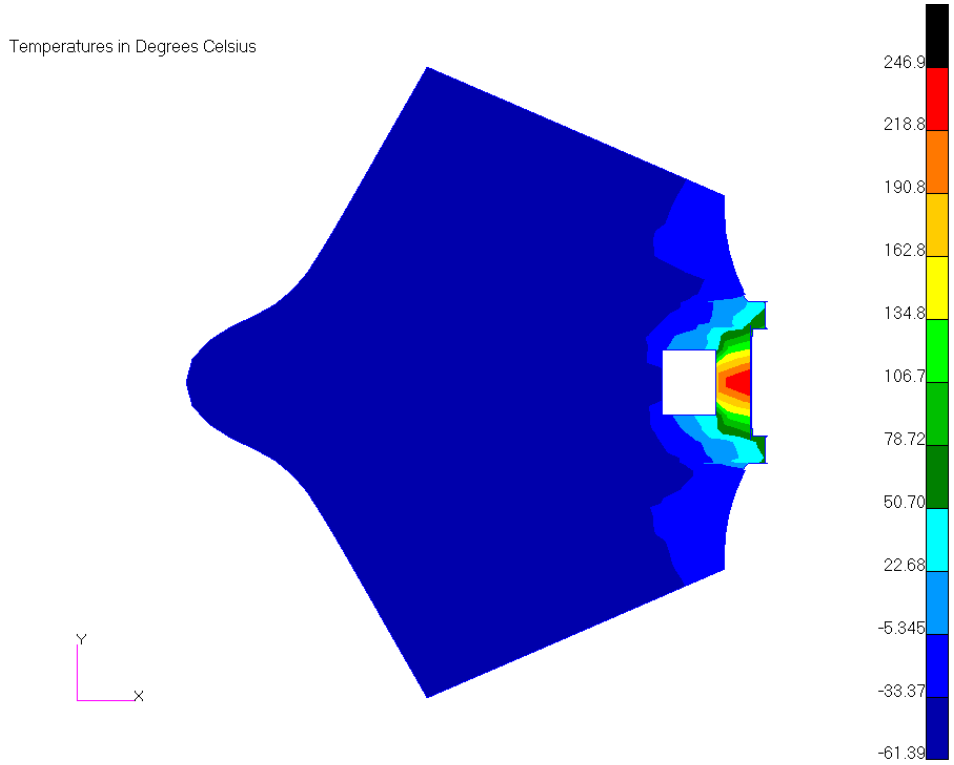

Figure 46. Temperature profile, lower fuselage, triangular config., 700°C plume, low ε paint.
(Max Temperature= 247°C).

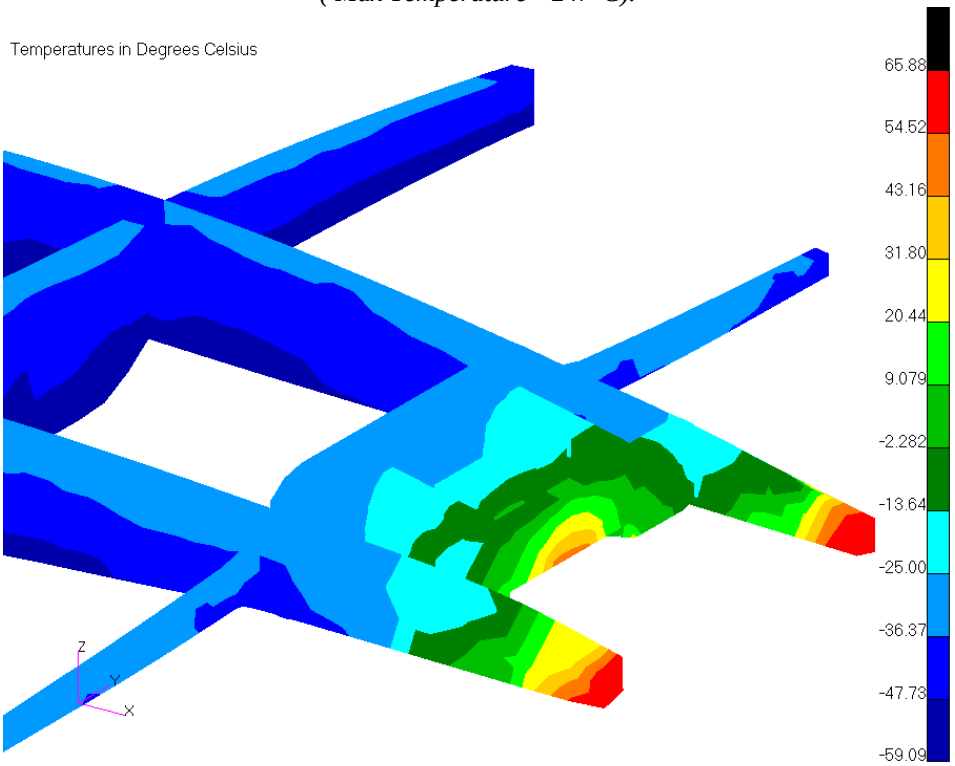

Figure 47. Temperature profile, support structure, triangular config., 700°C plume, low ε paint.
(Max Temperature= 66°C).

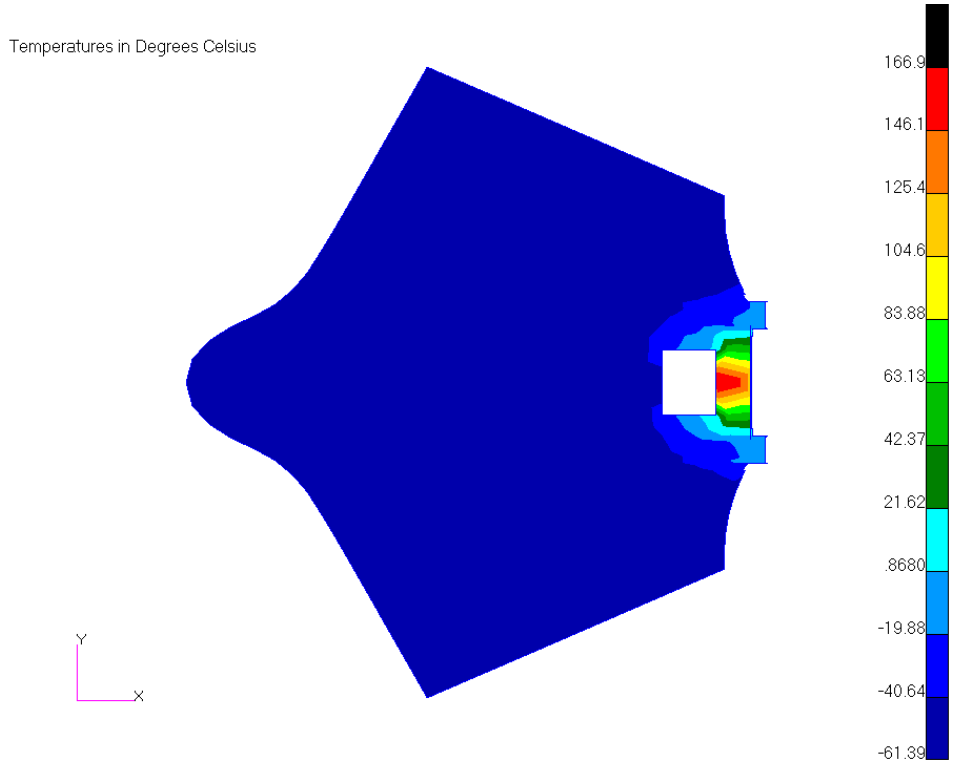

Figure 48. Temperature profile, lower fuselage, triangular config., 400°C plume, low ε paint.
(Max Temperature= 167°C).

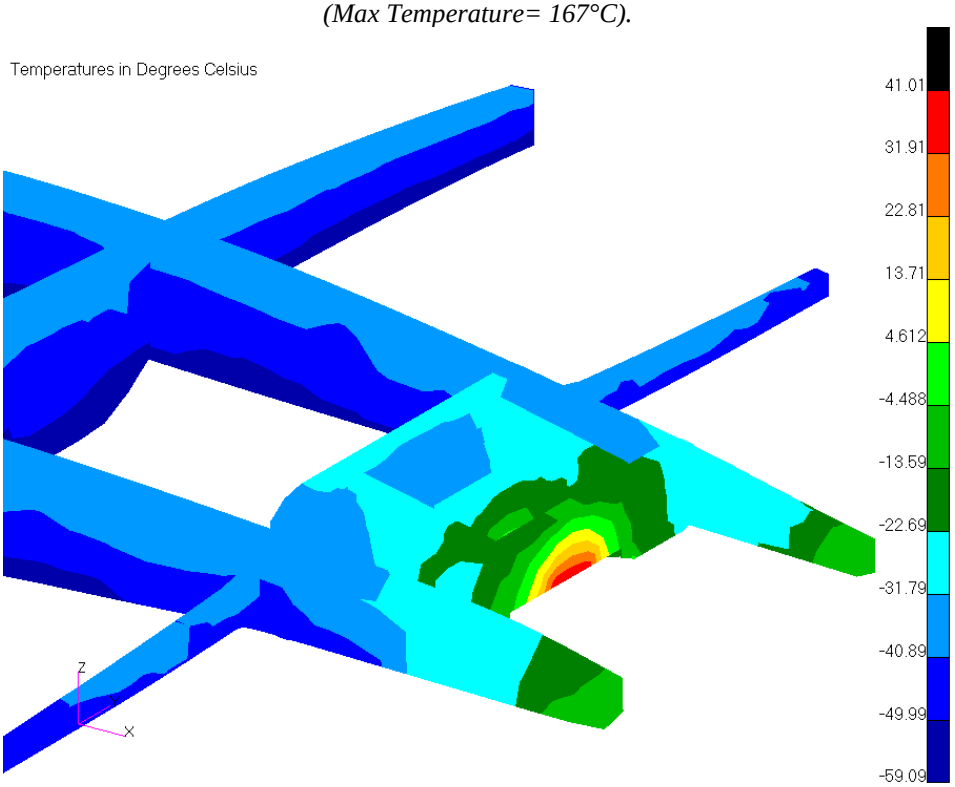

Figure 49. Temperature profile, support structure, triangular config., 400°C plume, low ε paint.
(Max Temperature= 41°C).

3.5.4.3.3 Heat Shield Study Results, 700 °C and 400 °C

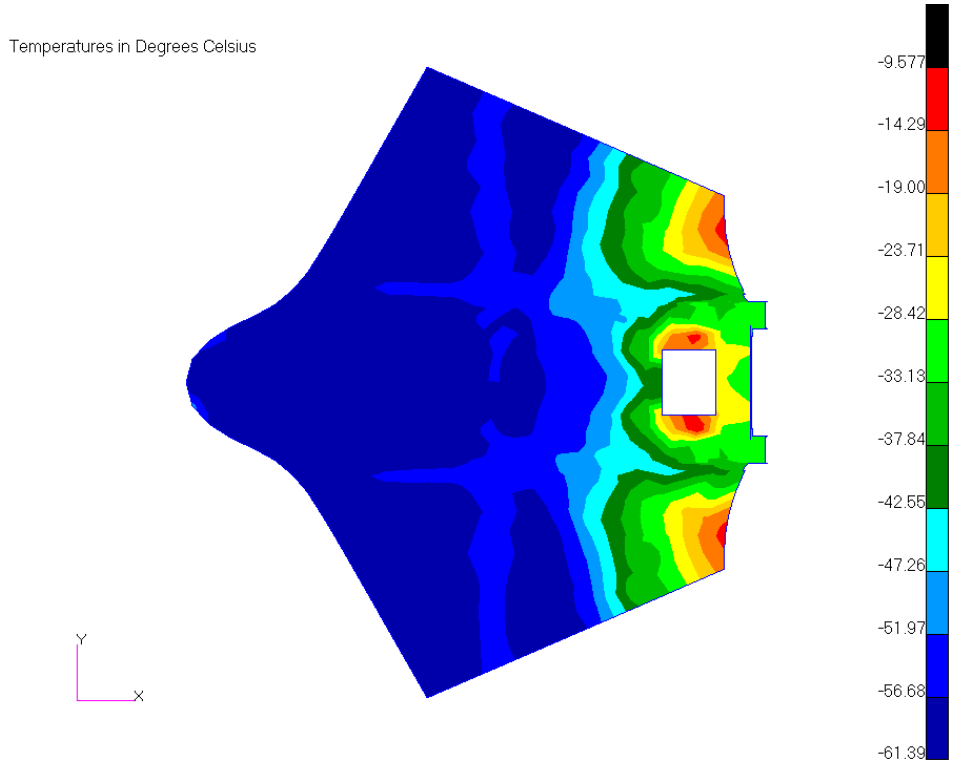

Figure 50. Temperature profile, lower fuselage, triangular config., 700°C plume, heat shield.
(Max Temperature= -9.5°C).

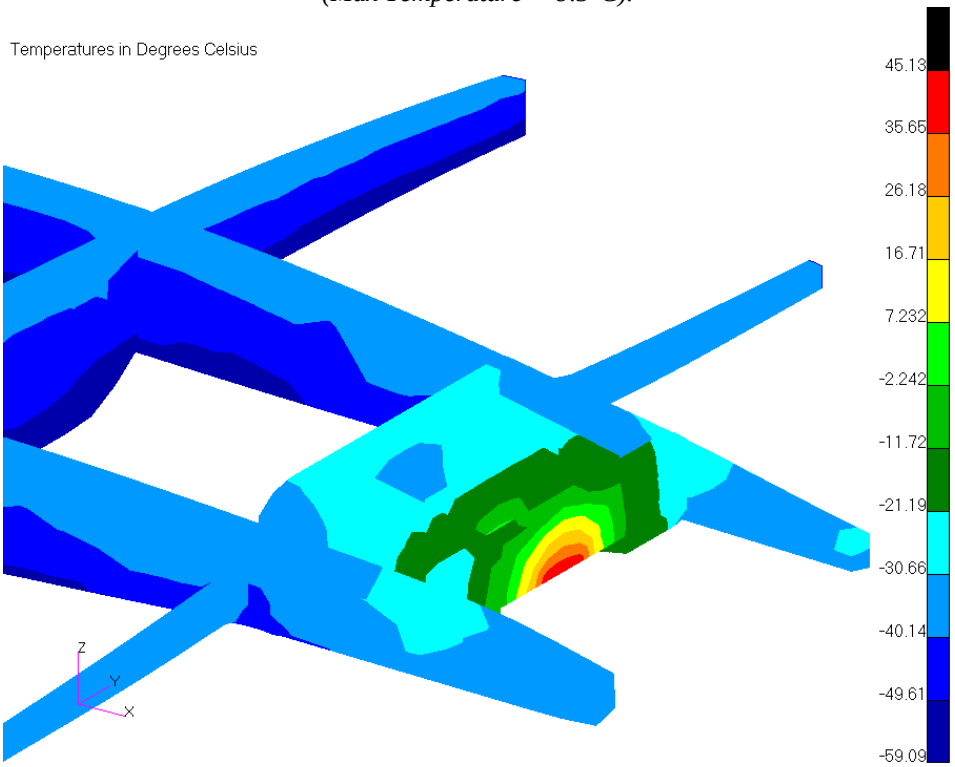

Figure 51. Temperature profile, support structure, triangular config., 700°C plume, heat shield.
(Max Temperature= 41°C).

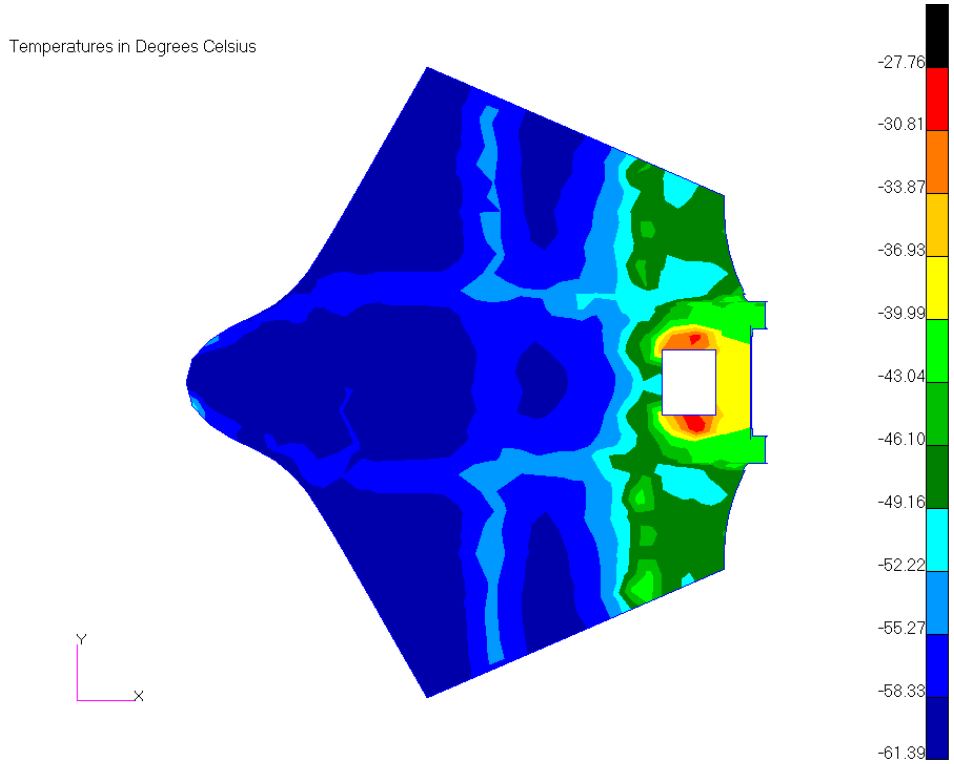

Figure 52. Temperature profile, lower fuselage, triangular config., 400°C plume, heat shield.
(Max Temperature= -28°C).

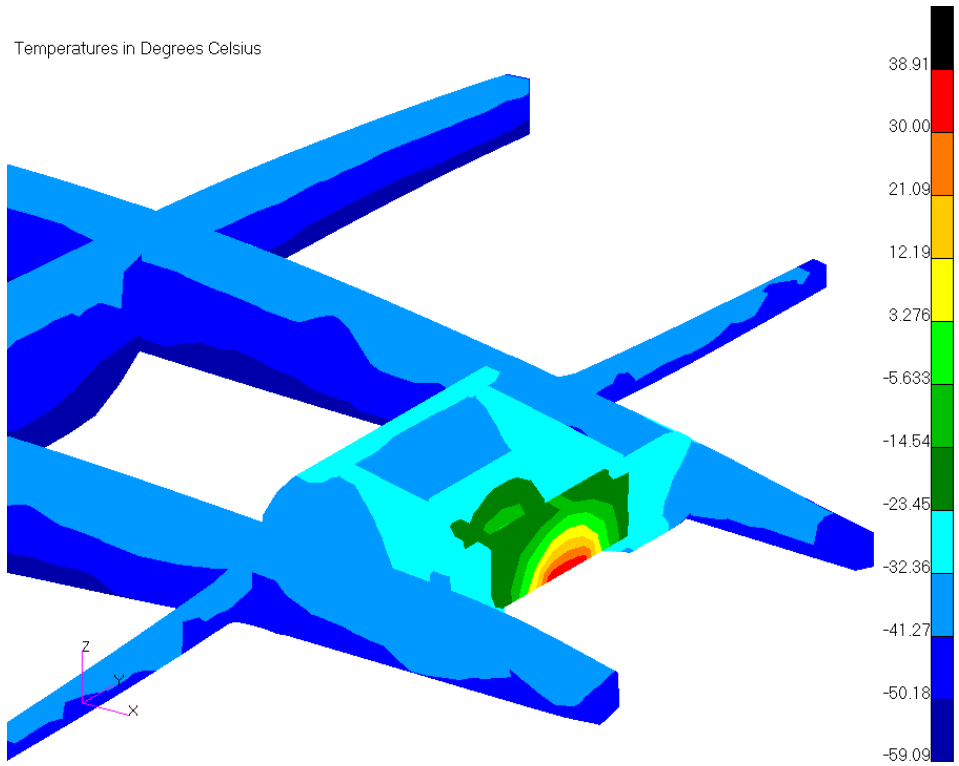

Figure 53. Temperature profile, support structure, triangular config., 400°C plume, heat shield.
(Max Temperature= 39°C).

3.5.5 Thermal Analysis Conclusion

If the plume is ignored, it appears that the fuselage will not exceed 250°C. The highest temperature reached is 209°C for the in-line configuration baseline study. The triangular thruster configuration results in the smallest fuselage temperatures for all studies. This seems physically reasonable since all three thrusters in the linear configuration have direct views to the lower fuselage, while one of the triangular thrusters is partially blocked by the other two. This blocked thruster is also further away from the fuselage which also reduces radiation transfer.

Adding the plume to the analysis clearly shows a large increase in the steady state temperatures on the aircraft. Assuming 0.5 for plume emissivity, and a plume temperature is 700°C, a paint with an emissivity of 0.3 will not be enough to keep the temperature below critical. A heat shield, or paint with a lower emissivity should be used if this is the case (see Figure 43, Figure 48, Figure 50, Figure 52). Paint with an emissivity of 0.3 should be sufficient however if the plume temperature is only 400°C. This analysis should be considered preliminary, as values for the plume are estimates.

The heat shield used in the plume study needed to cover a larger area than the one used in the non-plume studies (Figure 26). Depending on the plume temperature, the smaller shield could be used in combination with low emissivity paint. This would keep the fuselage temperatures closer to the ambient temperature if desired. For a high plume temperature, the larger heat shield should be used.

The last iteration for this trade study resulted in the plume temperature profile to be significantly lower than what was estimated for the thermal analysis. The plume temperature does not exceed 330K (66°C), which compared to the assumed 400°C and 700°C is significantly less. This suggests that the results obtained in the analyses ignoring the thruster plumes will more closely represent the expected airplane skin temperatures. The cases reported in the previous sections including the higher temperature plumes can be taken as worst case scenarios.

The smaller heat shield weighs approximately 0.068 kg, and the larger shield weighs approximately 0.16 kg. Both of these masses would increase to include any bonding material and/or fasteners needed to attach the shield to the aircraft. If a paint or shield is to be used, it does not appear that there will be any thermal benefit of using one configuration over the other. The triangular thruster does keep the lower fuselage temperature cooler, but not by enough to disqualify the use of the in-line thruster configuration.

3.6 Triple Thruster Plume Analysis and Characteristics

Computational fluid dynamics (CFD) simulation was used to evaluate possible plume interactions in the triple-thruster systems. This work considers the 3D thruster systems in a representative freestream environment, but does not include the aircraft outer mold line (OML) or influence of aircraft external aerodynamic flows.

CFD grids were created using the Langley "AXB" software, custom FORTRAN 95 codes, and the commercial "GridGen" tool. Thruster arrangements were modeled assuming spanwise symmetry about the vehicle centerline symmetry plane (X-Z plane at Y=0). Figure 54 and Figure 55 show the grids for the in-line and triangular arrangements as modeled for CFD.

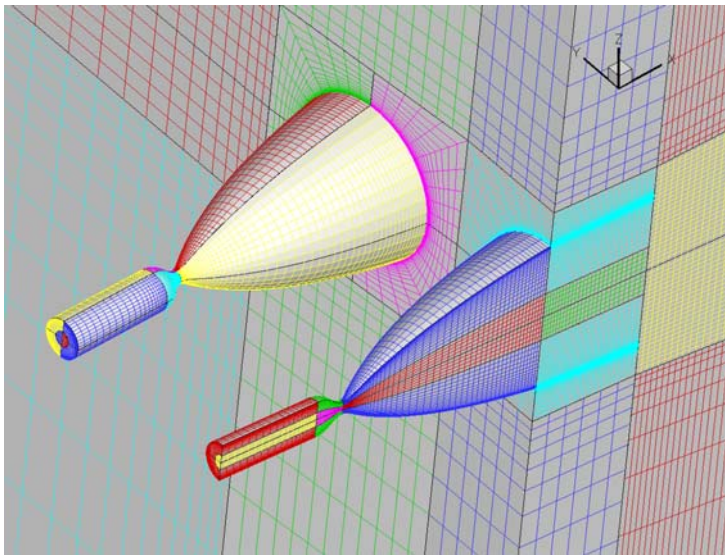

Figure 54. Triple 22N In-line thruster semi-span CFD model.
(Mesh shown at 1/2 resolution).

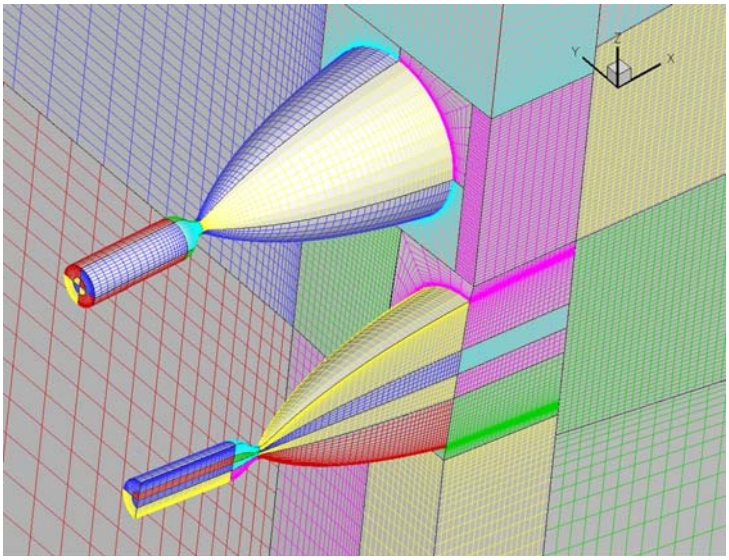

Figure 55. Triple 22N Triangular thruster semi-span CFD model.
(Mesh shown at 1/2 resolution).

The in-line CFD grid consisted of 120 blocks and 13.7 million cells. The triangular grid consisted of 84 blocks and 16.5 million cells. In both cases, the thruster nozzles discharge into an ambient freestream region with a 65 nozzle exit diameter downstream run. Reynolds-Averaged Navier-Stokes (RANS) simulations were run with the Langley "PAB3D" flow solver, using two-equation temperature-corrected k-ε turbulence closure and a linear Reynolds stress model. Freestream flow was set to M=0.55 with an ambient temperature of 346R (representative of ARES cruise conditions on Mars). Nozzle inflow was specified with a stagnation temperature of 1450R and a nozzle pressure ratio (NPR) of 2193 (corresponds to nozzle stagnation pressure of 125 psia and Mars ambient pressure 0.057 psia). A specific heat ratio of γ=1.23 (representative of thruster exhaust) was used everywhere.

Simulations were run in double precision on the 40-node ARES computer cluster, with 2.8GHz Intel Pentium4 CPUs and 1GB memory per node. Solutions were sequenced through coarse and medium mesh levels to evaluate grid dependence effects, and had run times of 350-1200 wall-clock hours per case. To accelerate convergence, simulations were initiated with local time-stepping, which drives towards a steady-state solution (steady RANS). The in-line case converged to a steady state solution after about 79,000 iterations. The triangular case did not converge to a steady state with local time-stepping after 72,000 iterations, and the simulation was switched to a constant-time-step "time-accurate" mode (unsteady RANS). After an additional 41,000 iterations (with 4 sub-iterations per time step) the triangular case converged to a stable steady-state solution.

3.6.1 Triple 22N In-line Thruster Plume Simulation Results

Results from the in-line case are presented in this section. In the following figures, the ARES OML is superimposed over the plume CFD simulation, with color contours of Mach number shown. Figure 56 shows a slice through the centerline plane of spanwise symmetry, with the center thruster plume visible. Here, the plume is seen to slowly bend from its initial 5.88° incidence to align with the freestream flow. Figure 57 shows a slice through the CFD simulation in a plane 5.88° from the horizontal, aligned with the thruster incidence. The individual thruster plumes are well isolated and maintain angular separation, with no major interactions apparent. Figure 58 shows a vertical slice through the CFD simulation at the tail mid-chord location. There is plenty of clearance between the tail and plumes. Very minor plume interactions are evident in the weakly three-dimensional (ie, non-round) plume shapes. Multiple slices through the plumes are shown in Figure 59 to give an idea of plume development going downstream. As in previous images, the three plumes are seen to be isolated with no major interactions. Figure 60 shows the temperature profile of the plume for the in-line configuration, the temperature does not exceed 330K (66°C).

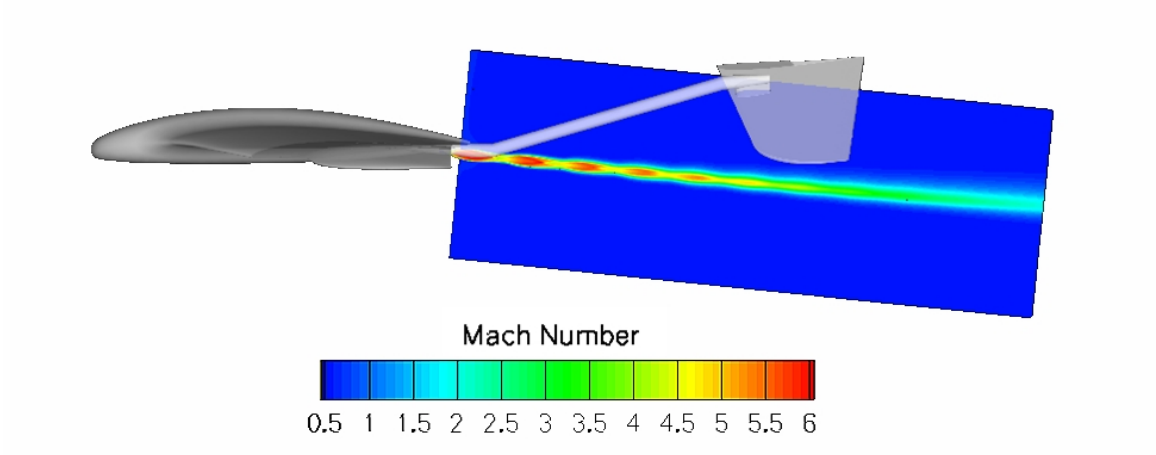

Figure 56. ARES OML superimposed over centerline slice through CFD simulation, in-line case.

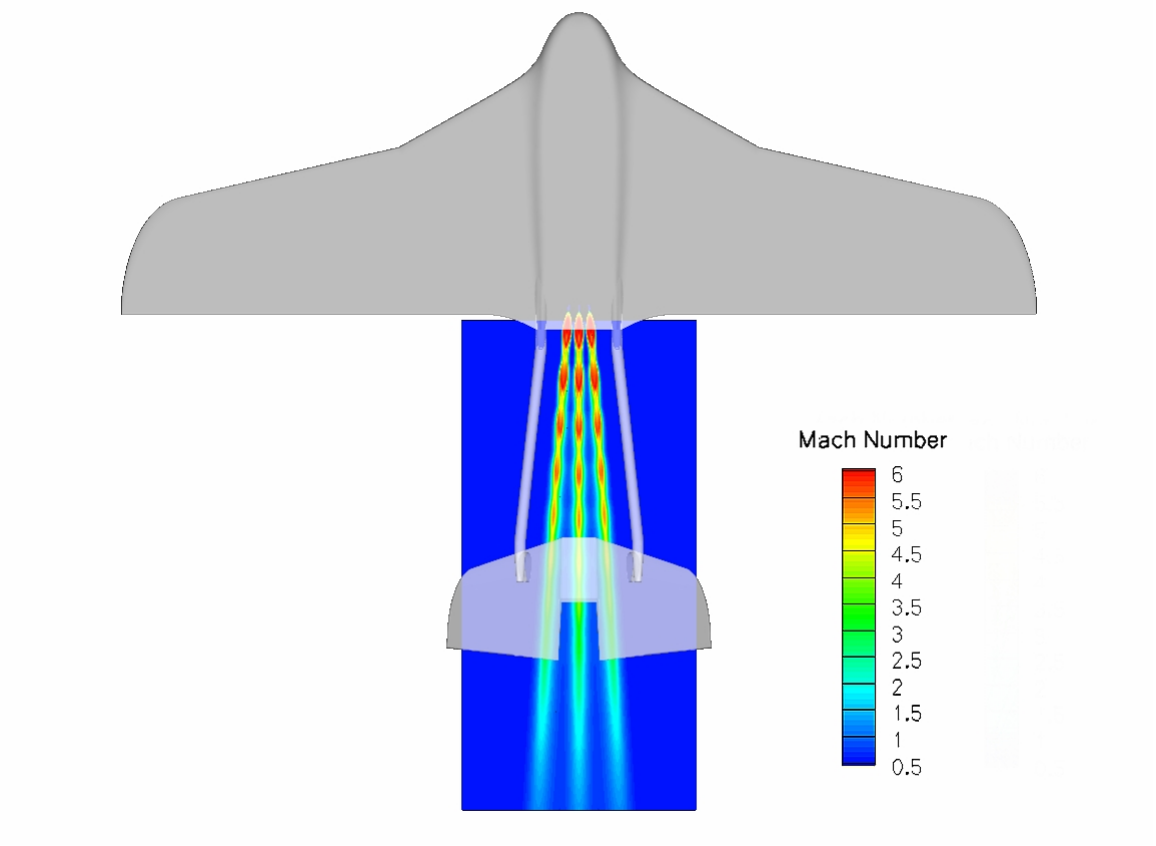

Figure 57. ARES OML superimposed over slice through CFD simulation, in-line case.

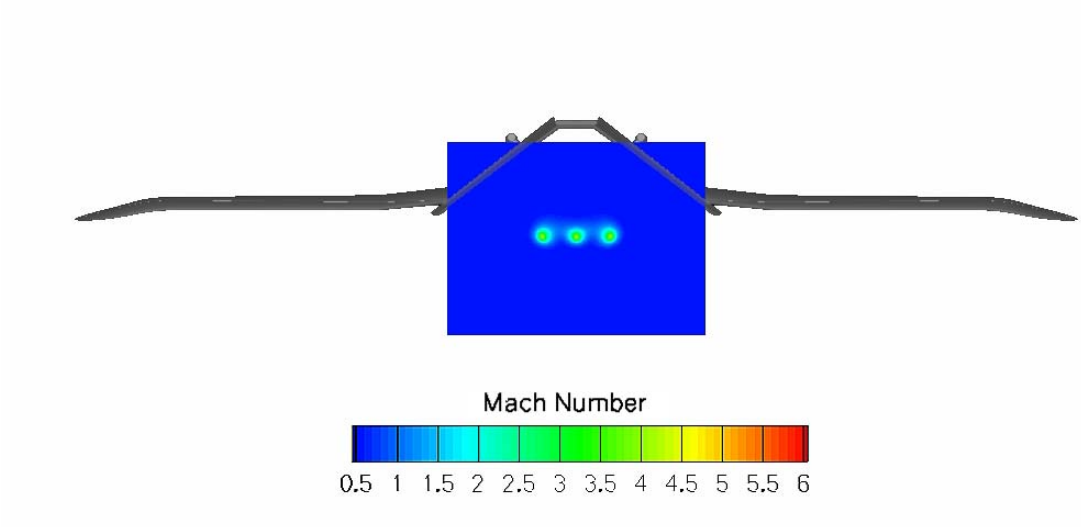

Figure 58. ARES OML superimposed over vertical slice through CFD simulation, in-line case.

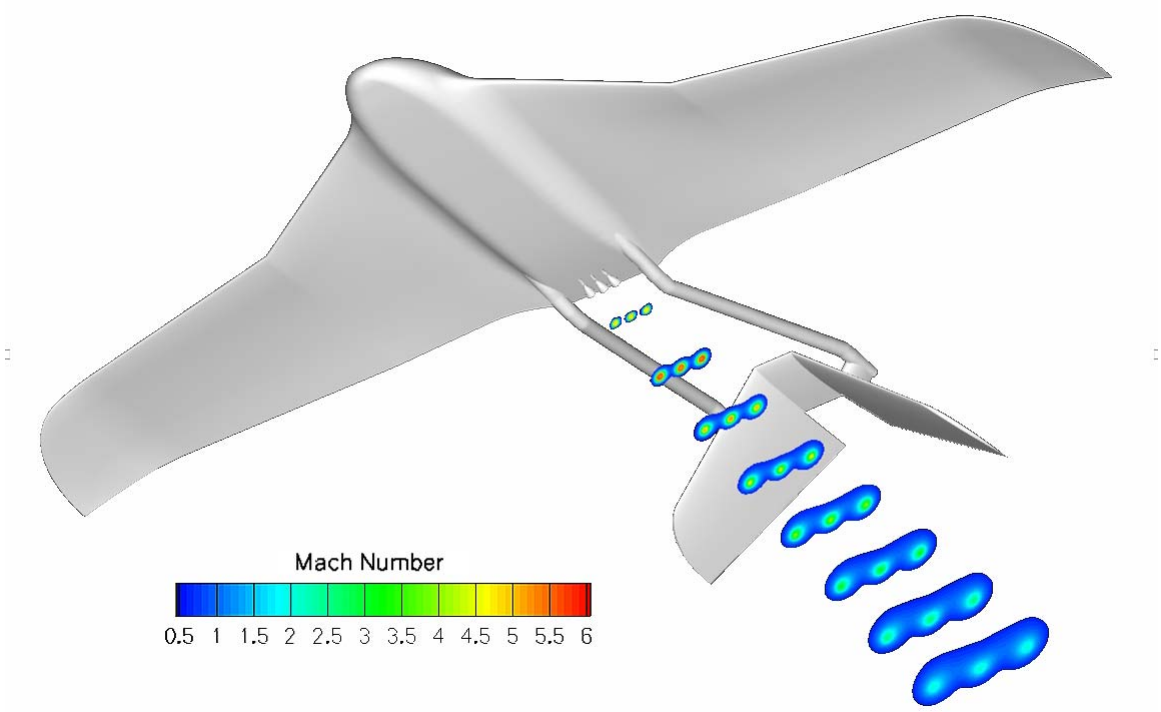

Figure 59. ARES OML superimposed over vertical slices through CFD simulation.
(Locations at X=2.5, 3.0, 3.5, 4.0, 4.5, 5.0, 5.5, and 6.0m (nozzle exits at X~2.3m), in-line case. Contours of Mach number above M=0.62 are shown).

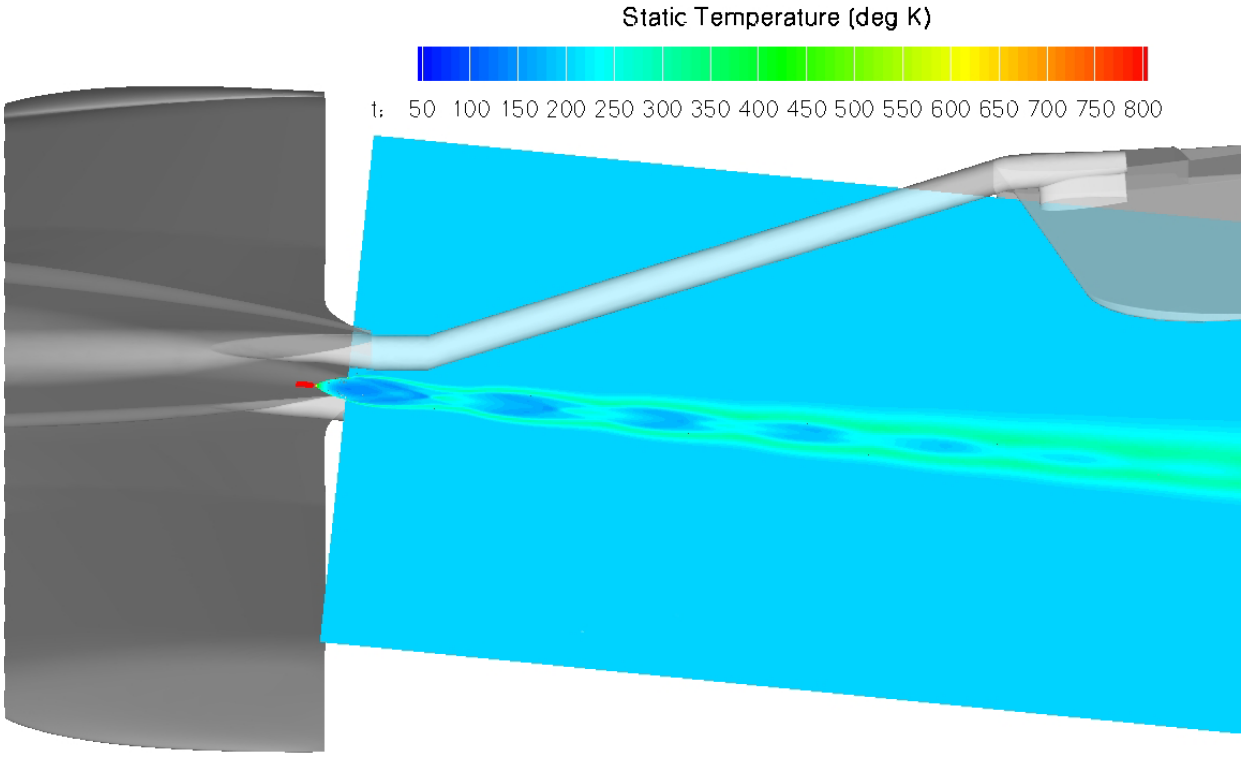

Figure 60. ARES OML superimposed over vertical slices through CFD in-line plume temperature profile.

3.6.2 Triple 22N Triangular Thruster Plume Simulation Results

Results from the triangular case are presented in this section. . Plume interactions are evident in Figure 61, as the top row plumes bend to align with the freestream flow and come together. Figure 61 shows a slice through the centerline plane of spanwise symmetry for the triangular case. Figure 62 and Figure 63 slice through the CFD simulation at incidence angles of 5.88° and 9.38°, aligned with the top and bottom rows of thrusters, respectivelyHere, the lower thruster plume is shown clearly, and the influence of the upper row plumes is visible at the centerline. Figure 64 shows a vertical slice through the CFD simulation at the tail mid-chord location for the triangular case. There is plenty of clearance between the tail and plumes. The plumes are still distinct, but are closer together and exhibit stronger interactions than the in-line case.

Multiple slices through the triangular plumes are shown in Figure 65 to give an idea of plume development going downstream. In this configuration, strong plume interactions start to develop around X=6m (approx. 1.5m downstream of the tail trailing edge) as the plumes begin to merge. Figure 66 shows the temperature profile of the plume for the in-line configuration, the temperature does not exceed 330K (66°C).

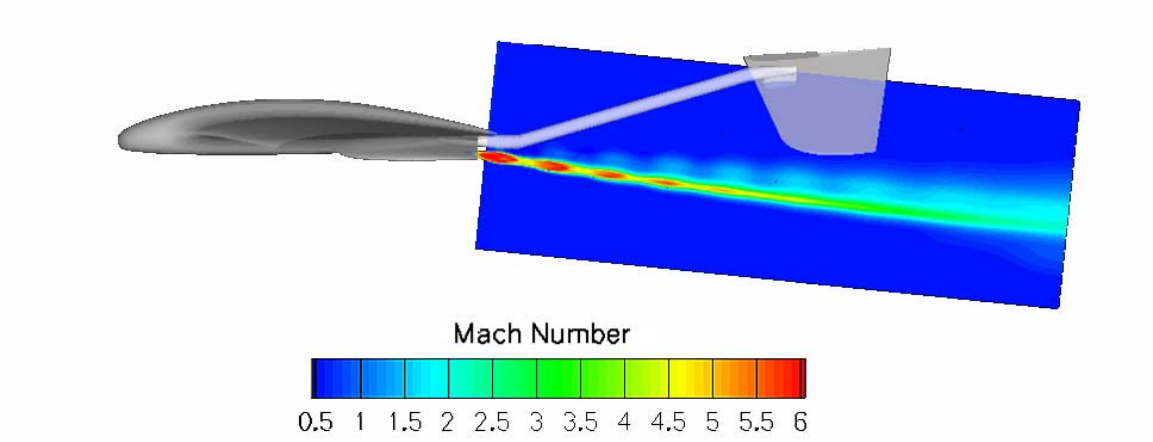

Figure 61. ARES OML superimposed over centerline slice through CFD simulation, triangular case.

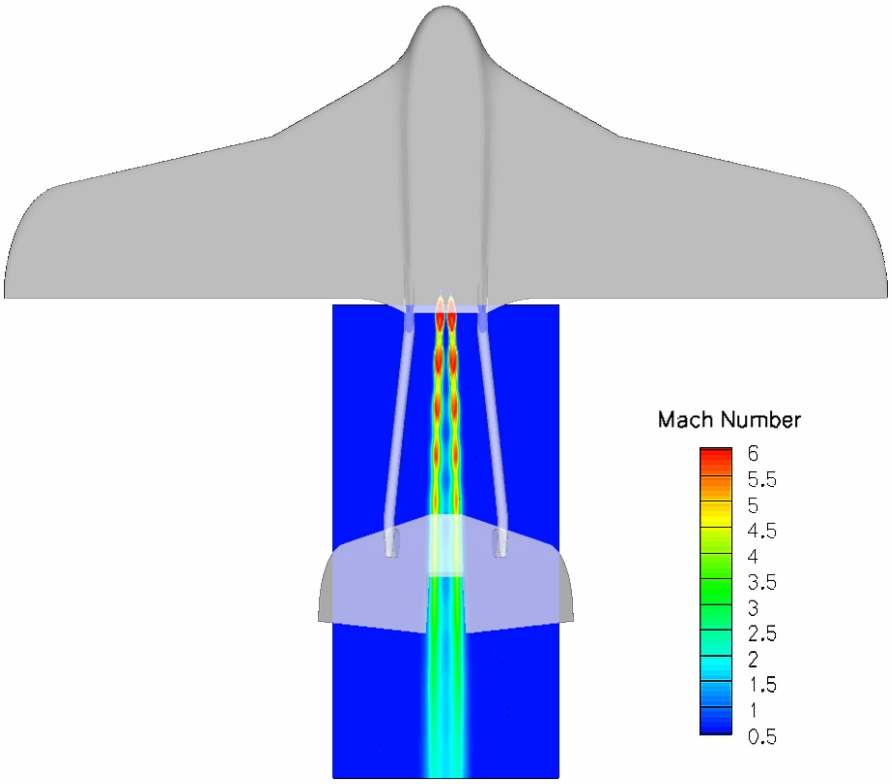

Figure 62. ARES OML superimposed over 5.88° slice through CFD simulation, triangular case.

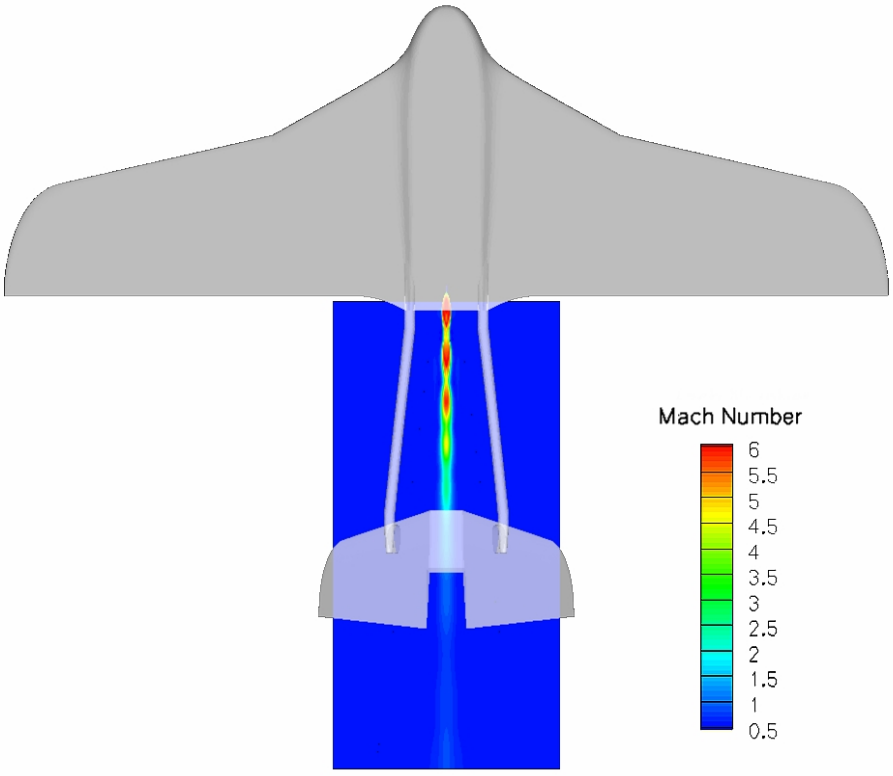

Figure 63. ARES OML superimposed over 9.38° slice through CFD simulation, triangular case.

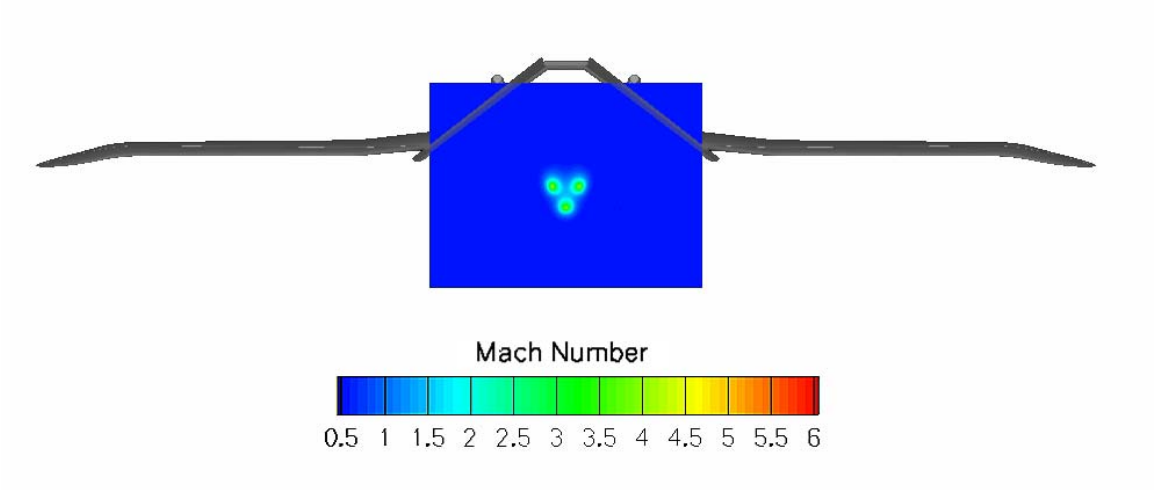

Figure 64. ARES OML superimposed over vertical slice through CFD simulation, triangular case.

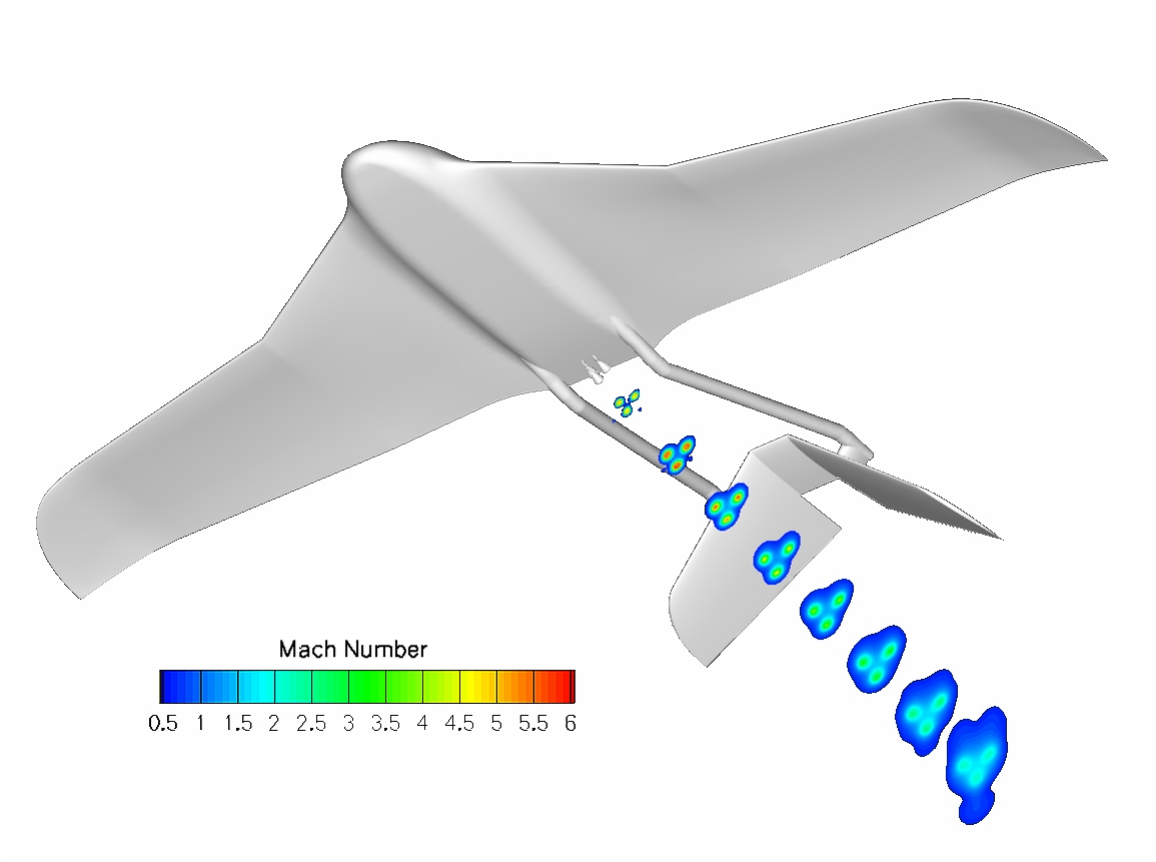

Figure 65. ARES OML superimposed over vertical slices through CFD simulation.
(Locations at X=2.5, 3.0, 3.5, 4.0, 4.5, 5.0, 5.5, and 6.0m (nozzle exits at X~2.3m), triangular case. Contours of Mach number above M=0.62 are shown).

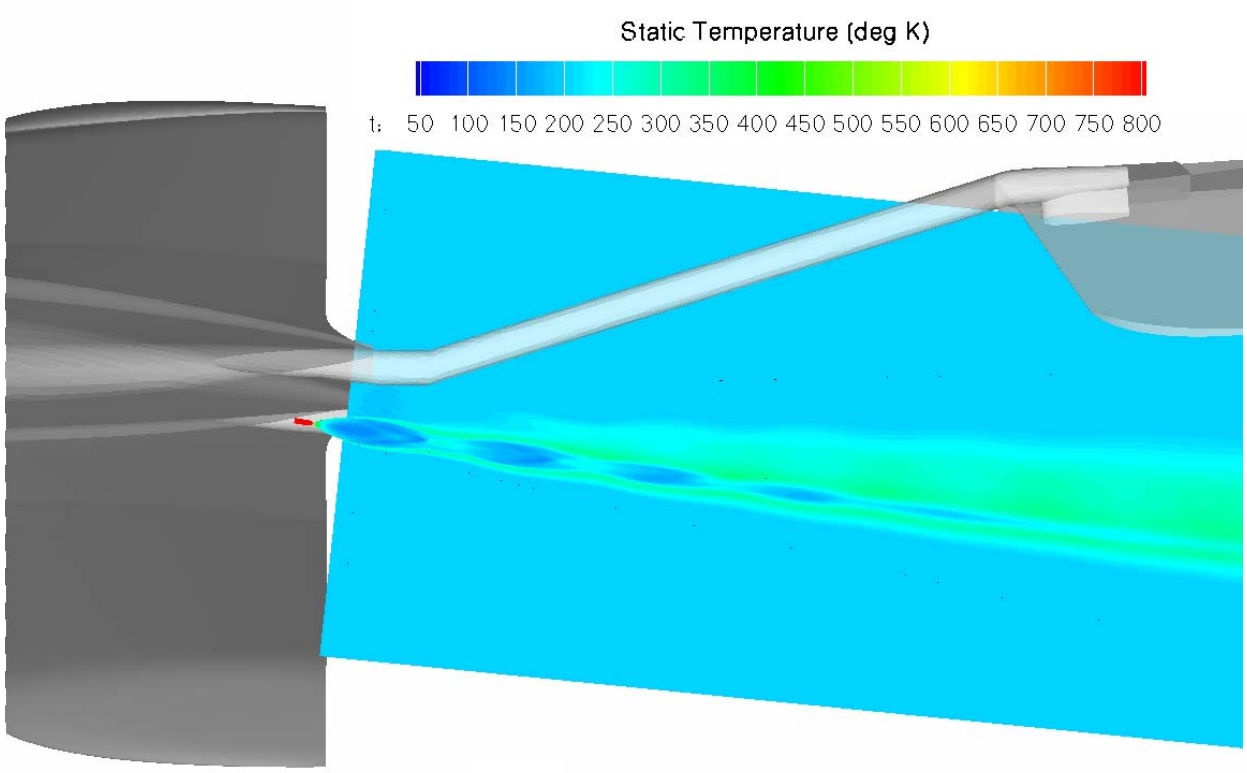

Figure 66. ARES OML superimposed over vertical slices through CFD triangular plume temperature profile.

3.6.3 Triple 22N Thruster Plume Analysis Conclusions

Both thruster configurations resulted in stable steady-state plumes, but the triangular case clearly showed stronger evidence of plume interactions. This is likely due to the fact that the top row thrusters were at a lower horizontal angle of incidence relative to the freestream (2.2°) compared to the in-line case (4.5°). This allowed the plumes to more easily bend to align with freestream flow, resulting in closer proximity going downstream. In contrast, the in-line plumes maintained an angular separation all the way downstream to the simulation boundary and had minimal interactions.

3.7 Triple Thruster Flight Simulation and Performance

Flight simulation of the Mars airplane with a three-thruster system was evaluated using the six degree-of-freedom model from the Langley Standard Real-Time Simulation application framework[5]. The firing logic for the thrusters was divided into two separate duty cycles. The primary duty cycle governed the firing of two thrusters simultaneously to provide the needed thrust to overcome drag while flying under normal conditions. The secondary duty cycle governed the firing of the third thruster and was invoked during instances where airplane acceleration or climbing was needed which required more than 44N of thrust. Similar to the single 62N system, two atmospheric conditions were simulated, one with no turbulence, and the other condition with severe atmospheric turbulence. Thruster duty cycle for the conditions of no turbulence is shown in Figure 67. The primary duty cycle is shown on the top chart and the secondary on the bottom. For conditions of no turbulence, the primary duty cycle stays predominantly around 70%, varying between 60% and 85% for the majority of flight. The secondary duty cycle shows that the third thruster is only slightly used during the initial stages of flight and stays off during the entire remainder of flight.

Figure 67. Duty Cycles of Triple Thruster System - No Turbulence Conditions

During severe turbulence, the data in Figure 68 shows that the two primary thrusters are fully firing at 100% duty cycle for a significant portion of the flight, and that the third thruster, or secondary duty cycle, is sparsely invoked throughout the flight and remains off for most of the flight.

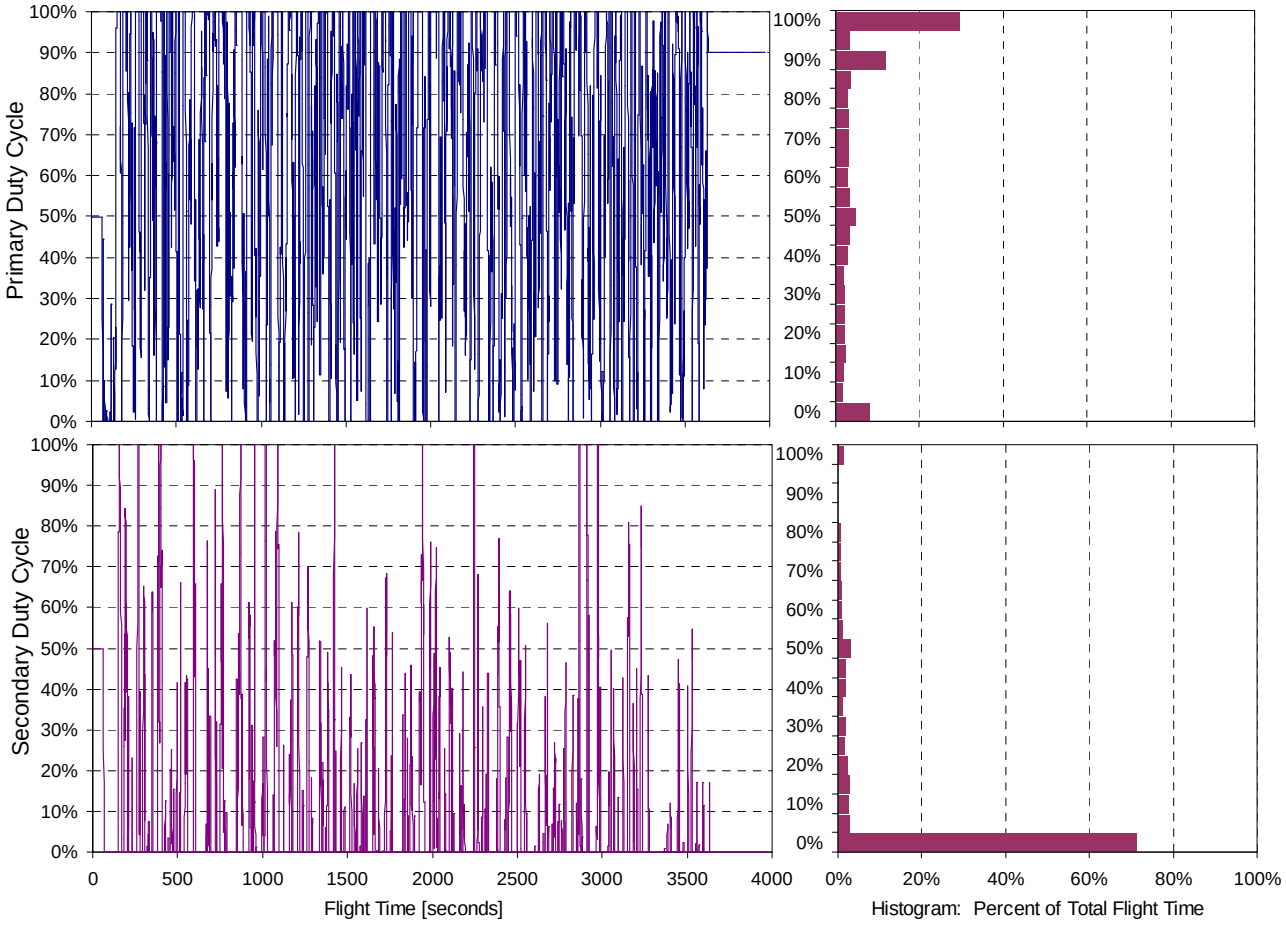

Figure 68. Duty Cycles of Triple Thruster System - Severe Turbulence Conditions

3.8 Triple 22N Thruster System Summary

The results of the simulation show that for the airplane with three 22N thrusters flying in no-turbulence conditions, the flight range with 40 kg of propellant is about 543 km. In severe turbulence conditions for the same fuel load, the flight range is reduced to about 536 km (Table 11).

The total mass of the triple thruster propulsion system is broken down into components shown in Table 12. Based on commercially available components, estimates from vendors, and analysis, the current best estimate for the triple thruster system is 16.31 kg for the in-line configuration and 16.26 kg for the triangular configuration. Incorporating the contingencies assigned to each component, the total mass increases to 19.40 kg for the in-line configuration and 19.34 kg for the triangular configuration.

Table 11. Triple Thruster Propulsion System Performance Summary – 40 kg Fuel Load

Parameter	Value
Total AFS Mass	145 kg
Propulsion Mass	18.06 – 18.12 kg
Propellant Load	40 kg
Fuel	15 kg - MMH
Oxidizer	25 kg - MON3
Thrust	Three - 22 N
Isp	~291 s
No Turbulence	
Flight Duration	67.63 min
Range	543 km
Avg Fuel Usage	13.6 km/kg
Severe Turbulence	
Flight Duration	66.22 min
Range	536 km
Avg Fuel Usage	13.4 km/kg

Table 12. Triple 22N Thruster Option - Propulsion System Mass Breakdown

Common Components	QTY	CBE Each [kg]	Total [kg]	Cont [%]	CBE + Cont [kg]	Vendor	Part Number
Pressure Transducer	5	0.15	0.75	20%	0.90	GP50	7200
Normally Closed Pyro Valve	5	0.15	0.75	15%	0.86	CONAX	1832-205
GHe Filter	1	0.25	0.25	25%	0.31	Vacco	F1D10636-01
High Pressure Service Valve	11	0.113	1.243	10%	1.37	Vacco	V1E10430-01
Helium Regulator	1	0.363	0.363	10%	0.40	Vacco	66250
Check Valve	4	0.02	0.08	25%	0.10	Vacco	V1D10856-02
Liquid Filter	2	0.18	0.36	25%	0.45	Vacco	F1D10638-01
GHe Tank	1	1.2	1.2	25%	1.50	Lincoln	220131-1
Oxidizer Tank	1	2.87	2.87	25%	3.59		
Fuel Tank	1	2.87	2.87	25%	3.59		
Tank Support Brackets	4	0.1	0.4	25%	0.50		
Subtotal			*10.74*		*13.07*		
Triple Thruster Components							
Thruster	3	0.8	2.4	10%	2.64	AMPAC	AJ10-220
Thruster Valves	6	0.19	1.14	10%	1.25	Moog	51-178
Additional Battery String	12	0.089	1.07	20%	1.28		
Flow Venturi	6	0.04	0.24	5%	0.25		
Misc Tubing, Brackets	1	0.3	0.3	25%	0.38		
PIA & PCA Plates	2	0.08	0.16	25%	0.20		
Subtotal			5.308		6.00		
In-Line Row Configuration							
Engine Support Structure	1	0.264	0.264	25%	0.33		
Total Propulsion Mass			*16.31*		***19.40***		
Triangular Configuration							
Engine Support Structure	1	0.214	0.214	25%	0.27		
Total Propulsion Mass			*16.26*		***19.34***		

4.0 Performance Comparison of the Triple Thruster and Single Thruster Systems

4.1 Performance Assumptions

The primary driver for comparing the triple thruster system with the single thruster system relies on the ultimate performance, or total flight range, achievable by the aircraft. This attribute can be subdivided into two categories; total achievable flight range with a fixed fuel load, and total achievable flight range given a fixed wet mass (i.e. the fuel load is reduced on the heavier system). In the case of fixed fuel load, the two systems were simulated using 40 kg of total propellant under conditions of both no-turbulence and severe turbulence. Comparing the performances assuming a fixed wet mass requires taking into account the differences in system mass of the three propulsion options studied, and adjusting the fuel loads of each system to result in identical system wet masses. The baseline configuration of the 62N thruster was assumed to carry a fuel load of 40 kg with a dry mass of 15.95 kg. Figure 69 recaps the mass breakdown of each of the systems being considered. Since the triple thruster "in-line" configuration has 3.4 kg more dry mass, the fuel load was reduced by this amount to 36.6 kg of fuel. Similarly, the triple thruster "triangular" configuration fuel load was reduced by the same amount. System mass and fuel loads for each case are summarized in Table 13.

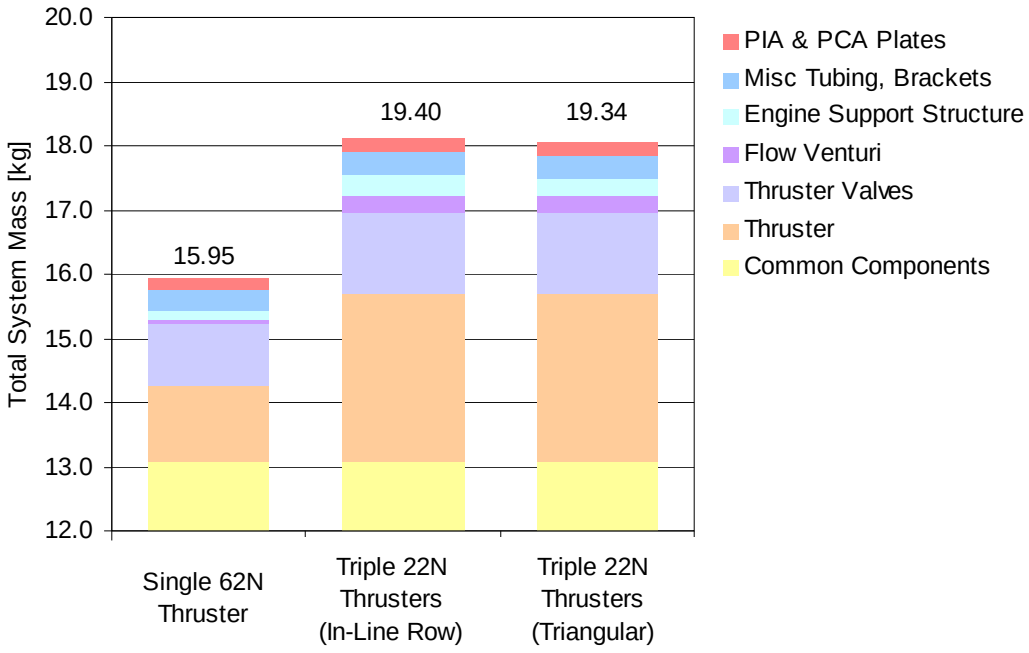

Figure 69. System Mass Breakdown Comparison

4.2 Performance Summary

The single thruster system was able to achieve a flight distances ranging from 520 km to 527 km. Both triple thruster configurations under fixed fuel load achieved the same flight distance ranging from 536 km to 543 km. A graph of these results is show in Figure 70, and summarized in Table 13. The "in-line" triple thruster configuration carries a fuel load of 36.56 kg and achieves a flight distance ranging from 490 km to 496 km. The "triangular" triple thruster configuration carries a fuel load of 36.62 kg and achieves a flight distance ranging from 491 km to 497 km. These results are shown in Figure 71.

Table 13. System Performance Comparison Summary

Fixed Fuel Load	Fuel	No Turb [km/kg]	Range [km]	Turb [km/kg]	Range [km]	Average Range
Single Thruster	40	13.2	527.1	13.0	519.7	523.4
Triple Thrusters (In-Line Row)	40	13.6	542.8	13.4	535.6	539.2
Triple Thrusters (Triangular)	40	13.6	542.8	13.4	535.6	539.2
Fixed System Wet Mass	Fuel	No Turb [km/kg]	Range [km]	Turb [km/kg]	Range [km]	Average Range
Single Thruster	40	13.2	527.1	13.0	519.7	523.4
Triple Thrusters (In-Line Row)	36.6	13.6	496.1	13.4	489.5	492.8
Triple Thrusters (Triangular)	36.6	13.6	496.9	13.4	490.3	493.6

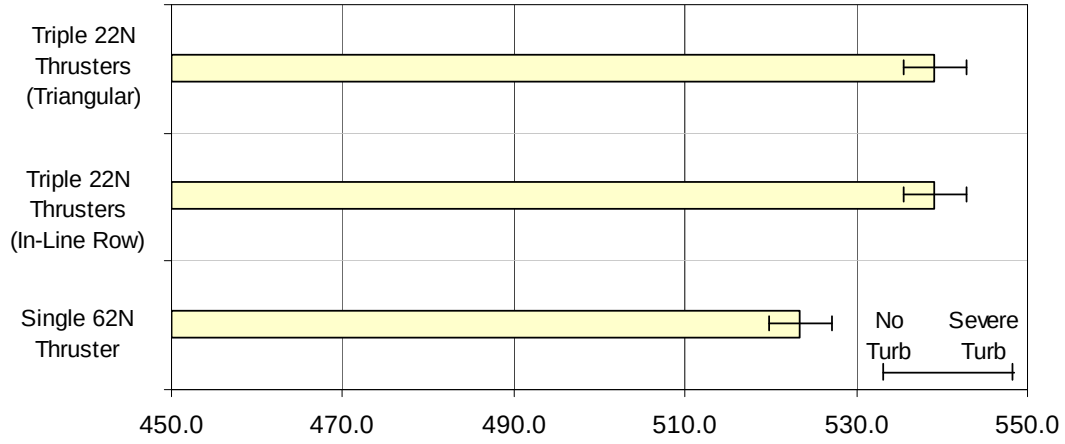

Figure 70. Comparison of Flight Range for Fixed Fuel Load

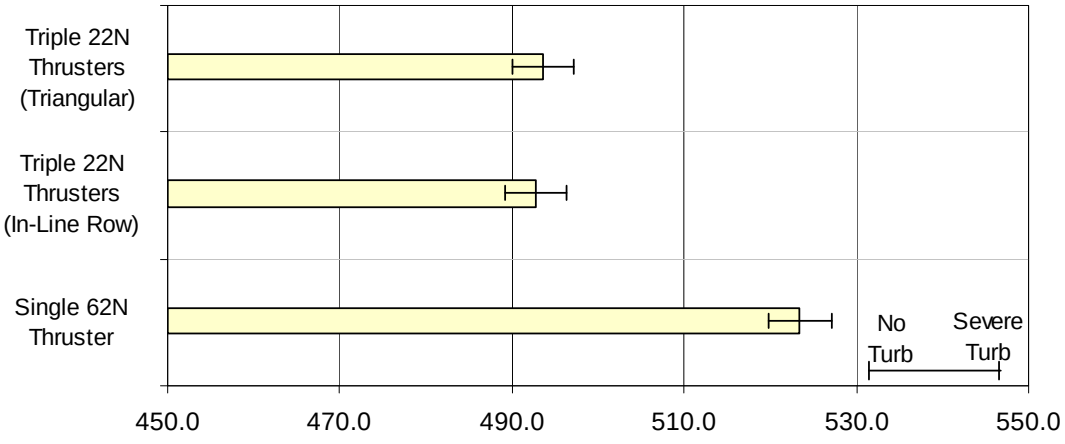

Figure 71. Comparison of Flight Range for Fixed Wet Mass

5.0 Decision Criteria for Thruster System Down-Select

5.1 Decision Criteria

The criteria for evaluating the three propulsion system options were derived based on the impact of each system on the airplane and overall mission performance, and on Mars Program cost and schedule. Out of the six criteria chosen, four relate to technical performance and two relate to program elements. However, based on the chosen weighting factors, the sum total of all technical attributes is equal to the sum total of all programmatic attributes. The decision criteria and weighting factors are listed in Table 15. There were other criteria considered in this evaluation process that could not be evaluated well quantitatively. A consideration was given to functional redundancy; the airplane is capable of flying under limited conditions with only two 22N thruster so the third thruster provides additional redundancy over the 62N single thruster system. Additionally, the impact on the center of gravity caused by additional thruster mass in the rear of the airplane was also considered, however it was judged to be insignificant.

Table 15. Decision Criteria and Weighting Factors

Criteria	Weight Factor
Energy Used by Thruster Valves	1
Peak Thruster Valve Power	2
Subsystem Dry Mass	3
Flight Range (fixed wet mass)	3
Total Thruster Costs	4
Thruster Heritage	5

The scores for each criterion were derived numerically with the exception of thruster heritage, which was derived by a combination of numerical and qualitative methods. Table 14 shows the supporting data used for determining the scores for each of the criterion. The scores are calculated based

Table 14. Supporting Data for Decision Criteria Scores

	62N Single	22N Inline	22N Tripod
Subsystem Dry Mass	**15.95**	**19.40**	**19.34**
Flight Range (fixed wet mass)	**523.42**	**492.76**	**493.60**
Thruster Non-Recurring Cost	1000	125	125
Unit Cost	125	100	100
Units Needed	3	7	7
Total Thruster Costs	**1375**	**825**	**825**
Thruster Valve Power (each) [watts]	23	26	26
Total Number of Thruster Valves	2	6	6
Peak Thruster Valve Power	**46**	**156**	**156**
Total Thruster On Time (Primary)	2011.48	2744.73	2744.73
Total Thruster On Time (Secondary)	0.00	250.23	250.23
Energy Used by Thruster Valves [Whr]	**25.70**	**82.91**	**82.91**
Thruster Developed	1	1	1
Thruster Flight Qualified/Flown	1	1	1
Current Thruster Design/Production	0	2	2
Total Units Flown in Space	*~100*	*~1000*	*~1000*
LOGARITHM of Total Units Flown	2	3	3
Thruster Heritage	**4**	**7**	**7**

on a ratio relative to the baseline single 62N thruster system. Regarding thruster heritage, the scores were derived by subdividing this criterion into four parts; *Development*: one point is given if the thruster has been previously designed and developed, *Qualification*: one point if the thruster has been flight qualified and flown on a mission, *Current Production*: two points if the design is current and the thruster is in production, one point if the design is relatively current but the thruster is not in production, and zero points if the design is not current and the unit is not in production, *Total Flight Units*: the score is determined by taking the logarithm of the total units that have flown, therefore one flight unit would equal a score of zero, 10 units a score of 1 and so on.

Table 16. Decision Criteria Scores

Criteria	Weight Factor	Baseline Single 14-lbf Thruster	Weighted Score	Tri-Thruster 22N In-Line	Weighted Score	Tri-Thruster 22N Tripod	Weighted Score
Subsystem Dry Mass	3	1	3	0.8	2.5	0.8	2.5
Flight Range (fixed wet mass)	3	1	3	0.9	2.8	0.9	2.8
Peak Thruster Valve Power	2	1	2	0.3	0.6	0.3	0.6
Energy Used by Thruster Valves	1	1	1	0.3	0.3	0.3	0.3
Total Thruster Flight Unit Cost	4	1	4	1.7	6.7	1.7	6.7
Thruster Heritage	5	1	5	1.8	8.8	1.8	8.8
Total			**18**		**21.6**		**21.6**

The final results are summarized in Table 16 and shown graphically in Figure 72. The total score for the 62N baseline system, which is simply the sum of the weight factors, is 18. The two tri-thruster systems both scored equally higher than the baseline at a total score of 21.6. An examination of the scores shows that there are four criteria having the largest divergence between the single thruster and triple-thruster systems; the baseline system scores better under Peak Thruster Valve Power and Energy Used by Thruster Valves and the triple-thruster systems scores better under Total Thruster Costs and Thruster Heritage. Figure 72 shows that the sum of five of the six scores for all three propulsion systems are relatively equal, with the Thruster Heritage being the decisive factor between the options considered.

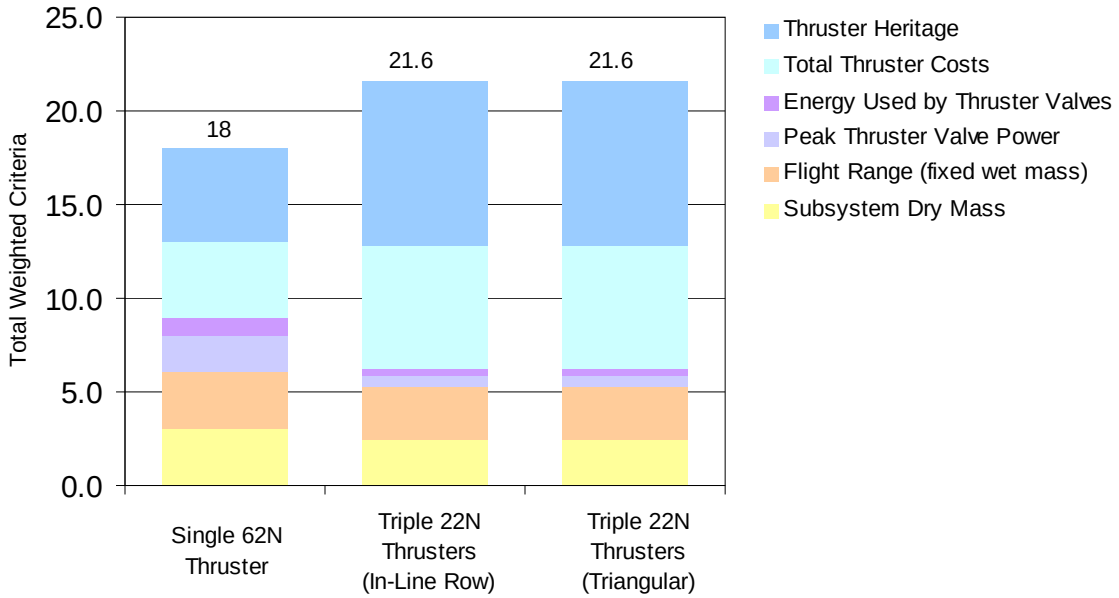

Figure 72. Decision Criteria Scores

5.2 Propulsion System Selection

The thruster options considered in this trade study are shown again in Figure 73. The triple thruster options score almost 21% higher on the decision criteria than the single thruster option. The triple in-line configuration option and the triple triangular configuration option scored essentially the same on the decision criteria. As stated in Section 3.6.3, both triple thruster configurations resulted in stable steady-state plumes, but the triangular case clearly showed stronger evidence of plume interactions and the in-line plumes maintained an angular separation all the way downstream to the simulation boundary and had minimal interactions.

The results of this study conclude that the triple 22N in-line thruster configuration is recommended for the new baseline Mars Airplane propulsion system.

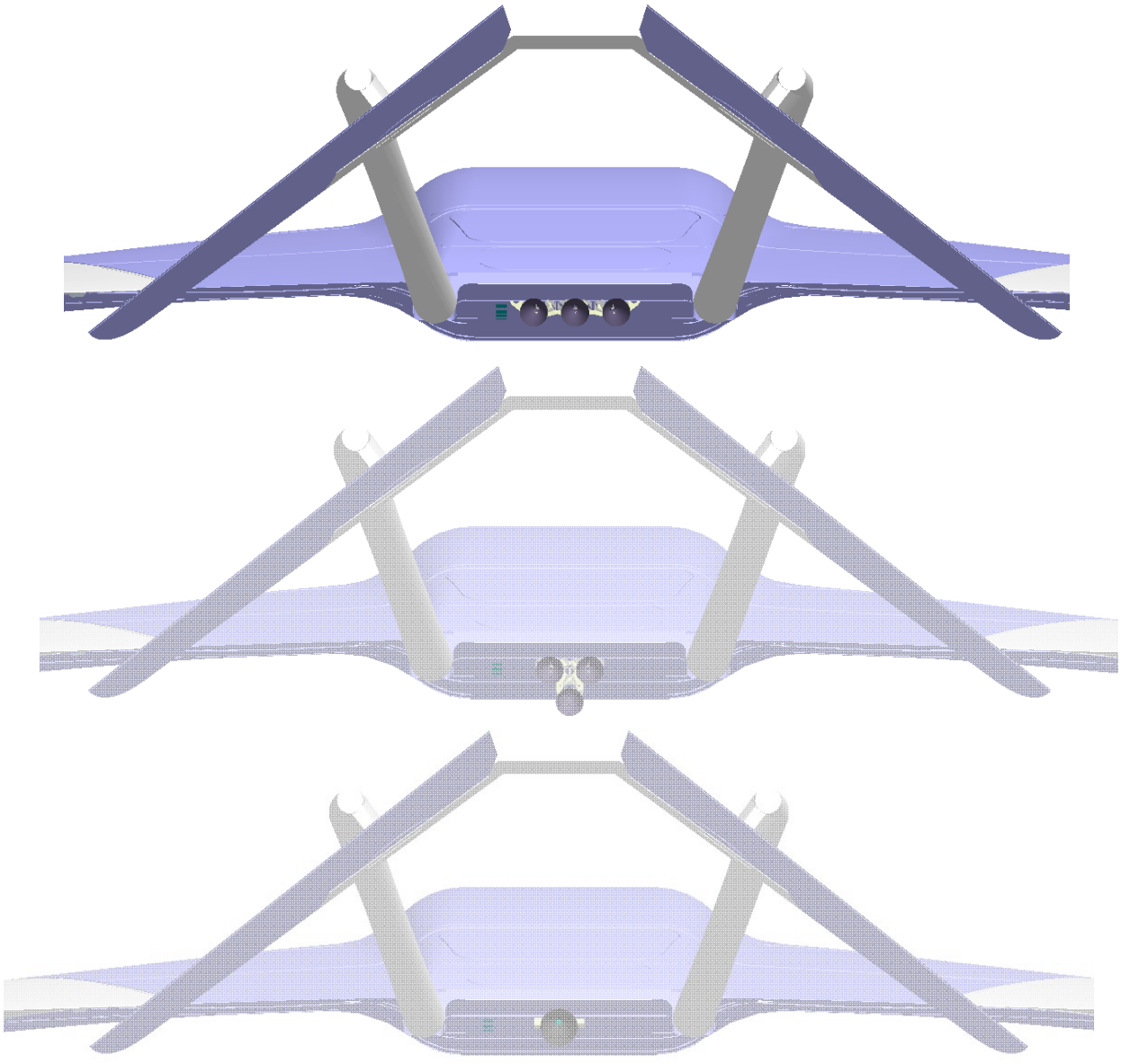

Figure 73. Recap of Trade Study Thruster Options

6.0 Appendix A – Other Thrusters Considered

6.1.1 Thruster Candidate #2 - Aerojet 5-lbf Thruster

The Aerojet Model R-6C 5.0 lbf earth storable bipropellant rocket engine (MON-3/MMH) is flight qualified and is currently operational on the Lockheed Martin MILSTAR satellite, NASA GOES, ISRO Insat 2B and others. The R-6C is distinguished from some other attitude control 5.0 lbf thrusters by its unique ability to operate at any duty cycle, including both pulse mode and steady state. This ability, enabled by a regeneratively cooled injector design, has been fully mapped over a broad spectrum of duty cycles and equilibrium long-term steady state firings.

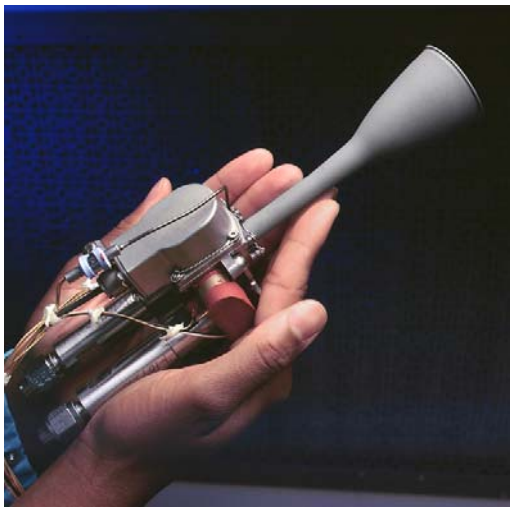

Figure 74. Photos of Alternate Thruster - Aerojet 5-lbf Thruster

The Aerojet Model R-6DM 5-lbf (22N) bipropellant (nitrogen tetroxide oxidizer and monomethylhydrazine fuel) rocket engine (Figure 1) which incorporates a single seat Moog bipropellant torque motor valve was qualified for space flight in 1989. The engine uses a fuel boundary layer film cooled combustion chamber and an unlike impinging multi-doublet injector to provide a specific impulse of approximately 294 seconds (2884 N Sec/Kg). This design provides a 100% increase in combustion chamber life when compared to the previously qualified and flight proven R-6C configuration which uses a single unlike impinging injector and active cooling of the injector head with fuel. The R-6D engine design will also interface with the Aerojet produced flexure guided single seat (R-6D), series redundant seat valves (R-6DSR) and the Moog series redundant torque motor valve. The R-6D rocket engine accumulated 61,818 seconds of firing time (341 full thermal cycles) during design verification tests at Aerojet and during the subsequent qualification program demonstrated 336,331 pulses.

6.1.2 Thruster Candidate #3 - Astrium (DASA) 22N Thruster

Astrium is a company from Munich, Germany with a new 22 N thruster that is a non-coated bipropellant rocket engine for pressurized propellant feed system using the storable propellants N2O4, MON-1 or MON-3 as oxidizer, MMH as fuel and helium as pressurant. The thruster is designed for both long term steady state operation and pulse mode down to 8 ms on-times. It operates with regulated pressure as well as in blown down mode. In addition it can be pulse operated far outside its nominal operating range in certain pulse modes if e.g. system tank pressures are exceeding tolerable limits. This thruster is a consequent evolution of the well proven Astrium 10N Pt/Rh thruster of which Astrium has already delivered several hundreds for numerous satellite programs.

Figure 75. Model of Alternate Thruster - Astrium 22N

7.0 Appendix B – Structural Analysis Assumptions

7.1 Structure Load Cases

No.	Description	Value	FS: Metals	FS: Composite
0	Launch Natural Frequency	Axial > 50 Hz Lateral > 20 Hz	N/A	N/A
1a	Launch (Use total thruster mass for MAC)	Axial = MAC+2.8 g Lateral = 4.5 g	Yield = 1.25 Ult. = 1.5	2.0
1b	Launch (Use total thruster mass for MAC)	Any = MAC g	Yield = 1.25 Ult. = 1.5	2.0
2	3rd Stage Cutoff	Axial = 15.3 g Lateral = 0.1 g Angular Vel = 80 RPM	Yield = 1.25 Ult. = 1.5	2.0
3a	3rd Stage Spin-Up	Angular Vel = 80 RPM Angular Accel = 11 rad/s^2	Yield = 1.25 Ult. = 1.5	2.0
3b	3rd Stage Ignition	Axial = 7.5 g Lateral = 0.1 g Angular Vel = 80 RPM	Yield = 1.25 Ult. = 1.5	2.0
4a	Parachute deployment	Axial = 15 g Angular Vel = 2 RPM	Yield = 1.25 Ult. = 1.5	2.0
4b	Parachute deployment – off axis	Axial = 10 g Lateral = 3 g Angular Vel = 2 RPM	Yield = 1.25 Ult. = 1.5	2.0
5	AES Impact	Axial = 15 g	Yield = 1.25 Ult. = 1.5	2.0
6	Thruster Ignition	5 lbf (ARC SW0003) 14 lbf (AJ10-220)	Yield = 1.25 Ult. = 1.5	2.0

Table 17. Mission Structural Load Cases

7.2 Load Case Definitions

- Orientation
  - Axial is defined as the longitudinal direction of the launch vehicle and the aeroshell (or perpendicular to the plane of the center-body)
  - Lateral is any direction orthogonal to the axial direction
- g's = 1 Earth g – 9.807m/sec^2

- Ultimate Margin of Safety:
  - Margin shall be positive

$$MS_{Ult} = \frac{Allow\_Ult\_Stress}{FS_{ult} * Stress} - 1$$

- Yield Margin of Safety:
  - Margin shall be positive

$$MS_{Yield} = \frac{Allow\_Yield\_Stress}{FS_{Yield} * Stress} - 1$$

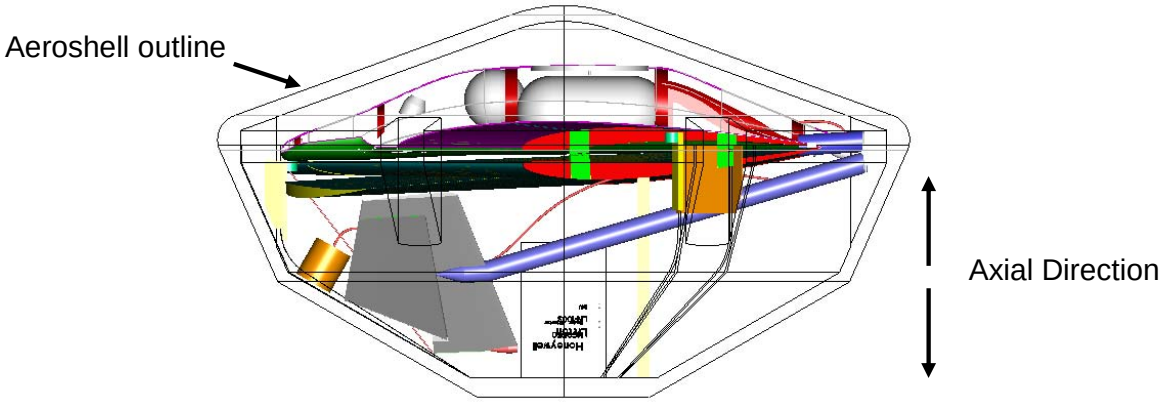

Figure 76. Flight vehicle folded in aeroshell.

7.3 Mass Acceleration Curve

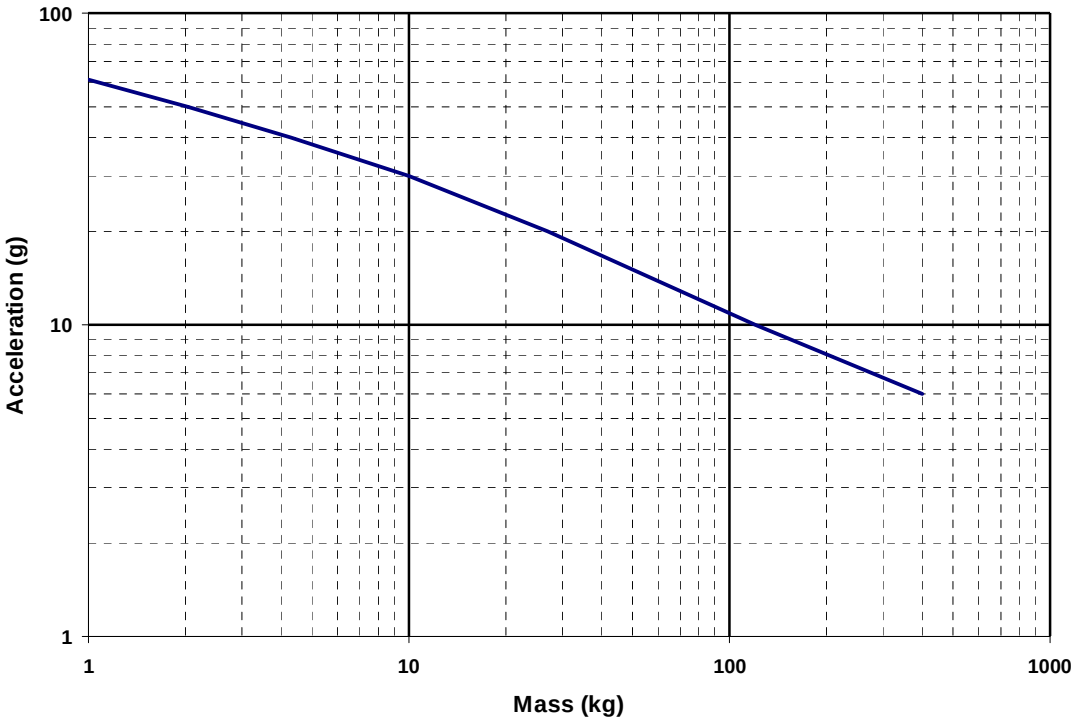

Figure 77. Mass Acceleration Curve (MAC)

8.0 Appendix C - Thermal Analysis Assumptions and Load Cases

Table 18. Source and value for all surface thicknesses used in the model

Component	Thickness (mm)	Source
Carbon Face Sheets, fuselage skin outer & inner	0.381 (used estimate of 3 fabric sheets, actually thicker or thinner in some locations)	Aurora Assembly Schematics[Error! Bookmark not defined.]
Carbon Face Sheets, inner c-channel of spars, ribs & bulkheads	1 (estimate, may be thicker in some spots)	Aurora Assembly Schematics[Error! Bookmark not defined.]
Carbon Face Sheets, outer c-channel of spars, ribs & bulkheads	4.2	Aurora Assembly Schematics[Error! Bookmark not defined.]
Carbon Face Sheets, c-channel caps	8.636 (this value is for the carbon sheets plus the carbon tape)	Aurora Assembly Schematics[Error! Bookmark not defined.]
Honeycomb Core, all	6.35	Aurora Assembly Schematics[Error! Bookmark not defined.]
Thruster nozzle	1.04	CAD Geometry Measurement
Thruster injector coupling	1.157	CAD Geometry Measurement
Thruster valves	1.71	CAD Geometry Measurement
Heat Shield	0.5	Picked value

Table 19. Sources for material properties used in this study

COMPONENT	MATERIAL	PROPERTY SOURCE
Carbon Face Sheets	Carbon Fabric, Newport Composites	Previous ARES analysis[1], Graphite/Epoxy example[11]
Honeycomb Core	Aluminum Honeycomb, Hexcel	Previous ARES analysis[1], Aluminum Honeycomb, HexWeb, HexWeb Manual - 5056 Al, 3/8" cell
Thruster nozzle, combustion chamber, & injector bracket	Columbium	Reference 11
Thruster valve mounting flange and mounting brackets	Titanium 5Al-2.5Sn	Reference 11
Thruster valves	Stainless Steel 304	Reference 11
Heat Shield	Aluminum	Patran Thermal Database

Table 20. Boundary conditions used in thermal analysis

Boundary Conditions	Value	Description/Source
Martian Ambient Air Temperature	-70 °C	Taken from previous model[1]. MarsGRAM 2001, Dick Davis (NASA GSFC)
Martian Ground Temperature	-68 °C	Taken from previous model[1]. MarsGRAM 2001, Dick Davis (NASA GSFC)
Space Temperature	-269 °C	Standard 4 K space temperature
Thruster temperature profile	Varying, °C	Using the data provided in Figure 24, two linear distributions were created for the thrusters, one from the T0 through T6 to the nozzle end, and one from T0 through T1 to the end of the combustion chamber. This may actually make the end of the combustion chamber hotter that it actually gets, but is a conservative estimate. The injector bracket faces were set at T2 and T4. The valve mounting flange was set to T5. All other components were not given fixed temperatures.

Table 21. Loads used in thermal analysis

Loads	Value	Description/Source
Contact conductance between Al honeycomb and carbon fiber face sheets, all components	0.006299 W/mm^{2}K	Taken from previous model[1]. Based on a gap with k = 4E-4 W/mmK and L = 0.0635 mm,
Contact conductance between support structure bonds (bulkheads to ribs, spars to ribs, mounting brackets to bulkheads, upper hatches to rest of fuselage)	0.006299 W/mm^{2}K	Used same as skin core convection. Heat transfer will be through the titanium corner brackets and possibly through any glue or bonding material in the joint. Contact resistance for a titanium-carbon fiber joint is not readily available. A brass alloy – brass Alloy bond with the highest roughness has a contact conductance of 0.0025 W/mm^{2}K at low pressure[12]. The value being used is most likely high if there is no adhesive or low if there is adhesive.
Contact conductance between all metal – metal bonds (valve mounting flange contact, mounting brackets to thruster connections)	0.0033 W/mm^{2}K	Used SS 416 at 1 MPa, (502.5 pg 7 curve i)[12]. This value is for standard atmospheric pressure. On Mars the pressure will be much less so for the same contact pressure, this should be a conservative estimate.
Mars albedo heating to bottom of aircraft	4.513 x 10^{-5} W/mm^2	Taken from previous model.
Solar and diffuse heating to top of aircraft	0.000285 W/mm^2	Taken from previous model[1]. Heating value was calculated assuming a coating of white paint 293 (α = 0.19, ε = 0.85)[13].
Radiation to ground from aircraft bottom	ε = 0.85	Common emissivity for carbon fabric. Radiation is to ground temperature BC which is set at an emissivity of 1. The Martian surface probably does not have an emissivity of 1, and future studies should take this into account.
Radiation to space from aircraft top	ε = 0.85	Common emissivity for carbon fabric. Radiation is to space temperature BC which has an emissivity of 1
CO_2 convection on fuselage	varying convection coefficient based on boundary layer growth over the fuselage	Taken from previous model[1]. Value for h was derived by Joseph Gasbarre (NASA Langley, STSB).
View factor radiation calculations	$\varepsilon_{columbium}$ = 0.19 $\varepsilon_{titanium}$ = 0.31 $\varepsilon_{stainless}$ = 0.31 $\varepsilon_{fuselage}$ = 0.85 $\varepsilon_{low\ \varepsilon\ paint}$ = 0.3 (when used) $\varepsilon_{heat\ shield}$ = 0.05 (when used)	Applied to thruster components and portions of the fuselage. All metal values are from Reference 11. Polished aluminum heat shield value from Reference 13 The low ε coating is an estimate, can probably find one lower.
Thruster exhaust plume properties, estimates	T = 400 °C, 700 °C ε = 0.5	The temperatures represent an estimated range for the plume. The emissivity is estimated as the highest value of H_2O vapor at 700 °C contained in Figure 9-16 in Reference 14. Since the combustion products do not contain H_2O vapor, this it is difficult to gage the accuracy of this assumption.

9.0 References

[1] "ARES, an Aerial Regional-scale Environmental Survey of Mars – Concept Study Report," proposed in response to the NASA Office of Space Science Announcement of Opportunity AO 02-OSS-02 for Mars Scout investigations, April 30, 2003.

[2] "Aerojet 14 lbf Satellite Propulsion Program", Aerojet Internal Document AP98AL313-F, Provided to NASA LaRC in support of Phase-2 Mars Scout Proposal, April 2003.

[3] "Advanced Small Rocket Chambers, Option 1 – 14 lbf IR/Re Rocket Final Report," NASA CR-191014, D. M. Jassowski, M.L. Gage, GenCorp Aerojet, August 1992.

[4] "Liquid Rocket Propulsion for Atmospheric Flight in the Proposed ARES Mars Scout Mission," C. Kuhl, H. Wright, C. Hunter, NASA Langley Research Center, Hampton, VA; C. Guernsey, Jet Propulsion Laboratory, Pasadena, CA; A. Colozza, NASA Glenn Research Center, Cleveland, OH; AIAA-2004-3696. 40th AIAA/ASME/SAE/ASEE Joint Propulsion Conference and Exhibit, Fort Lauderdale, Florida, July 11-14, 2004

[5] "Simulating the ARES Aircraft in the Mars Environment," Kenney, P.S., AIAA-2003-6579, 2nd AIAA "Unmanned Unlimited" Systems, Technologies, and Operations – Aerospace Conference, San Diego, California, September 15-18, 2003.

[6] "Mars Airplane Propulsion Study – Final Report," NASA Contract NAS1-00141, Lockheed Martin Astronautics, April 19, 2005.

[7] "Long Life 5 LBF Bipropellant Engines," AIAA-85-1378, Chazen, M.L., Bell Aerospace Textron, AIAA/SAE/ASME/ASEE 21st Joint Propulsion Conference, Monterey, California, July 8-10, 1985.

[8] "Development Tests on a 5-LBF Bipropellant Thruster Using a Platinum/Rhodium Thrust Chamber," Driscoll, R.J., Yager, J., Roy, M.J., Kammerer, H.G., Atlantic Research Corporation, AIAA-98-3357, AIAA/ASME/SAE/ASEE Joint Propulsion Conference and Exhibit, 34th, Cleveland, OH, July 13-15, 1998.

[9] HADD2 Assembly Drawings, H2-SF101, H2-SF102, H2-SF104, H2-SF105, June 24, 2003, Aurora Flight Sciences Corporation, Manassas, Va.

[10] "Transient thermal model of a film-cooled bipropellant thruster ," G. P. Purohit, P. A. Donatelli, J. R. Ellison (Hughes Space and Communications Co., El Segundo, CA), and V. K. Dhir (California, Univ., Los Angeles), AIAA-2000-1072, Aerospace Sciences Meeting and Exhibit, 38th, Reno, NV, Jan. 10-13, 2000.

[11] TPSX Material Properties Database, Web Edition. http://tpsx.arc.nasa.gov/, NASA

[12] Heat Transfer and Fluid Flow Data Books. Genium Publishing Co., Schenectady, NY, 1985.

[13] Spacecraft Thermal Control Handbook., Gilmore, David G., The Aerospace Corporation Press, 1994.

[14] Radiative Heat Transfer. Modest, Michael F., McGraw-Hill Inc. 1993.

REPORT DOCUMENTATION PAGE

Form Approved
OMB No. 0704-0188

1. REPORT DATE *(DD-MM-YYYY)*	2. REPORT TYPE	3. DATES COVERED *(From - To)*
01- 03 - 2009	Technical Memorandum	

4. TITLE AND SUBTITLE
Trade Study of Multiple Thruster Options for the Mars Airplane Concept

5a. CONTRACT NUMBER

5b. GRANT NUMBER

5c. PROGRAM ELEMENT NUMBER

6. AUTHOR(S)
Kuhl, Christopher A.; Gayle, Steven W.; Hunter, Craig A.; Kenney, Patrick S.; Scola, Salvatore; Paddock, David A.; Wright, Henry S.; Gasbarre, Joseph F.

5d. PROJECT NUMBER

5e. TASK NUMBER

5f. WORK UNIT NUMBER
698671.02.07.02.01

7. PERFORMING ORGANIZATION NAME(S) AND ADDRESS(ES)
NASA Langley Research Center
Hampton, VA 23681-2199

8. PERFORMING ORGANIZATION REPORT NUMBER
L-19371

9. SPONSORING/MONITORING AGENCY NAME(S) AND ADDRESS(ES)
National Aeronautics and Space Administration
Washington, DC 20546-0001

10. SPONSOR/MONITOR'S ACRONYM(S)
NASA

11. SPONSOR/MONITOR'S REPORT NUMBER(S)
NASA/TM-2009-215699

12. DISTRIBUTION/AVAILABILITY STATEMENT
Unclassified - Unlimited
Subject Category 20
Availability: NASA CASI (443) 757-5802

13. SUPPLEMENTARY NOTES

14. ABSTRACT

A trade study was performed at NASA Langley Research Center under the Planetary Airplane Risk Reduction (PARR) project (2004-2005) to examine the option of using multiple, smaller thrusters in place of a single large thruster on the Mars airplane concept with the goal to reduce overall cost, schedule, and technical risk. The 5-lbf (22N) thruster is a common reaction control thruster on many satellites. Thousands of these types of thrusters have been built and flown on numerous programs, including MILSTAR and Intelsat VI. This study has examined the use of three 22N thrusters for the Mars airplane propulsion system and compared the results to those of the baseline single thruster system.

15. SUBJECT TERMS
Airplane; Bipropellant; Propulsion; Rocket; Thruster

16. SECURITY CLASSIFICATION OF:			17. LIMITATION OF ABSTRACT	18. NUMBER OF PAGES	19a. NAME OF RESPONSIBLE PERSON
a. REPORT	b. ABSTRACT	c. THIS PAGE			STI Help Desk (email: help@sti.nasa.gov)
					19b. TELEPHONE NUMBER *(Include area code)*
U	U	U	UU	77	(443) 757-5802